Titre: Title:	Geostatistics and Machine Learning Applied to Recoverable Resources Assessment and Uncertainty Quantification
Auteur: Author:	Nadia Macarena Mery Guerrero
Date:	2022
Type:	Mémoire ou thèse / Dissertation or Thesis
Référence: Citation:	Mery Guerrero, N. M. (2022). Geostatistics and Machine Learning Applied to Recoverable Resources Assessment and Uncertainty Quantification [Thèse de doctorat, Polytechnique Montréal]. PolyPublie. https://publications.polymtl.ca/10246/

URL de PolyPublie: PolyPublie URL:	https://publications.polymtl.ca/10246/
Directeurs de recherche: Advisors:	Denis Marcotte
Programme: Program:	Génie minéral

POLYTECHNIQUE MONTRÉAL
affiliée à l'Université de Montréal

Geostatistics and machine learning applied to recoverable resources assessment and uncertainty quantification

NADIA MACARENA MERY GUERRERO
Département des génies civil, géologique et des mines

Thèse présentée en vue de l'obtention du diplôme de *Philosophiæ Doctor*
Génie minéral

Mars 2022

POLYTECHNIQUE MONTRÉAL
affiliée à l'Université de Montréal

Cette thèse intitulée :

Geostatistics and machine learning applied to recoverable resources assessment and uncertainty quantification

présentée par **Nadia Macarena MERY GUERRERO**
en vue de l'obtention du diplôme de *Philosophiæ Doctor*
a été dûment acceptée par le jury d'examen constitué de :

Michel GAMACHE, président
Denis MARCOTTE, membre et directeur de recherche
Erwan GLOAGUEN, membre
Oy LEUANGTHONG, membre externe

DEDICATION

To my nephews and nieces

ACKNOWLEDGEMENTS

I would like to thank my research supervisor, Professor Denis Marcotte, for his guidance, support and infinite patience during all my studies. His invaluable expertise and motivation really encouraged me to move to sharpen my professional career. Thanks for every meeting and all the time you spent with me, and thanks for your patience during the challenging moments. You are, without a doubt, a great supervisor.

I also would like to thank Xavier Emery, who has supported me since I was an undergraduate student. You pushed me to continue my studies and encouraged me to follow an academic career. Thanks for your fully confidence.

I also would like to thank Dr. Gamache, Dr. Gloaguen, and Dr. Leuangthong for the valuable comments and constructive suggestions on this document. Your comments helped me significantly improve the thesis.

Finally, I would like to thank my parents, brothers, and family for their continuous support during this adventure. My partner Diego for being part of this process, thanks for walking along with me even at a distance, brightening the darkness, for helping me in my rough days, and thanks for always believing in me. Thanks to my close friends Anne and Julio for every conversation trying to change the world, our fabulous trips, and the classical dinners on Fridays; I really miss you guys. Also, thanks to those who kept in touch with me during the pandemic, with a call, a message, or a meme. Thank you friends!

RÉSUMÉ

Cette thèse porte sur l'évaluation des ressources récupérables et de leur incertitude dans les gisements minéraux. Une caractérisation adéquate des ressources minérales et de l'incertitude associée est fondamentale dans la décision de poursuivre où arrêter les projets miniers, en particulier aux étapes préliminaires, où des données d'échantillonnage limitées sont disponibles. Trois contributions sont proposées répondant aux principaux défis identifiés dans les pratiques actuelles d'évaluation des ressources minérales, à savoir la génération de prédictions non lissées et la quantification de l'incertitude sur la prédiction des ressources récupérables pour les gisements uni- et multivariés. Une série de comparaisons avec les techniques géostatistiques traditionnelles est effectuée pour évaluer la pertinence des approches proposées en vue de leur possible intégration dans les pratiques du domaine minier.

La première proposition est le krigeage contraint (CK, *constrained kriging*), une approche qui génère des prédictions non lissées des ressources récupérables. Les performances de prédiction sont validées à l'aide d'un ensemble de données synthétiques et de deux études de cas réels, dont un gisement aurifère. Le CK surpasse le krigeage ordinaire, qui est la norme utilisée dans les rapports techniques et réglementaires d'évaluation des ressources. Il permet une meilleure prédiction du tonnage, de la teneur du minerai et du profit conventionnel. Bien que CK donne des résultats comparables à ceux du conditionnement uniforme, ce dernier ne localise pas directement les ressources et repose sur une hypothèse forte sur la distribution des teneurs. La méthode CK est robuste à la densité d'échantillonnage et les ressources récupérables prévues ne sont pas fortement affectées par les paramètres du variogramme sélectionnés. Cependant, même si CK peut devenir une alternative aux approches géostatistiques traditionnelles, il ne peut pas fournir une évaluation de l'incertitude des ressources récupérables prévues.

L'utilisation de techniques d'apprentissage automatique supervisé (ML, *machine learning*) est suggérée pour remédier à l'absence de mesure d'incertitude des ressources tout en s'accommodant de variogrammes expérimentaux souvent très bruités. L'idée de base est de fournir une quantification de l'incertitude évitant la définition d'un modèle de variogramme unique comme cela se fait habituellement avec le krigeage ou la simulation géostatistique. À cette fin, de nombreuses simulations non conditionnelles de teneurs sont générées avec des paramètres de modèle de variogramme choisi dans des intervalles de valeurs possibles. A partir de chaque simulation, un gisement de référence est utilisé pour déterminer les variables d'entrée, et les réalisations établissent les variables de sortie (c'est-à-dire les courbes de tonnage et les intervalles de confiance associés). L'apprentissage supervisé est effectué en utilisant les variables

d'entrée-sortie pour restituer des modèles prédictifs, qui peuvent ensuite être appliqués pour obtenir les ressources récupérables, et leur incertitude, à l'aide de caractéristiques extraites des données disponibles. Parmi les techniques de ML, la régression linéaire multiple (MLR, *multiple linear regression*) est considérée comme l'approche la plus appropriée car elle fournit sur des cas synthétiques des résultats similaires à d'autres techniques de ML, telles que le réseau de neurones artificiels, tout en étant plus simple d'utilisation et beaucoup plus rapide en temps de calcul. MLR caractérise mieux les ressources récupérables que les approches géostatistiques traditionnelles, et aussi bien que le modèle gaussien discret. Néanmoins, ce dernier modèle montre une assez forte sensibilité aux variations du modèle de variogramme choisi et il ne peut quantifier l'incertitude sur les ressources. La capacité de MLR à quantifier correctement l'incertitude est validée sur des données test par des probabilités de couverture très voisines des probabilités nominales.

Une extension multivariée de l'approche ML est proposée pour le cas des gisements multi-éléments ou des gisements avec la présence de contaminants venant diminuer la valeur du minerai. Cette approche utilise une série de modèles linéaires de corégionalisation avec des paramètres choisis aléatoirement dans des intervalles de valeurs possibles et générant des modèles admissibles. L'approche ML multivariée proposée est validée à l'aide d'un gisement de nickel latéritique où le traitement métallurgique de la variable primaire (teneur en nickel) est limité par un seuil maximal pour le rapport silice/magnésie. Un apprentissage MLR bivarié de la teneur en nickel et du rapport silice/magnésie est effectué en utilisant des surfaces de tonnage. L'approche ML multivariée fournit des prédictions précises et une évaluation de l'incertitude des ressources récupérables en nickel avec ou sans contrainte sur le rapport silice/magnésie. De plus, des analyses complémentaires valident la robustesse et l'applicabilité de l'approche ML. Ainsi l'approche est appliquée avec succès à des modèles physiques qui, à priori, ne présentent pas de distribution multigaussienne. Le comportement des intervalles de confiance en fonction du nombre de données est examiné de même que la capacité de la méthode à fournir des intervalles de confiance crédibles en fonction de la catégorie de ressources. Finalement, l'approche est appliquée à la fonction de récupération profit conventionnel où l'on observe que les intervalles de confiance apparaissent significativement plus larges pour cette fonction que pour la fonction tonnage.

La thèse contribue à prouver l'applicabilité du CK dans le domaine minier, soulignant son adéquation lorsqu'une localisation des ressources est requise tout en évitant l'effet lissant du krigeage ordinaire. De plus, la thèse fournit des approches ML nouvelles et robustes non-sujettes à des décisions subjectives des approches géostatistiques touchant les paramètres caractérisant la structure spatiale. Les approches ML sont applicables aux gisements univariés et multivariés. De plus, les approches ML peuvent évaluer l'incertitude des ressources

prévues et cette incertitude coïncide bien avec les niveaux des intervalles de confiance. Les trois approches sont recommandées principalement aux étapes initiales de l'évaluation des ressources minérales récupérables lorsque la quantité limitée de données disponibles nuit à l'utilisation des méthodes géostatistiques traditionnelles. On s'attend à ce que ces approches puissent améliorer la prévision des ressources récupérables et surtout permettre de quantifier leur incertitude pour aider à prendre des décisions mieux informées tout au long de l'évaluation des projets miniers.

ABSTRACT

The thesis focuses on the assessment of recoverable resources and their uncertainty in mineral deposits. A proper mineral resources characterization and their associated uncertainty are fundamental in mining projects, especially at preliminary stages, where limited sample data is available, to decide whether to continue or abandon a project. Three approaches are proposed to address the main challenges identified in current practices for mineral resource assessment, namely the generation of non-smoothed predictions and the uncertainty quantification on recoverable resources for univariate and multi-element deposits. A series of comparisons against traditional geostatistical techniques are carried out to evaluate the suitability of the proposed approaches to be incorporated as part of current practices within the mining field.

The first proposal is constrained kriging (CK), an approach that generates non-smoothed predictions of recoverable resources. The prediction performance is validated by using a synthetic dataset and two real case studies, including a gold deposit. CK outperforms ordinary kriging, which is the standard used in technical and statutory resource assessment reports, as it renders a better prediction of the tonnage, ore grade, and conventional benefit. Although CK yields results comparable to those of uniform conditioning, the latter does not directly localize the resources and relies on a strong assumption on the grade distribution. CK exhibits robustness under different sampling densities, and the predicted recoverable resources are not highly affected by the selected variogram parameters. However, even though CK may become an alternative to the traditional geostatistical approaches, it cannot provide an uncertainty assessment of the predicted recoverable resources.

The use of supervised machine learning (ML) techniques is suggested to address the drawback of the previous method, i.e., the lack of uncertainty quantification while dealing with erratic experimental variograms. The basic idea is to provide an uncertainty quantification avoiding the definition of a unique variogram model as usually done with kriging or geostatistical simulation. To this end, numerous non-conditional grade simulations are generated with variogram model parameters defined in intervals of possible values. From each simulation, a reference deposit is used to determine the input variables, and the realizations establish the output variables (i.e., tonnage and confidence interval curves). The supervised learning is carried out employing the input-output variables to render predictive models, which can be subsequently applied to obtain the recoverable resources and their uncertainty using features extracted from the available data. Among the ML techniques, multiple linear regression (MLR) is deemed the most suitable approach since it provides similar results faster and eas-

ier compared to other ML techniques, such as artificial neural networks, in a synthetic study. MLR characterizes recoverable resources better than traditional geostatistical approaches, and as well as the discrete Gaussian model. Nevertheless, the latter model shows a relatively strong sensitivity to variations on the chosen variogram model and cannot provide an uncertainty assessment. The appropriate MLR capability to quantify uncertainty is obtained by using a correction function that allows the coverage probabilities to achieve the nominal probabilities for a set of defined cut-off grades.

A multivariate extension of the ML approach is included as the third proposal, which allows assessing multi-element ore deposits characterized by several spatially correlated variables and deposits where contaminants can affect the recoverability and quality of the primary variable. This approach avoids the complex definition of a linear coregionalization model by utilizing intervals of possible values to generate admissible models. The proposed multivariate ML approach is validated using a lateritic nickel deposit, where the metallurgical processing of the primary variable (nickel grade) is restricted by a maximum threshold for the silica/magnesia ratio. A bivariate MLR training of nickel grade and silica/magnesia ratio is carried out employing tonnage surfaces. As a result, the multivariate ML approach provides accurate predictions and an uncertainty assessment of the recoverable resources of nickel and of the nickel constrained by the silica/magnesia ratio. Furthermore, complementary analyses validate the robustness and applicability of the ML approach. First, the resources of physical models that, a priori, do not exhibit a multivariate Gaussian distribution are properly assessed. This approach is able not only to incorporate the effect of the amount of data on the estimated confidence intervals, but also to adequately predict tonnage for resource categories (i.e., measured and indicated). Finally, the results indicate a precise quantification of the conventional benefit and provide credible confidence intervals on the benefit assessment. In addition, these confidence intervals are wider compared to those obtained for the tonnage function.

Ultimately, the research contributes to proving the applicability of CK in the mining field, emphasizing its suitability when a localization of the resources is required while avoiding the smoothing effect of ordinary kriging. Moreover, the study provides novel and robust ML approaches to overcome subjective decisions behind the parameter definition to characterize the spatial structure in geostatistical approaches. The ML approaches are appropriate to evaluate univariate and multivariate ore deposits. Furthermore, the ML approaches can assess predicted resources uncertainty and reproduce the nominal confidence intervals. Overall, the three proposed approaches are recommended at initial stages of recoverable mineral resources evaluation because the limited amount of available data may be insufficient for the use of traditional geostatistical methods. It is expected that these approaches can improve the

recoverable resources prediction and their uncertainty quantification to help make better-informed decisions throughout mining projects evaluation.

TABLE OF CONTENTS

DEDICATION iii

ACKNOWLEDGEMENTS iv

RÉSUMÉ v

ABSTRACT viii

TABLE OF CONTENTS xi

LIST OF TABLES xv

LIST OF FIGURES xvii

LIST OF SYMBOLS AND ACRONYMS xxi

LIST OF APPENDICES xxiii

CHAPTER 1 INTRODUCTION 1
1.1 Context 1
1.2 Problem statement 1
1.3 Research objectives 3
1.3.1 General 3
1.3.2 Specifics 3
1.4 Scope 4

CHAPTER 2 LITERATURE REVIEW 5
2.1 Recovery functions 5
2.2 Change of support 5
2.3 Common practices in mineral resources assessment 6
2.4 Model-driven methods for the assessment of recoverable mineral resources . 9
2.4.1 Global change-of-support models 9
2.4.2 Local geostatistical methods 10
2.4.3 Multivariate approaches for mineral resources assessment 17
2.5 Data-driven methods for the assessment of recoverable mineral resources . . 19
2.5.1 Mineral resource assessment applications 20

2.6 Gap of knowledge in recoverable resource assessment 21

CHAPTER 3 THESIS ORGANIZATION AND COHERENCE OF THE ARTICLES IN RELATION TO THE RESEARCH GOALS 23
3.1 Thesis outline 23
3.2 Coherence of articles 23

CHAPTER 4 ARTICLE 1: CONSTRAINED KRIGING: AN ALTERNATIVE TO PREDICT GLOBAL RECOVERABLE RESOURCES 26
4.1 Abstract 26
4.2 Introduction 26
4.3 Methods 28
4.3.1 Constrained kriging (CK) equations 28
4.3.2 Computational aspects 30
4.3.3 Kriging neighborhood analysis (KNA) 30
4.4 Results 31
4.4.1 Synthetic data 31
4.4.2 Real datasets 35
4.5 Discussion 43
4.6 Conclusions 46
4.7 Appendix 46

CHAPTER 5 ARTICLE 2: QUANTIFYING MINERAL RESOURCES AND THEIR UNCERTAINTY USING TWO EXISTING MACHINE LEARNING METHODS 48
5.1 Abstract 48
5.2 Introduction 49
5.3 Methods 51
5.3.1 Assumptions 51
5.3.2 Machine Learning Algorithms 52
5.3.3 Output (target) Data 53
5.3.4 Input Data 53
5.3.5 Settings for the Synthetic Case 55
5.4 Results 56
5.4.1 Point Grade Distributions 56
5.4.2 Input Data 57
5.4.3 Network Architecture of ANN 57
5.4.4 Tonnage Curve Prediction 58

5.4.5 Assessment of Uncertainty over Resource Predictions 60
5.4.6 Comparison between Curves Predicted by ML Methods and Traditional Geostatistical Methods 61
5.4.7 Computational Aspects 63
5.5 Case Studies 64
5.5.1 Synthetic Data of non-Gaussian Fields 64
5.5.2 Gold Deposit 68
5.6 Discussion 70
5.7 Conclusions 73
5.8 Amendment 73

CHAPTER 6 ARTICLE 3: ASSESSMENT OF RECOVERABLE RESOURCES UNCERTAINTY IN MULTIVARIATE DEPOSITS THROUGH A SIMPLE MACHINE LEARNING TECHNIQUE TRAINED USING GEOSTATISTICAL SIMULATIONS 74
6.1 Abstract 74
6.2 Introduction 75
6.3 Methods 77
6.3.1 General assumptions 77
6.3.2 MLR for multivariate recoverable resource prediction and uncertainty quantification 77
6.3.3 Definition of input variables 81
6.3.4 Definition of target variables 82
6.3.5 Uncertainty quantification 83
6.3.6 Model evaluation 84
6.4 Results 85
6.4.1 3D synthetic bivariate deposit 85
6.4.2 MLR training 86
6.4.3 Tonnage curves predicted by bivariate MLR training 87
6.4.4 Comparison of univariate and bivariate MLR training for constrained tonnage curves 89
6.5 Case study: Multi-element nickel deposit 90
6.5.1 Reference deposit 91
6.5.2 MLR training 91
6.5.3 Nickel tonnage curve prediction 93
6.5.4 Comparison of univariate and bivariate predictions for nickel tonnage curves constrained to the SiO_2/MgO ratio 93

6.6 Discussion 96
6.7 Conclusions 98

CHAPTER 7 COMPLEMENTARY RESULTS 99
7.1 3D synthetic non-Gaussian deposits 99
7.2 Influence of the sampling density 102
7.3 Application using mineral resources categories 103
7.4 Another recovery function: the conventional benefit 105

CHAPTER 8 GENERAL DISCUSSION 106

CHAPTER 9 CONCLUSION AND RECOMMENDATIONS 111
9.1 Summary of Works 111
9.2 Limitations 113
9.3 Future Research 113

REFERENCES 115

APPENDICES 135

LIST OF TABLES

4.1	RMSPE and R results using OK and CK and different neighborhood sizes.	34
4.2	Comparison of statistics obtained with UC, OK, and CK methods for blocks 5×5, Walker Lake.	37
4.3	Declusterized capped (at 30 ppm) and uncapped statistics for DDH and RC	40
4.4	Comparison of statistics obtained with UC, OK, and CK methods for blocks $5 \times 5 \times 5$ m, gold deposit.	41
5.1	Summary of assumptions and choices made for ML training.	52
5.2	Summary of parameters utilized to generate each of the $K = 5,000$ cases for training.	56
5.3	Summary of input variables.	58
5.4	Sensitivity analysis of activation function.	59
5.5	MAE and RMSE for training and testing datasets obtained by ANN and MLR.	59
5.6	Summary of MAE and RMSE of tonnage curves and success rate of different prediction methods: ANN, MLR, CK, UC, OK, IL and DG.	62
5.7	Pairwise comparison between prediction methods.	63
5.8	Summary of parameters utilized to generate each of the $K = 5,000$ cases for training. Synthetic non-Gaussian case.	66
5.9	MAE and RMSE of tonnage curves and success rate of prediction methods MLR, CK, UC, OK, IL and DG. Training on synthetic Gaussian case, prediction for images of Fig. 5.8.	66
5.10	Basic statistics of RC data.	68
5.11	Summary of the parameters utilized to generate each of the $K = 3,000$ cases for training. Gold deposit dataset.	69
5.12	Summary of MAE and RMSE for tonnage curves computed using different prediction methods: MLR, CK, UC, OK, IL and DG. Gold deposit dataset.	70
6.1	Summary of the input variables for univariate and bivariate training .	82
6.2	Summary of the output variables for univariate and bivariate training	83
6.3	Basic statistics	86

6.4 Summary of the parameters utilized to generate the $k = 3,000$ cases used for MLR training. 3D synthetic bivariate analysis 87
6.5 Metrics to evaluate MLR learning for the training and testing sets. 3D synthetic bivariate analysis 89
6.6 Basic statistics of the 1,054 samples of the reference deposit 92
6.7 Summary of the parameters utilized to generate the k =3,000 cases used for MLR training. Nickel deposit 93
6.8 Summary of the input and output variables for tonnage surface prediction. Nickel deposit 94
6.9 Metrics to evaluate MLR learning for the training and testing sets. Nickel deposit 96
7.1 Basic statistics 100
7.2 Summary of the parameters to generate the $k = 3,000$ cases used for each MLR training. 3D synthetic carbonate and sand cases 101
8.1 Summary of features in the proposed geostatistical and machine learning techniques 110

LIST OF FIGURES

2.1 Example of the loss of selectivity in the conventional benefit curve as a function of cut-off grades. SMU support (red) and point support (blue) 6

2.2 Smoothing effect on tonnage resources. Kriging (red) and real (blue) 11

4.1 Histogram (a) and variogram (b) of synthetic dataset. Experimental variogram (blue crosses) and theoretical model (solid line): $\gamma(h) = 1.89\ nug + 1.36\ exp(h, a = 8.05) + 1.46\ sph(h, a = 17.88)$. 33

4.2 KNA results for SR (blue), KE (black) and OSR (red) as a function of number of boreholes per quadrant, synthetic dataset. Theoretical values (solid lines) and experimental values (dashed lines). 34

4.3 OK and CK recovery functions using one borehole in three quadrants (dots) and three boreholes per quadrant (dashed lines). Real recoveries with synthetic dataset (solid red line). 35

4.4 Location maps of variable V, Walker Lake. The exhaustive dataset (a) and the sample dataset (b). 36

4.5 Experimental block variograms of OK (blue), CK (black) and real block values (red dashed). Walker Lake dataset. 37

4.6 Recovery functions for OK (blue), CK (black), UC (cyan) and real values (red dashed). Walker Lake dataset. 38

4.7 Swath plots along east-west (a) and north-south (b) directions. Walker Lake dataset. 38

4.8 Recovery functions for OK (blue), CK (black), UC (cyan) and real values (red dashed). Walker Lake dataset. 39

4.9 Plan views of gold variable. Reverse circulations drilling (a) and diamond drill samples (b) at level 443 m. 40

4.10 Experimental block variograms of OK (blue), CK (black) and real values (red dashed). Gold deposit dataset. 42

4.11 Recovery functions for OK (blue), CK (black), UC (cyan) and real values (red dashed). Gold deposit dataset. 42

4.12 Plan view (level 443 m) of predicted gold variable using OK (a) and CK (b). 43

4.13 Swath plots along east-west (a), north-south directions (b) and elevation (c). Gold deposit. 44

5.1 Neural network architecture schematic composed of two hidden layers. 55

5.2 Probability density function of histogram values generated from defined Gaussian anamorphosis used in the synthetic controlled case. Lognormal (a) and bimodal (b) distributions. 57

5.3 Sensitivity analysis of network architecture. 58

5.4 Real and predicted tonnage by MLR, predicted upper-bound (UB 97.5%) and lower-bound (LB 2.5%) defining 95% CI. Lognormal (a) and bimodal (b) distributions. 60

5.5 Coverage probability vs CI width in testing dataset: Original coverage (blue squares), ANN (red squares) and MLR (yellow circles). Lognormal (a) and bimodal (b) distributions. 61

5.6 Coverage probabilities for 95% CI at different cut-off values in testing dataset. Original coverage (blue squares), ANN (red squares) and MLR (yellow circles). Lognormal (a) and bimodal (b) distributions. 62

5.7 Sensitivity analysis of varying block variance s_v^2 by a factor, lognormal and bimodal distributions. Success rate of MLR (a) and MAE ratio DG/MLR (b). 64

5.8 Images used in the synthetic non-Gaussian case. Lognormal (a) and bimodal (b) distributions. 65

5.9 Real (solid blue) and predicted (dashed red) tonnage curves with predicted upper-bound 95% and lower-bound 5%, for the images of Fig. 5.8. Lognormal (a) and bimodal (b) distributions. 67

5.10 Real and predicted tonnage curves and 90% CI for the amalgam of the ten images of Fig. 5.8. Lognormal (a) and bimodal (b) distributions. 68

5.11 Real and predicted tonnage curves and 95% CI obtained with samples taken from RC data. 69

6.1 Scheme of the proposed multivariate ML algorithm 80

6.2 Section view at elevation 120 (a) v_1 and (b) v_2 85

6.3 Samples from (a) v_1 and (b) v_2 86

6.4 (a) Heat map of mean CP as a function of cutoff values for the testing set and (b) difference between real tonnage curve and predicted LB/UB as a function of the cutoff on v_1 for the testing set 88

6.5 Coverage probability vs nominal CI in testing dataset 88

6.6 Predicted mean tonnage curve (orange dashed line) and its 95% CI (yellow and purple dashed lines) along with the real tonnage curve (blue line) for (a) v_1 and (b) v_2. Bivariate predictions 89

6.7 Predicted constrained tonnage curve (orange dashed line) and its 95% CI (yellow and purple dashed lines) along with the real constrained tonnage curve (blue line). (a) Univariate MLR training and (b) bivariate MLR training 90

6.8 (a) Isometric view of nickel samples and (b) histogram of nickel grades 91

6.9 (a) Heat map of mean CP as a function of cutoff values for the testing set and (b) difference between real tonnage curve and predicted LB/UB as a function of the nickel cutoff for the testing set 92

6.10 (a) Predicted tonnage surface (orange surface) and its 95% CI (yellow and purple surfaces) along with a cross-section at ratio<2 (white) and (b) predicted mean tonnage curve (orange dashed line) and its 95% CI (yellow and purple dashed lines) along with the real tonnage curve (blue line) for nickel resources 95

6.11 Predicted mean tonnage curve (orange dashed line) and its 95% CI (yellow and purple dashed lines) along with the real tonnage curve (blue line) for nickel grades constrained by SiO_2/MgO<2. (a) Univariate MLR training and (b) multivariate MLR training 95

7.1 Section view at elevation 120 (a) carbonate cube and (b) sand cube . 99

7.2 Samples of (a) carbonate cube and (b) sand cube 100

7.3 Predicted mean tonnage curve (orange dashed line) and its 95% CI (yellow and purple dashed lines) along with the real tonnage curve (blue line) for (a) carbonate cube and (b) sand cube 101

7.4 Sample configurations. (a) 3 boreholes, (b) 6 boreholes, and (c) 12 boreholes 102

7.5 Predicted mean tonnage curve (orange dashed line) and its 95% CI (yellow and purple dashed lines) along with the real tonnage curve (blue line) using as conditioning data (a) 3 boreholes, (b) 6 boreholes, and (c) 12 boreholes 102

7.6 (a) Section view of the kriging variance at elevation 120. (b) Resources categories obtained using the kriging efficiency. Measured resources (blue) and indicated resources (yellow) along with sampling data (red dots) 104

7.7 Predicted mean tonnage curve (orange dashed line) and its 95% CI (yellow and purple dashed lines) along with the real tonnage curve (blue line). (a) Measured resources and (b) indicated resources 104

7.8 Predicted mean conventional benefit curve (orange dashed line) and its 95% CI (yellow and purple dashed lines) along with the real conventional benefit curve (blue line) 105
A.1 Normalized probability distribution varying the change-of-support coefficient 136

LIST OF SYMBOLS AND ACRONYMS

ANN	Artificial neural network
CV	Coefficient of variation
CS	Conditional simulation
CI	Confidence interval
CK	Constrained kriging
$B(z)$	Conventional benefit function
R	Correlation coefficient
CM	Covariance matching constrained kriging
CP	Coverage probability
z	Cut-off grade
DD	Data-driven
DGM	Discrete Gaussian model
DK	Disjunctive kriging
FFT-MA	Fast Fourier transform moving average
GP	Gaussian process
IK	Indicator kriging
IL	Indirect lognormal
IDW	Inverse distance weighting
KE	Kriging efficiency
KNA	Kriging neighborhood analysis
KED	Kriging with external drift
LCM	Linear coregionalization model
LUC	Localised uniform conditioning
LB	Lower bound
ML	Machine learning
MAE	Mean absolute error
m	Mean grade
$m(z)$	Mean grade function
MSPE	Mean square prediction error
$Q(z)$	Metal quantity function
MK	MultiGaussian kriging
MLR	Multiple linear regression
NI-43-101	National instrument 43-101

NN	Nearest-neighbor
OK	Ordinary kriging
OSR	Over-smoothing ratio
$P(x)$	Probability
PPMT	Projection pursuit multivariate transform
QRF	Quantile random forest
RC	Reverse circulation
RMSE	Root mean square error
SMU	Selective mining unit
SK	Simple kriging
SR	Slope of regression
3D	Three-dimensional
$T(z)$	Tonnage function
’	Transpose operator
TB	Turning Band
2D	Two-dimensional
UC	Uniform conditioning
UK	Universal kriging
UB	Upper bound
$\gamma(h)$	Variogram function

LIST OF APPENDICES

Appendix A DISCRETE GAUSSIAN MODEL 135

Appendix B UNIFORM CONDITIONING 139

CHAPTER 1 INTRODUCTION

1.1 Context

Recoverable resources are conventionally defined as the portion of *in situ* mineral resources that could be recovered depending on the selectivity of the mining method (Vann & Guibal, 2001). Global recoverable resources allow the whole ore deposit to be characterized, whereas local recoverable resources are employed to determine the grade and tonnage values at block or panel supports. The mineral resources assessment directly affects the ore reserves definition, and therefore, the revenues expected from mining projects. An incorrect prediction of those resources and reserves may lead to severe repercussions on project investment decisions (e.g., determining whether or not to proceed with the project) or mine design (e.g., life-of-mine estimation, mining method) (Goldsmith, 2002; Wellmer et al., 2007; Jones et al., 2019). McManus et al. (2021) state that numerous mining projects fail because of misleading geological interpretations or defining inappropriately spatial domains, i.e., because of an inaccurate appraisal of the mineral resources.

Several methods and good practices have been proposed to predict recoverable resources based on sampling data availability and ore deposit characteristics. At initial stages, defining a resource model that provides both conditionally unbiased (i.e., conditionally to the predicted value, the expected error is zero) and precise (i.e., the error variance is minimal) predictions is desired. At the same time, another key feature is dealing with the variability of the grade and tonnage distributions at selective mining unit (SMU) support, owing to the so-called support effect (Matheron, 1984). This is critical since mining operations require extracting mining units that are more voluminous than the quasi-point support of sample data gathered from exploration, and then, recoverable resources have to be determined at the SMU support. Moreover, enhancing the knowledge on resources is vital because there is a limited amount of drill holes at early stages of mining projects. Therefore, an appropriate approach to quantify uncertainty is needed as it may provide valuable key information for decision-making through the life-of-mine, principally when multi-elements ore deposits are of interest.

1.2 Problem statement

Despite the numerous geostatistical methods proposed to predict the recoverable resources, and the fact that the assessment of those resources is crucial for the success of mining projects, there is still no consensus about how to address the features mentioned earlier related to

the mineral resources quantification. Hence, there is a need to explore reliable alternative methods to overcome the following main challenges.

Reproduction of grade variability: The grades predicted with ordinary kriging (OK) do not reflect the real variability of geological phenomena, which is an issue called smoothing effect (Isaaks & Srivastava, 1989). This challenge is critical for the recoverable resources assessment since biased responses occur when a non-linear operator (e.g., a cut-off grade) is applied to the predicted kriging values. Even though some alternatives have been proposed to circumvent the smoothed predicted values, such as non-linear geostatistical methods (Matheron, 1976a,b; Rendu, 1980; Verly, 1983; Yates & Yates, 1988; Emery, 2005), they are complex and rely on assumptions that reduce their applicability (Vann et al., 2000; Rivoirard, 1994). Therefore, constrained kriging (CK) (Cressie, 1993) may arise as a promising alternative capable of providing non-smoothed predictions at SMU support, ensuring that the variance of the predicted values is the same as that of the target values. Since CK has been mainly applied in environmental domains (Hosseini et al., 1994; Hofer & Papritz, 2010; Hofer et al., 2013), there is an opportunity to examine its suitability for the recoverable resources assessment.

Uncertainty quantification: Although CK can deal with the change of support and smoothing effect, it cannot provide a measurement of the reliability of the predicted resources. In this line, uncertainty quantification should be characterized as mineral resources are determined from exploration drill holes usually known on widely spaced sampling. Conditional simulations (CSs) (Journel & Huijbregts, 1978; Lantuéjoul, 2002; Journel & Kyriakidis, 2004; Chilès & Delfiner, 2012) allow for uncertainty quantification of the simulated resources through multiple realizations of the element of interest. CSs can be applied to simulate resources at SMU support while surpassing the smoothing effect of OK; nevertheless, they suffer from significant shortcomings, such as assuming strong stationarity and multiGaussianity hypotheses, as well as the non-suitability for variables that exhibit a spatial continuity of their extreme values. Moreover, traditional geostatistical approaches need to define parameters. The measure of uncertainty provided by CSs is certainly dependent on the exact specification of the variogram model parameters. Any error on the model parameters would significantly impact the uncertainty assessment obtained by CS. Hence, considering the accelerated growth of data-driven techniques (e.g., machine learning (ML)), the usefulness of these methods for the evaluation of recoverable resources and their uncertainty should be assessed. This is key because finding a data-driven method to avoid the sensitive variogram fitting may improve the recoverable resources assessment. Some mining applications of ML can be found for mineral resource assessment (Matías et al., 2004; Samanta et al., 2006; Jalloh et al., 2016), but no further work is conducted for the prediction of recoverable resources and their uncertainty quantification.

Multivariate modeling: Since ore deposits commonly host several elements of interest, the application of multivariate approaches is of significant relevance as they surpass univariate techniques for the prediction of recoverable mineral resources (Battalgazy & Madani, 2019; Hosseini & Asghari, 2019). Cokriging and cosimulation appear as options for the joint prediction and simulation of coregionalized variables through the incorporation of the correlation between data and their spatial continuity (Journel & Huijbregts, 1978; Myers, 1982; Wackernagel, 2003; Chilès & Delfiner, 2012). However, the pitfalls advocated for kriging and CS remain valid for their multivariate extensions. A possible alternative is exploring the use of ML techniques to assess multi-element mineral resources. In this regard, a multivariate prediction may allow for the prediction of tonnages and grades of primary variables and by-products, or the resources of a primary variable constrained by the threshold of a contaminant. Essentially, an appropriate assessment of multi-element mineral resources and their uncertainty is fundamental to achieve the correct development of mining projects.

1.3 Research objectives

1.3.1 General

The research aims to verify the suitability of alternative approaches for predicting recoverable resources and quantifying their uncertainty. The proposed geostatistical and machine learning techniques have to deal with the main pitfalls of traditional practices to enhance the mineral resource assessment in the mining industry.

1.3.2 Specifics

In order to achieve the general objective of this study, three main specific objectives are defined as follows.

1. To determine the applicability of CK for the quantification of recoverable mineral resources by avoiding the smoothing of ordinary kriging estimates. To this end, the performance of CK is compared with traditional geostatistical methods and its robustness is tested under the application of different data types (i.e., synthetic data and real mining cases).

2. To verify the suitability of supervised machine learning techniques for assessing recoverable resources and quantifying their uncertainty. It is required to determine the most proper ML technique for the recoverable resources prediction, and then, compare it with

traditional geostatistical approaches. Moreover, the robustness of the ML approach is verified under different data type distributions and real case studies.

3. To apply the ML approach for multivariate ore deposits, providing a method of assessing recoverable resources and their uncertainty in complex scenarios (e.g., prediction of either non-additive variables or mineral resources of a primary variable constrained by a threshold of a contaminant).

1.4 Scope

The main scopes of the research are the following:

1. The research is developed in a multiGaussian framework since this model is widely used within the mining industry for modeling ore grades and, also, has the most efficient simulation algorithms available.

2. Machine learning is the preferred approach to explore the applicability of data-driven techniques for assessing recoverable mineral resources.

3. Case studies using synthetic datasets and real deposits are carried out in order to analyze the performance of the proposed approaches and to compare them against traditional geostatistical methods.

CHAPTER 2 LITERATURE REVIEW

2.1 Recovery functions

The recovery functions are used to quantify the global recoverable resources with respect to given cut-off grades (z) in an ore deposit (Lantuéjoul, 1990; Chilès & Delfiner, 2012). These functions allow modeling the global distribution of a regionalized variable, represented by the cumulative distribution function of a parent random field.

Four main recovery functions are defined in the mining context: (i) the tonnage $T(z)$, which corresponds to the proportion of values greater than or equal to z, representing the fraction of total tonnage above the cut-off. The tonnage is a decreasing function of the cut-off grade, (ii) the metal quantity $Q(z)$ which is a decreasing function of the cut-off grade, (iii) the mean grade $m(z)$, which corresponds to the ratio between the metal quantity and the tonnage, an increasing function of cut-off grade, and (iv) the conventional benefit $B(z)$ that is a decreasing function of the cut-off grade. The conventional benefit is defined by the difference between real recovered metal quantity and the minimum quantity that is supposed to be recovered above the cut-off grade, that is $B(z) = Q(z) - zT(z)$. It should be noted that tonnage is referred to the relative tonnage with regards to the total tonnage in the studied domain, T_0. The same is applied to the metal quantity. Hereinafter, tonnage and metal quantity are used to refer to relative terms. At zero cut-off grade, $T(0) = 1$ and $Q(0) = m(0) = B(0) = m$, which is equivalent to the global mean value. $Q(0) = m(0)$ is valid only if $Q(0)$ is normalized by T_0.

2.2 Change of support

During the mine operation, the material extracted is defined in a greater support than the quasi-point support of the exploration drill hole samples. Thus, it is required to understand how the recovery functions will be affected by this change of support.

The aforementioned recovery functions can be mathematically defined at SMU support (v) as follows:

$$T_v(z) = \mathbb{E}\{\mathbb{1}_{Z(v)\geq z}\} \tag{2.1}$$

$$Q_v(z) = \mathbb{E}\{Z(v)\mathbb{1}_{Z(v)\geq z}\} \tag{2.2}$$

$$m_v(z) = \mathbb{E}\{Z(v)|Z(v) \geq z\} \tag{2.3}$$

$$B_v(z) = \mathbb{E}\{(Z(v) - z)\mathbb{1}_{Z(v)\geq z}\} \tag{2.4}$$

where $Z(v)$ is the SMU grade and $\mathbb{1}$ is the indicator function equal to 1 when $Z(v) \geq z$ and 0 otherwise. These formulae generalize the previous definitions of the recovery functions at a point support.

The change of support has an impact on the distribution (hence, on the recovery functions) of the studied variable. For instance, a higher support implies less variability, and consequently, a loss of selectivity will occur when the mine is developed (Matheron, 1984; Chilès & Delfiner, 2012). An example of the loss of selectivity is depicted in Fig. 2.1, where conventional benefit at SMU support is shown to be less selective than the point support, i.e., $B_v(z) \leq B(z)$.

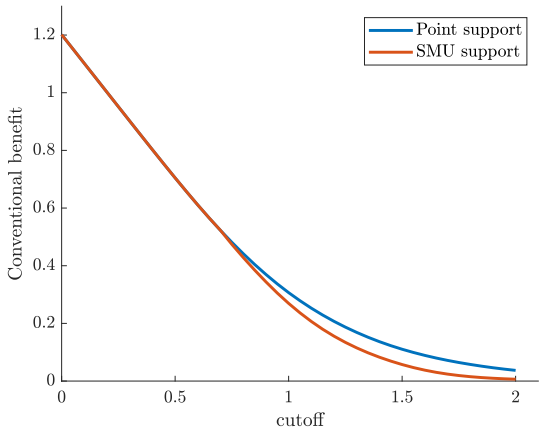

Figure 2.1 Example of the loss of selectivity in the conventional benefit curve as a function of cut-off grades. SMU support (red) and point support (blue)

The loss of selectivity at SMU support can be explained by Cartier's relationship, which implies that the expected grade at random point chosen within the SMU with a known grade must be equal to the SMU grade (Matheron, 1984). This relationship is the basis for the construction of change-of-support models such as the well-known discrete Gaussian model (DGM) (Matheron, 1976a, 1984; Rivoirard, 1994).

2.3 Common practices in mineral resources assessment

Several studies have been conducted to determine the best practices and techniques associated with the prediction of mineral resources. A comprehensive review can be found in Rossi & Deutsch (2014), where the traditional approaches, their main issues, and several case studies are presented.

The main steps required for assessing mineral resources generally include the definition of geological domains, data analysis, the quantification of the spatial variability, and the ap-

plication of geostatistical methods accounting for a change of support (Glacken & Snowden, 2001). Commonly, a reconciliation process is performed throughout the mine operation to validate the predicted mineral resources. The approaches to assess mineral resources can be divided between global and local techniques. The former focuses on predicting resources as a whole without localizing them in the field, while the latter provides a characterization of each SMU. Although traditional methods such as inverse distance weighting (IDW) can be used to evaluate mineral resources (Glacken & Snowden, 2001), geostatistical approaches are recommended as they account for the spatial continuity of regionalized variables. Kriging (Matheron, 1963) has been the principal method employed to this end. Depending on whether the mean value is known or unknown, the evaluation of mineral resources can be carried out using simple kriging (SK), ordinary kriging (OK), universal kriging (UK), or kriging with external drift (KED) (Chilès & Delfiner, 2012).

Depending on the goal sought for the predictions, three main types of mineral resources can be considered (Deutsch et al., 2014). The initial predictions are performed for visualization and geological understanding, where SK is the preferred method. The interim predictions are employed for long-term evaluations considering limited data, where global accuracy is the desired property. To accomplish this, OK with a restrictive kriging neighborhood is suggested, in order to attenuate the smoothing effect and to obtain an unbiased (i.e., the expected error is zero) or not-too-biased prediction of the recovery functions. Final predictions are used for the decision-making process of sending material to either the mill or dump and consequently, the focus is set on providing local precision (i.e., the conditional bias has to be reduced by applying a large neighborhood) (Deutsch et al., 2014; Rossi & Deutsch, 2014). The definition of the kriging neighborhood is therefore essential because the predictions are highly affected by their parameters (Vann et al., 2003). These parameters can be selected taking into account practical factors and the experience of practitioners. Some metrics to define the kriging neighborhood were proposed by Rivoirard (1987), and later formalized as quantitative kriging neighborhood analysis (QKNA) by Vann et al. (2003). Further details on the criteria are found in Section 4.3.3. Despite applications of QKNA are still being carried out in the prediction of mineral resources (Boyle, 2010; Khakestar et al., 2013; Hundelshaussen et al., 2018), its criteria cover a limited range of the possible parameters. Until now, there is no consensus about which criterion to prefer, leaving the geologists or mining engineers to decide the parameters used in the prediction based on their prior knowledge or expertise. Furthermore, it is worthwhile to mention that reducing conditional bias and enhancing local precision implies a greater smoothing effect, hence, the prediction of the recovery functions may be inaccurate (Isaaks, 2004). The optimal prediction of the mineral resources may not provide a good prediction of the recoverable resources above a given cut-off grade. Advanced

techniques for recoverable resources assessment are presented in the next sections.

In order to compute the global recoverable resources and the grades and tonnage at SMU support, the studied variables should be additive (i.e., their average must have a meaning (Journel & Huijbregts, 1978)). Some counterexamples found in orebody evaluation are related to the ratio between elements (e.g., solubility ratio), geometallurgical variables (e.g., metallurgical recovery) or to deposits where the rock density varies with the ore grade (e.g., iron deposits). The traditional approach to deal with non-additive variables is to identify, when possible, additive variables to carry out their prediction, and later, obtain the non-additive responses minimizing the bias (Carrasco et al., 2008). For instance, Adeli et al. (2021) perform the prediction of the additive variables mass of metal in feed and mass of metal in the concentrate, inferring the recovery by computing the ratio between them. Moreover, an appropriate assessment of recoverable resources has to consider the contaminants or by-products that affect the primary variables. Since these variables usually are statistically and spatially correlated, it is highly recommended to utilize methods that incorporate these relationships. As an example, Vergara & Emery (2013) apply arsenic grades as a conditional constraint on the predicted copper grades, resulting in a higher conditional bias when both variables are predicted separately compared to the joint prediction of them.

A missing aspect in almost all the mineral resources reports is a measure of uncertainty on the predicted resources. Most of the initial decisions in mining projects are based on the declared information of these reports, even though they are carried out with scarce data that is unlikely to be enough to characterize the inherent uncertainty of the ore deposits. For instance, the national instrument NI-43-101 (CSA, 2016) requires disclosure of mineral resources to be founded in reliable information through defined standards and best practices. Specific details regarding data quality, laboratory assays or drilling results have to be reported; however, an uncertainty assessment is not explicitly required. The measure of uncertainty in NI-43-101 aims to classify the mineral resources as measured, indicated, and inferred. However, within each category, the uncertainty on the tonnage and ore grade is not reported. Instead, NI-43-101 only requests a significant discussion on risks and uncertainties that can be expected (refer to Item 25), although no standards or guides are officially defined. Dimitrakopoulos (1998) indicates that a complete block resource model must include an assessment of uncertainty on the mineral resources and the possible effects of their uncertainty on downstream stages of mining projects. Today, uncertainty quantification has still not been incorporated as a common practice in the industry, despite its significant impact on mining projects (Chiquini & Deutsch, 2020).

An additional gap in current industrial practices, particularly in technical and statutory min-

eral resources reports, is that machine learning techniques are not deemed to be incorporated despite their rapid evolution and numerous applications carried out for academic purposes.

2.4 Model-driven methods for the assessment of recoverable mineral resources

2.4.1 Global change-of-support models

The basic approach to provide global recoverable resources at SMU support are denominated change-of-support models. The central idea is to relate the distribution at point and SMU supports, assuming that the SMU distribution has the same mean, a reduced variance (considering a variance correction factor that can be computed from the point-support variogram), and a more symmetrical shape compared to the point support distribution as a consequence of the support effect. Several change-of-support models have been proposed to compute global resources at SMU support, e.g., affine correction, mosaic correction, direct lognormal correction, indirect lognormal (IL) correction, among others (Journel & Huijbregts, 1978; Isaaks & Srivastava, 1989; Lantuéjoul, 1990; Rivoirard, 1994; Lajaunie, 2000; Chilès & Delfiner, 2012). The most used methods are affine and IL correction. Although these methods are simple alternatives able to reproduce the loss of selectivity of distributions at SMU support, they suffer from drawbacks, such as the selected distribution does not get more symmetrical when increasing the support (affine correction), or the proportion of zero grade values does not decrease when increasing the support (IL correction) (Emery, 2007).

The discrete Gaussian model (Matheron, 1976a) is capable of predicting local and global resources avoiding the shortcoming of the previous models. This method is based on a transformation of the point and block-support grades into Gaussian equivalents and on satisfying Cartier's relationship, which provides a relationship between point and SMU distribution, allowing for obtaining the recoverable resources at SMU support (Machuca-Mory et al., 2008). Further mathematical details on DGM are presented in Appendix A. DGM is a robust alternative compared to the before-mentioned change-of-support models because it relies on relatively mild assumptions. Nevertheless, DGM can be unsuitable when the variables under analysis have zero grades as the SMU support distribution must have fewer zero values (Matheron, 1980).

Many applications of the change-of-support models are theoretical studies focused on analyzing how the methods modify the point distribution and comparing the predicted resources with different models. For example, Emery & Torres (2005) conclude that the affine correction lead to unrealistic global distributions. In contrast, DGM and mosaic correction are more effective approaches based on the results of a synthetic case study that mimics a gold

deposit with connectivity of high grades and positive highly skewed distribution. The authors mention that the so-called simple approaches (e.g., the affine correction) require the same amount of defined parameters as DGM. Therefore, this is not a major argument to justify using these simple approaches. The superiority of DGM is in line with the findings of Demange et al. (1987); Lantuejoul (1988) and Rossi & Parker (1994). Dutaut & Marcotte (2019) study the effect of the variogram estimator type (i.e., traditional, normal score, correlogram, and pairwise) on the change-of-support models. The results indicate that DGM overcomes the IL correction on the tonnage-grade curves prediction. The authors conclude that DGM is a robust method under different distribution types and sampling densities. Even though DGM is the preferred alternative for assessing recoverable mineral resources, it does not provide a measure of resources uncertainty.

2.4.2 Local geostatistical methods

Numerous geostatistical approaches have been utilized to assess mineral resources at a local scale. Kriging, non-linear methods, constrained kriging, and simulations for local recoverable mineral resources evaluation are discussed below.

Kriging

Ordinary kriging (Matheron, 1963) is one of the most used geostatistical predictor in the mining industry. It considers the redundancy between the available sampling data and their spatial continuity. A kriging neighborhood, that defines which subset of the available sample data are used, and a covariance model are required to carry out the prediction. The fitting of the covariance model is often derived from an experimental covariance or an experimental variogram using a set of known basic models (i.e., nested structures). Further discussion of the covariance fitting process can be found in David (1977), Journel & Huijbregts (1978), Guibal (2001), and Chilès & Delfiner (2012), while a detailed elaboration of kriging can be found in Goovaerts (1997) and Chilès & Delfiner (2012).

Isaaks (2004) demonstrates that this predictor cannot be conditionally unbiased and accurate at the same time (i.e., the kriging oxymoron). In particular, the conditionally unbiased prediction leads to a smoothed histogram of the predicted values, generating inaccurate predictions when applying a non-linear function (e.g., a cut-off). In addition, the author indicates that the decision of which property (precision or conditional unbiasedness) will be prioritized depends on how the predictions will be used during the mine operation. For instance, non-smoothness will be preferred when evaluating long-term scenarios (annual or semi-annual periods of the life-of-mine), while (conditional) unbiasedness has to be chosen

in a short-term scenario (ore-waste classification).

The extensive use of OK as an interpolation method is mainly explained by its properties, such as the unbiasedness, the exact interpolation and the additivity property (Chilès & Delfiner, 2012). Nevertheless, kriging generates values with reduced variability. Some consequences of this undesired property imply (i) predicted grades less variable than real grades, (ii) histogram of predicted grades narrower than the histogram of real grades, (iii) non-reproduction of the covariance model, (iv) issues in the representation of patterns of extremes values (Goovaerts, 1997), (v) biased predictions when a non-linear function is applied, and (vi) maps where the densest sampling areas exhibit a high artificial variability compared with more sparse sampling areas since the smoothing effect is non the same over the domain (Journel et al., 2000). For instance, Fig. 2.2 shows the bias that appears when cut-off grades are applied to the tonnage resources. An overestimation occurs if cut-off grades are lower than the mean grade of the deposit, and otherwise, an underestimation is obtained.

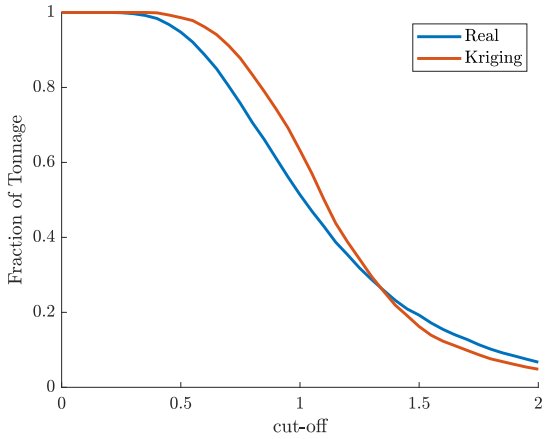

Figure 2.2 Smoothing effect on tonnage resources. Kriging (red) and real (blue)

One common approach that deals with the smoothed predictions is the use of a restrictive neighborhood when OK is applied. A comparison between DGM, optimized OK (i.e., OK set to reduce the smoothing effect), and OK is performed by De-Vitry et al. (2007) for predicting recoverable resources in an iron deposit. It is concluded that kriging methods are not able to eliminate the smoothing effect, even when OK is adjusted to reduce the smoothing. As a result, OK predictions are conditionally biased at low cut-offs and generate greater tonnage values than DGM. Moreover, the authors criticize the decision to use optimized OK in most technical reports, stating that it is not recommended because local accuracy can also be important in long-term planning. Therefore, DGM can be a good alternative to move from linear (*in-situ* resources) to non-linear (recoverable resources) predictions, as well as

conditional simulation (CS) that will be explored later in this chapter.

Several other alternatives have been proposed to minimize the smoothing effect on the predictions. Guertin (1984) suggests the use of a binormal model distribution, while Olea & Pawlowsky (1996) utilize cross-validation to define the coefficients of a linear regression used to generate non-smoothed predicted values. Journel et al. (2000) apply the spectral approach proposed by Yao (1998) as a post-processing of the kriging results to furthermore incorporate the appropriate covariance model in the prediction process. The predicted results do not exhibit artifacts generated by the smoothing effect; however, a reduction in the local accuracy is introduced using this method. Yamamoto (2005) proposes a post-processing approach based on a four-step procedure able to reproduce the covariance to generate accurate local predictions. This approach has been validated by Yao et al. (2014) and Yamamoto (2007, 2008). Nonetheless, this approach suffers from a complex formulation because it requires additional steps to generate the non-smoothed results.

Since the thesis aims to assess mineral resources accurately, one goal is to determine a predictor capable of reducing or eliminating the smoothing effect.

Non-linear geostatistical methods

Non-linear approaches such as disjunctive kriging (DK) (Matheron, 1976b; Rendu, 1980; Yates & Yates, 1988), bi-Gaussian kriging (Marcotte & David, 1985), multiGaussian kriging (MK) (Verly, 1983; Emery, 2005), and uniform conditioning (UC) (Rivoirard, 1994) may also be considered as alternatives to avoid the smoothing effect of kriging (Vann et al., 2000). DK and MK are able to estimate a non-linear function of the variable under study (e.g., tonnage at given cut-off values). Apart from its mathematical complexity, one drawback of DK is the order relation problems that produce inconsistencies on the predicted recoverable resources (Emery & Ortiz, 2004). MK assumes that the transformed variables follow a multiGaussian distribution. This hypothesis can be inappropriate for variables with extreme values that are highly spatially correlated (Rivoirard, 1994). Both DK and MK may be applied for resource prediction at SMU support using the DGM. UC enables the prediction of recoverable resources at SMU support located within a panel (i.e., the union of several SMUs) conditioned to a prediction of the panel value, alleviating the strict stationarity hypothesis stated for DK and MK. Nevertheless, UC may be sensitive to the misspecification of the covariance model, requires extending the DGM hypotheses to the panel support, and does not allow distinguishing the predictions of the SMUs within the same panel. Further mathematical details on UC can be found in Appendix B.

Within the mining industry, few applications of DK and MK are found due to the theoretical

complexity behind these methods, where most of the studies involve academic research. Conversely, UC and localised uniform conditioning (LUC) (an extension of UC that provides SMU grades within the predicted UC panels, see Abzalov (2006)) are more widely used to assess recoverable resources. For instance, Guibal & Remacre (1984) argue that UC leads to predictions comparable to DK or MK, while Remacre (1989) finds that UC outperforms indicator kriging. Millad & Zammit (2014) compare the tonnage and grade resources obtained by LUC and OK in a porphyry copper deposit, concluding that LUC outperforms OK in the reproduction of the mineral resources of the grade control model. Govindsammy (2016) derives the same conclusion from a gold deposit in an underground mine, where UC provides superior accuracy compared to OK. Hansmann (2016) performs an analysis of whether UC can be adequately applied, indicating that the non-linear method is more effective than OK when data is widely spaced and follows a lognormal distribution. The influence of the amount of data in the mineral resource assessment by UC is investigated by Assibey-Bonsu & Muller (2014). The authors suggest that a conditional bias appears when limited data is considered, which is common in pre-feasibility and feasibility studies, and hence, UC can be unsuitable in such cases.

Constrained kriging

Cressie (1993) proposes a variant of kriging to obtain unbiased and non-smoothed predictions. The predictor, known as constrained kriging (CK), ensures that the predictions have the same theoretical variance as the true values. Further elaboration of the CK equations can be found in Section 4.3. Aldworth & Cressie (2003) propose an extension of CK called covariance matching constrained kriging (CM). This predictor is capable of matching not only the variance of the target values, but also the covariance between the predicted and target values. Because they do not smooth the variability, CK and CM are expected to generate unbiased predictions when non-linear functions are applied to the predictions. The main applications of CK and CM and its comparison with traditional approaches are summarized below.

Cressie (1993) conducts a synthetic study where CK generates less biased predictions compared to OK, suggesting that CK should be used in resource evaluation when unbiasedness is a desired property. Nevertheless, the mean square prediction error (MSPE) increases between 20% and 50% for CK compared to OK. In the environmental domain, Hosseini et al. (1994) analyze the interpolation of soil salinity data by geographic information systems employing different methods, where thin plate smoothing splines and OK are the best predictors regarding precision. Although CK presents the lesser smoothing effect, it is less precise than the

other methods. Cressie & Aldworth (1997) carry out numerical experiments to analyze the impact of sampling designs. The authors state that OK and CK present acceptable MSPE, even in cases where measurement errors are observed. OK is smoother than CK when the spatial mean and spatial cumulative distribution function are studied. As a general conclusion, CK performs better than OK regardless of the considered scenarios. Later, Aldworth & Cressie (1999) conduct several experiments to compare the performance of OK and CK. Although OK is the preferred predictor for spatial predictions over a local region, CK shows similar results to OK. Regarding global predictions, OK and CK perform adequately.

Several studies have been developed to compare CK, CM, and traditional geostatistical methods. First, Aldworth (1998) performs a comparison between OK, CK, and CM using simulated data. The author concludes that OK is the best predictor for linear predictands, and the performance of OK, CK, and CM is similar if the spatial correlation is strong. In addition, under the application of non-linear functions and Gaussian distributions, CK outperforms OK. Cressie & Johannesson (2001) compare the performance of CM with OK and CK using data of scallop abundance within the environmental field. As a result, CM and CK avoid the smoothness of OK and generate heavier tails than OK. The authors suggest that CM have to be selected instead of CK, even though specific cases have to be analyzed, such as the effect of distributions far from Gaussian. Aldworth & Cressie (2003) introduce CS into the comparison using synthetic data that consider Gaussian and non-Gaussian random fields. For linear functions and Gaussian data, the best results are obtained through OK and CS. CS fails when data do not follow a Gaussian distribution. For non-linear functions, CK and CM show a robust performance, with slight biases and intermediate MSPE with respect to the other methods. In general, the performance of CM is better than CK based on the lower prediction error. Exploring a robust method to predict threshold exceedance, Hofer & Papritz (2010) carry out several simulation experiments to compare UK, CK, CM, and CS considering different data distributions, non-stationary mean functions, and different incorporation of errors. The results indicate that CK and CM provide lower precision in sparse sampling density cases but outperform UK in all the non-linear scenarios. When skewed data distributions are analyzed, CS shows a strong bias while CK and CM generate unbiased and precise predictions. In general, CK and CM are the best predictors in most of the studied cases. Even though no clear advantages of utilizing CK instead of CM are presented in their work, the authors firmly recommend the use of CK because of its simplicity and robustness. Hofer et al. (2013) perform an application using heavy metal values in soils around a metal smelter to compare the performance of lognormal CK, lognormal CM, lognormal UK, and CS. CS reaches the best precision for the block mean and threshold exceedance evaluation, but it does not exhibit a notable advantage. Lognormal UK outperforms the other methods

when non-linear functions are applied, which is unexpected due to the bias of traditional kriging approaches but can be explained by the high-density sampling. Notwithstanding, the authors recommend using either CK, CM or CS when non-linear functions are applied.

Most of the CK applications have been carried out using numerical experiments and within the environmental field. Thus, research on the mining field is needed to explore CK as an alternative for assessing recoverable resources, especially considering the seemingly satisfactory results of CK under the application of non-linear functions. Furthermore, the robustness of CK has not been thoroughly studied, where case studies and numerical experiments using different data distributions have to be performed.

Simulation of mineral resources

None of the previous methods provide uncertainty quantification on the predicted recoverable resources as geostatistical simulations (Chilès & Delfiner, 2012). The approach aims to generate values reproducing the spatial variability of the available data. These simulated values are a realization of a random field, which could be interpreted as the stochastic representation of the regionalized variable under study.

Simulations are classified as non-conditional and conditional simulations. The former provides realizations with the same variability as the available data without reproducing values at sampling locations. The latter reproduces both the spatial variability and data at sampling locations. A non-conditional simulation can be converted into a conditional simulation in the case of Gaussian random fields, where an additional step known as residual kriging is required (Chilès & Delfiner, 2012):

$$Y_{CS}(x) = Y^{SK}(x) + Y_S(x) - Y_S^{SK}(x) \tag{2.5}$$

where $Y_{CS}(x)$ is the conditional simulation value obtained at location x, $Y^{SK}(x)$ is SK of the conditioning data, $Y_S(x)$ is a non-conditional simulation at location x, and $Y_S^{SK}(x)$ is the SK of the non-conditional simulation values at the conditioning data locations.

The multiGaussian model is typically employed in the mineral resources assessment. Some algorithms such as sequential (Ripley, 1987; Deutsch & Journel, 1998) and matrix decomposition (Davis, 1987; Alabert, 1987) can directly provide conditional simulations. In contrast, spectral (Shinozuka & Jan, 1972) and turning bands (TB) algorithms (Journel, 1974; Emery & Lantuéjoul, 2006) require the additional step specified in Eq. 2.5. Other approaches such as fast Fourier transform and fast Fourier transform moving average (FFT-MA) (Ravalec et al., 2000) can also be used. Applications and comparisons of the simulation methods are

found in Vann et al. (2002), Benndorf (2013), and Paravarzar et al. (2015). Paravarzar et al. (2015) conclude that TB outperforms sequential simulation because a better reproduction of the spatial structure (covariance function or variogram) is observed. An error propagation due to the use of a moving neighborhood explains the inaccurate reproduction of the spatial structure in sequential simulation during the simulation process (Emery & Peláez, 2011).

High-resolution CSs are commonly performed, and then, the simulated SMUs are obtained by averaging the simulated point-support values within the SMU (Verly, 1984). Consequently, this process is demanding in terms of computational resources. Some alternatives have been provided to deal with this issue, for example, direct block simulation at the SMU support using sequential simulation (Marcotte, 1994) or incorporating a change-of-support model into the simulation algorithm (Boucher & Dimitrakopoulos, 2009; Emery & Ortiz, 2011). Nonetheless, additional assumptions have to be considered when applying the direct simulations, and therefore, the current practice of block-averaging point-support simulations is still suggested (Journel & Kyriakidis, 2004).

The outcomes of geostatistical simulations may be used to perform either risk analysis, uncertainty assessment, or the predictions of recoverable resources (considering the average of recovery functions calculated over several realizations). A typical barrier to the use of CS appears since common practice in assessing mineral resources is to determine the resources taking into account only one resources model. This may be surpassed since all the calculations that commonly consider a single model could be carried out on all the realizations, providing a range of results, hence an uncertainty quantification of recoverable resources. If necessary, a subsequent calculation can be performed to generate one result model, for instance, using the average of the recoverable resources calculated over all the realizations.

Verly & Parker (2021) provide a valuable insight into the application of CS for mineral resource classification and mining dilution assessment from the 1990s until now. Numerous considerations are given to select the simulation parameters, and, also, four case studies are shown where simulations outperform traditional methods such as DGM, DK and others. The authors highlight improvements in simulations associated with speed, computer capacity, memory, storage, and development of algorithms. In addition, they indicate that CSs provide a valuable tool for not only classification and dilution assessment, but also stochastic mining optimization and operational efficiency improvement.

Some drawbacks significantly affect CSs. This approach does not ensure local accuracy, and the resulting error variance is larger than the kriging error variance. CSs often rely on strong hypotheses (e.g., the multiGaussianity and stationarity) and cannot be suitable when the regionalized variable exhibits correlation of the extreme values or patterns of spatial connec-

tivity of high or low values. Finally, CSs require parameters to be specified for their correct application, where some inaccurate responses may be obtained if the covariance or variogram model is misspecified (Englund & Heravi, 1993). These pitfalls as well as the complexity associated with geostatistical simulations, limit their usability in the mining industry. Despite this, much research has been conducted to validate their applicability, emphasizing the importance of incorporating uncertainty into the complete mining project evaluation. It is then suggested to account for uncertainty assessment in mineral resources reports.

2.4.3 Multivariate approaches for mineral resources assessment

Primary variables are commonly observed alongside by-products and contaminants in mining operations since deposits can host several elements of interest. These elements are usually spatially correlated, and thus, the application of multivariate approaches rather than univariate methods is highly recommended. The first attempt to reproduce the relationship between the variables of interest is the use of a linear combination of these variables. This defines an equivalent grade that can be employed with traditional geostatistical methods (Myers, 1983; Davis & Jalkanen, 1988). Nonetheless, the meaning of the equivalent grade is generally not practical. Therefore, multivariate approaches are required so as to obtain a prediction of each underlying variable, not only of a combination of these variables.

Cokriging arises as an alternative to the joint prediction by utilizing the correlation between data and their spatial continuity (Journel & Huijbregts, 1978; Myers, 1982; Wackernagel, 2003; Chilès & Delfiner, 2012). In order to incorporate the spatial dependency between variables, experimental direct and cross-covariance functions are calculated and then usually fitted through a linear coregionalization model (LCM). The LCM relies on a set of basic nested structures, where the sill matrix of each nested structure has to be symmetric positive semi-definite for mathematical consistency (Chilès & Delfiner, 2012). Cokriging minimizes the prediction error variance and provides unbiased predictions; however, it suffers from the same limitations as kriging, in particular, the smoothing effect.

In terms of non-linear methods, several applications for multi-element deposits consider the use of multivariate LUC. Refer to Deraismes et al. (2008) for further details on porphyry copper deposits and Deraisme & Assibey-Bonsu (2012) and Assibey-Bonsu et al. (2014) on porphyry copper-gold deposits. Assibey-Bonsu et al. (2014) demonstrate that multivariate LUC provides consistent results for the predicted resources through reconciliation employing production data. Geostatistical simulations can also be extended to a multivariate setting, incorporating the spatial correlation between the variables by using a LCM in the multiGaussian model. Since fitting the LCM can be challenging, an alternative approach for parameters

inference of LCM is the use of Bayesian inference (Kitanidis, 1986). The estimates of the parameters are obtained from the posterior distribution, which links the prior distribution of the parameters and the likelihood referring to the conditional probability of the observations given the values of the parameters. This method suffers from issues in the definition of the prior distribution, which is typically selected based on expertise and assuming a multiGaussian distribution for the likelihood. Moreover, the approach is limited by the number of data. Other approaches to avoid the LCM fitting are based on the spatial decorrelation of the variables, for example, principal component analysis (Goovaerts, 1993a), minimum-maximum autocorrelation factorization (Desbarats & Dimitrakopoulos, 2000), and stepwise conditional transformation (Leuangthong & Deutsch, 2003). Their major limitation is the spatial decorrelation, which is approximate. An alternative, in the LCM setting, is coregionalization analysis (Wackernagel, 2003), which provides factors with no spatial cross-correlation, at the cost of a larger number of factors. Projection pursuit multivariate transform (PPMT) (Barnett et al., 2014) can overcome this problem by transforming multiple variables into uncorrelated multivariate Gaussian distribution. Traditional univariate geostatistical simulation can then be employed, and a posterior back transformation is used to restore the correlation of the original variables. However, PPMT is not always able to reproduce the original multivariate distribution due to univariate realizations far from Gaussian distribution.

Several studies confirm the validity of using multivariate approaches instead of the univariate methods for the mineral resources assessment. For instance, Dhaher & Lee (2013) obtain better predictions for the metal quantity of copper and nickel with cokriging compared to kriging. Through geostatistical simulations, Madani & Ortiz (2017) perform an analysis in a nickel-laterite deposit. The results demonstrate that the joint simulation of iron and magnesia outperforms the univariate simulation in terms of both reproducing the correlation between variables and generating a lower relative error for the validation set. Consequently, it is recommended to evaluate recoverable resources of several variables of interest and account for their correlations, which is usually required in the mining operation. As an example, in iron deposits, where industrial steel is the expected product, the ore concentrate is restricted by the content of phosphorus and sulphur, e.g., 0.05% P and 0.1% S (Svoboda, 2004). In copper-silver deposits, Montoya et al. (2012) consider five variables in the mineral resource evaluation: copper and its by-products, silver and molybdenum, as well as arsenic and antimony, contaminants that determine the quality of the predicted grade of the primary variable affecting its mineral processing.

De-Vitry et al. (2007) provide a guideline to help in deciding the most appropriate techniques to assess multivariate iron deposits. They indicate that few applications of non-linear techniques can be found in iron deposits evaluation due to numerous relationships between

the variables that have to be reproduced. It is proposed the use of DGM as an effective tool to decide when to move from traditional linear predictors to non-linear geostatistical techniques, including conditional simulations.

Ultimately, the recovery functions representation as selectivity curves (tonnage, metal quantity, mean grade and conventional benefit above a cut-off) can be extended to selectivity surfaces in a bivariate context. For instance, the tonnage can be obtained as a function of the cut-off grades of both variables of interest. So far, this idea has not been thoroughly explored within the mining field. A concept close to the selectivity surface is developed by Silva & Almeida (2017), where the tonnage of copper is illustrated as a function of copper cut-offs for massive and stockwork ores. Hence, there is a significant opportunity to explore the applicability of selectivity surfaces for assessing bivariate recoverable resources.

The aforementioned approaches typically rely on strong assumptions or parameter definitions to be correctly applied. Therefore, it is noteworthy to contemplate analyzing the suitability of data-driven techniques to assess mineral resources and their uncertainty, primarily focused on recoverable resources.

2.5 Data-driven methods for the assessment of recoverable mineral resources

Data science has become an attractive field in geosciences and natural resources engineering, where significant contributions are related to solving challenging problems such as non-linear relationships and complex interactions. In the mining field, the amount of available information from different processes is heterogeneous and large. Then, data-driven methods (e.g., machine learning (ML) techniques) have the potential to significantly make decisions more accurate than experience or prior knowledge from practitioners.

Machine learning techniques are categorized as supervised, unsupervised, and reinforcement learning. Depending on whether the data is labelled, the learning can be considered supervised or unsupervised, respectively, while reinforcement learning trains the model founded on a reward system. In the supervised environment, the main tasks are classification and regression. Their goal is to learn the relationships or patterns of a labeled dataset to establish the underlying relationship between input and output variables and to apply this relationship to new data for which only the input is known. Methods employed to this end may be random forest, multiple linear regression (MLR), decision tree, nearest neighbors, support vector machines (SVM), and artificial neural network (ANN). Further details on ML techniques can be found in Mitchell (1997), Murphy (2012), and Kuhn et al. (2013).

Several ML techniques have been applied to the study of earth sciences, for example, in geo-

logical mapping (Cracknell & Reading, 2014; Harris & Grunsky, 2015; Harvey & Fotopoulos, 2016), mineral exploration using geochemical and petrophysical data (Kirkwood et al., 2016; Caté et al., 2017), classification of categorical geological data (Caté et al., 2018; Ishitsuka et al., 2021), among others.

2.5.1 Mineral resource assessment applications

A comprehensive review of ML applications for the mineral resources assessment can be found in Dumakor-Dupey & Arya (2021). A detailed description of the applications includes the ore deposit type, type of datasets (e.g., field, synthetic, or laboratory-scale data), the ML technique selected, and main results. The authors found 51 published scientific articles associated with ML and mineral resources assessment from 1993 to 2021. ANN is the preferred technique, followed by SVM. The studies cover a wide range of deposits, including bauxite, iron ore, nickel, coal, gold-silver, copper, among others. Most of the works are related to the idea of predicting ore grades at unsampled locations given the relationships between data locations and known grade values, which can be extracted through supervised learning under the assumption of a homogeneous geology. Several results indicate a good performance of ML techniques since the mean absolute errors are smalls and the correlation coefficient between predicted and true values is close to one. Different conclusions are derived when ML techniques are compared with traditional geostatistical methods. For instance, Zhang et al. (2013) show that least-square SVM outperforms IDW, OK, and ANN, being a robust method with a high generalization capability in predicting ore grades in a seafloor hydrothermal sulphide deposit. Conversely, Afeni et al. (2020) indicate that OK surpasses ANN in the prediction of iron grades as OK is able to explain a higher variability, as well as to provide a better generalization capacity and prediction performance.

The prediction of local recoverable resources (recovery functions) has been reviewed only in one work. Jafrasteh et al. (2018) compare Gaussian process (GP), OK, and indicator kriging (IK) for assessing the tonnage and grade at different cut-off grades in a copper deposit. They conclude that OK and GP perform similarly, while IK shows more tonnage resources and low grades at the same cut-offs compared with the other methods. The main difference between OK and GP is revealed at low cut-off grades, where GP significantly exhibits less tonnage than OK. Nevertheless, this study is non-conclusive as there are no real recoveries to contrast with the results.

In a global resource quantification setting, Nezamolhosseini et al. (2017) perform the tonnage prediction using ANN and OK in an iron deposit. The results are similar for both methods, but they slightly differ in the shallowest of the deposit. Based on the idea of predicting

multi-element ore deposits, Chatterjee et al. (2006) utilize ANN to assess four elements of interest (silica, alumina, calcium oxide and ferrous oxide). As a result, ANN exhibits better performance than OK for all the analyzed variables.

Few studies have been focused on employing ML for the uncertainty quantification of spatial variables. Fouedjio & Klump (2019) compare a traditional geostatistical method (i.e., kriging with external drift) with quantile random forest (QRF) to examine their uncertainty assessment on synthetic and real case studies. The uncertainty accuracy is measured by the accuracy plot, probability interval width plot, and goodness statistic. The authors conclude that one method can perform better than the other depending on the data characteristics. Although QRF can be a valuable technique for assessing regionalized variables, it fails to provide accurate uncertainty quantification when a strong spatial correlation is observed. However, no further research has been conducted to determine recoverable resources while providing a measure of uncertainty on the predicted resources.

Some difficulties experienced during the use of ML techniques for the mineral resource evaluation are related to the input dimensionality and singularities of each ore deposit. Hence, each mineral resource evaluation may require applying a specific ML technique (Kapageridis, 2005).

2.6 Gap of knowledge in recoverable resource assessment

After reviewing traditional approaches in the resource evaluation domain, there are various opportunities to explore alternative geostatistical and ML techniques capable of dealing with current challenges in assessing global or local recoverable mineral resources, accounting for a change of support from point-support samples to voluminous SMUs.

- Constrained kriging is able to provide unbiased and non-smoothed predictions. Despite these significant features, this predictor has not been thoroughly used to assess local recoverable resources, and its applications take a limited type of datasets into account. Therefore, there is still a lack of certainty about the performance and robustness of CK for the characterization of recoverable resources. Since non-smoothness is the desired property in preliminary studies, it is expected that CK may provide appropriate results, avoiding the assumptions and complexity of traditional approaches.
- Machine learning techniques may be suitable to provide resources prediction and uncertainty quantification for variables of interest. Nevertheless, there are no relevant applications within the literature that assess recoverable mineral resources and quantify their uncertainty, and thus, it is not clear whether ML can be properly applied

to this purpose. Circumventing complex parameter definitions, surpassing the limited amount of data gathered at initial project stages, and avoiding the assumptions considered in traditional geostatistical approaches can be strength features of ML techniques.

- Multivariate assessment plays a key role in predicting the recoverable resources of mining projects. Until now, there is no research focused on predicting variables of interest in multi-element ore deposits and providing a measure of their uncertainty using ML techniques. Consequently, there is an opportunity to examine the effectiveness of ML in this matter. Avoiding the complex definition of a unique LCM for several spatially correlated variables through the use of ML may be beneficial for pre-feasibility and feasibility studies.

CHAPTER 3 THESIS ORGANIZATION AND COHERENCE OF THE ARTICLES IN RELATION TO THE RESEARCH GOALS

3.1 Thesis outline

The thesis is carried out in order to contribute to improving the recoverable mineral resources and uncertainty assessment by the application of new practices based on geostatistical and machine learning techniques. Each chapter aims to address a specific objective of the research through the development of scientific articles. The chapters are organized as follows:

Chapter 4 shows the article *Constrained kriging: an alternative to predict global recoverable resources* published in *Natural Resources Research*.

Chapter 5 exhibits the second article *Quantifying mineral resources and their uncertainty using two existing machine learning methods* published in *Mathematical Geosciences*.

Chapter 6 presents the article *Assessment of recoverable resource uncertainty in multivariate deposits through a simple machine learning technique trained using geostatistical simulations* published in *Natural Resources Research*.

Chapter 7 provides complementary results to the findings from Chapters 5 and 6 through additional analyses in order to evaluate the applicability and robustness of the ML approach.

Chapter 8 gives a general discussion of the research project.

Chapter 9 presents the conclusions and further research.

3.2 Coherence of articles

In this research thesis, three different articles are included in order to deal with the main challenges associated with *improving the recoverable mineral resources assessment and their uncertainty quantification*, which is the general research objective. These articles are founded on different approaches described as follows.

Article 1: Constrained kriging: an alternative to predict global recoverable resources

The undesired smoothing effect of kriging predictions may be avoided by using CK, a method seldom used in the mining industry. The article, submitted in April 2019 and accepted in 2019 in *Natural Resources Research*, aims to address the first specific objective: *determine*

the applicability of CK for the quantification of recoverable mineral resources by avoiding the smoothing of ordinary kriging estimates. This work shows the main findings of testing CK for the assessment of global recoverable resources. A comparison between CK and traditional geostatistical approaches, such as OK and UC, is performed employing a synthetic dataset and two case studies: a gold deposit and the Walker Lake dataset. As a result, CK provides better predictions than OK and similar to UC. Moreover, a sensitivity analysis for the variogram model parameters proves the robustness of CK compared to traditional methods, providing an alternative to predict non-smoothed resources at SMU support while allowing for their localization.

Article 2: Quantifying mineral resources and their uncertainty using two existing machine learning methods

Since CK is not able to quantify uncertainty and, also, data-driven methods arise as a promising option to predict recoverable resources and their uncertainty, a second article is submitted in May 2020 and accepted in 2021 in *Mathematical Geosciences*, whose goal is to reach to the second specific objective of this research: *verify the suitability of supervised machine learning techniques for assessing recoverable resources and quantifying their uncertainty*. The basic concept is to avoid the assumptions and variogram model definition required in traditional geostatistical approaches by replacing them with supervised learning of a series of input and output variables. These variables are obtained from conditional simulations whose parameters are defined within an interval of possible values. Two machine learning techniques are compared: multiple linear regression and multi-layer artificial neural network. Similar results are obtained with both methods, and therefore, the first technique is preferred as it is the most straightforward approach and easily allows for the corrections on the confidence intervals used to evaluate the uncertainty. Compared to traditional geostatistical methods (such as OK, CK, UC and IL correction), MLR exhibits better predictions of the recoverable resources, being only outperformed by DGM; however, the latter uses the true variogram model to provide the predictions, which may be an irrealistic assumption in practice. Two case studies demonstrate the validity of the ML approach, highlighting two critical aspects of this proposal: the recoverable resources assessment while providing a measurement of their uncertainty.

Article 3: Assessment of recoverable resource uncertainty in multivariate deposits through a simple machine learning technique trained using geostatistical simulations

Based on the results obtained with the proposed ML approach, a multivariate extension is carried out in the third article submitted in November 2021 and accepted in 2022 in *Natural Resources Research*, which addresses the third specific objective of this research: *apply the ML approach for multivariate ore deposits, providing a method of assessing recoverable resources and their uncertainty in complex scenarios*. This study is crucial as ore deposits typically host multiple elements of interest (e.g., main products, by-products and contaminants). Hence, the prediction of recoverable mineral resources may be markedly improved when considering their dependence relationships. Two challenges can be faced by using a multivariate approach: the prediction of non-additive variables and the prediction of joint recoveries of several elements of interest. The latter allows assessing the recoverable resources of each variable of interest and the resources of a primary variable constrained by the threshold of a secondary variable. The proposed multivariate ML approach is based on conditional simulations where features and targets can be extracted from each of these simulations, and consequently, they are used to perform the bivariate supervised learning. The outcomes of this research are validated by a synthetic case study and tested on a real application on a lateritic nickel deposit, where the ratio between silica and magnesia is a constrained on the recoverability of the nickel resources.

CHAPTER 4 ARTICLE 1: CONSTRAINED KRIGING: AN ALTERNATIVE TO PREDICT GLOBAL RECOVERABLE RESOURCES

Nadia Mery, Denis Marcotte and Raphael Dutaut
Natural Resources Research 29(4), 2275–2289, DOI 10.1007/s11053-019-09601-6
Accepted: November 2019

4.1 Abstract

In most NI-43-101 resource assessment reports the prediction of global *in-situ* resources is performed either by inverse distance weighting (IDW), ordinary kriging (OK) or uniform conditioning (UC). These methods have known drawbacks: OK estimates are over-smoothed and UC necessitates an additional step to localize resources within panels. An alternative, named constrained kriging (CK), enables to circumvent the smoothing issue of OK by imposing the desired theoretical variance to the interpolated variable. CK is not used in NI-43-101 reports, possibly due to a lack of real application examples and little detailed study of its properties. This paper seeks to fill the gap by comparing the prediction performance for global resources of OK, UC, and CK on a synthetic lognormal dataset, and two real datasets, the Walker Lake and a gold deposit. Results indicate that CK, although being slightly less precise than OK, provides better predictions of grade-tonnage curves than OK and predictions comparable to UC, a remarkable achievement considering that UC is a widespread non-linear method specifically designed to predict recovery functions. CK is also shown to provide resource estimates more robust than UC with respect to the variogram model specification. Hence, CK appears as a valuable tool allowing simultaneously to localize resources and easily account for change of support in resources estimation.

Keywords: Ordinary kriging - constrained kriging - uniform conditioning - kriging neighborhood analysis - recovery functions

4.2 Introduction

A suitable quantification of mineral resources is a significant stage within a mining project since it defines the value of the project and has direct implications on downstream stages (Morley et al., 1999; Goldsmith, 2002). The assessment is usually carried out employing ordinary kriging (OK) (Matheron, 1963). However, OK is known to have a smoothing effect, the variability of estimated block grades being less than the variability of the true block

grades. Applying a cut-off to the estimated grade can result in serious biased ore grade-tonnage curves. As the smoothing effect increases when less information is available, the bias is particularly severe for interim prediction of recoverable resources where data is less abundant than for final estimates. For interim resource estimates, NI-43-101 reports indicate that often small kriging neighborhood are rather used to reduce the smoothing effect. This is accomplished at the expense of a loss in precision and increased discontinuities in kriged maps. Finding a suitable neighborhood size is often performed using the Kriging Neighborhood Analysis (KNA) strategy (Rivoirard, 1987; Vann et al., 2003), which seeks a tradeoff between conflicting objectives of good precision and reduced smoothing. However, it is difficult on KNA to account for the fact that sampling density is rarely homogeneous over the whole deposit or even within sub-domains so that the best neighborhood can be unsatisfactory in the different parts of the deposit or domain.

Numerous alternatives exist to circumvent the pitfalls of smoothed values. For instance, nonlinear methods, such as indicator kriging, disjunctive kriging, multi-Gaussian kriging and conditional simulation have been developed (Journel, 1974; Verly, 1983; Rivoirard, 1994; Goovaerts, 1997; Chilès & Delfiner, 2012). These methods rely on stronger distributional hypothesis than OK and they try to estimate conditional distributions rather than to provide a single prediction. Indicator kriging requires, in addition, a change of support model to shift from point conditional distribution to block distribution. A simpler approach is uniform conditioning (UC) (Rivoirard, 1994), a method widely spread in the mining industry, as it is able to compute the grade-tonnage curves for the block support within each panel. However, UC does not localize the recoverable resources spatially at a finer scale than the panel. Abzalov (2006) proposed an extension to UC known as localized uniform conditioning (LUC), which produce block grades within the panel such as to recover the distributions predicted by UC for each panel. The method is based on ranking of block kriged estimates. The caveats are that it introduces discontinuities of the grades at panel boundaries and two blocks having the same OK estimate but taken in different panels do receive different LUC estimates, which appears a bit arbitrary.

A promising variant of kriging is constrained kriging (CK) (Cressie, 1993), which, by construction, produces unbiased and non-smoothed grade predictions at block support. CK was developed to ensure that the predicted values have, theoretically, the same variance as the target values. Basic CK equations may be found in Cressie (1993), while a thorough derivation of CK equations can be found in section 4.3. This predictor has been mostly studied within the environmental field at block support, where several comparisons between OK and CK have been carried out for different applications (Hosseini et al., 1994; Aldworth & Cressie, 1999). CK was further generalized to covariance matching constrained kriging (CM) (Cressie

& Johannesson, 2001; Aldworth & Cressie, 2003; Hofer & Papritz, 2011; Hofer et al., 2013), which additionally imposes constraints on covariance of predicted values. Hofer & Papritz (2010) performed a comparison between CK and CM, concluding that CM does not exhibit a significant benefit over CK. Furthermore, the additional constraints in CM increase its theoretical estimation variance. The authors firmly recommend the use of CK because of its simplicity and better robustness compared to CM.

We emphasize that CK was originally designed to be applied on block-support distributions (Cressie, 1993). When it is incorrectly used on point support, large negative and positive weights can be obtained, leading numerous negative estimates and poor precision of the estimates (Hosseini et al., 1994; Hofer & Papritz, 2010; Hofer et al., 2013).

Although CM was used for coal tonnage assessment (Tercan, 2004) and estimation of coal quality variables (Ertunç et al., 2013), no previous studies using CK for resources predictions have been performed in the mining field. This article assesses for the first time the capacity of CK to improve interim resource predictions compared to OK and UC. Different neighborhood sizes and case studies are considered herein and the sensitivity of results to the neighborhood choice and variogram model is appraised. Moreover, we introduce a new measure in KNA, the oversmoothing ratio (OSR), which helps to select the best neighborhood for resource prediction by OK.

The paper is structured as follows. Section 4.3 exhibits a complete derivation of CK equations and the main criteria used in KNA, including the new OSR criterion. Section 4.4.1 describes the KNA results obtained with OK and CK for a synthetic case study. Section 4.4.2 compares the performances of OK, CK, and UC on two case studies, one using the Walker Lake data and the other data from a gold deposit. Finally, section 4.5 discusses the main findings and conclusions of this research and its implications for the important problem of resource estimation as currently practiced.

4.3 Methods

4.3.1 Constrained kriging (CK) equations

A linear predictor has the form $Z_v^* = \boldsymbol{\lambda}'\mathbf{Z}$, where $\boldsymbol{\lambda}$ is the vector of weights and $\mathbf{Z}$ is the vector of observed values. The variance of the predictor is given as: $\boldsymbol{\lambda}'\mathbf{K}\boldsymbol{\lambda}$, where $\mathbf{K}$ is the covariance matrix between all known data points (usual simple kriging matrix). Let the prediction error variance be minimized under the constraints $\mathbf{1}'\boldsymbol{\lambda} = 1$ and $\boldsymbol{\lambda}'\mathbf{K}\boldsymbol{\lambda} = \sigma_v^2$, where $\mathbf{1}$ is a column vector of ones. Using the Lagrange method and posing derivatives equal to zero, one obtains

the following equations:

$$\mathbf{K}\boldsymbol{\lambda} + \mu_1\mathbf{1} + \mu_2\mathbf{K}\boldsymbol{\lambda} = \mathbf{k} \tag{4.1}$$

$$\mathbf{1}'\boldsymbol{\lambda} = 1 \tag{4.2}$$

$$\boldsymbol{\lambda}'\mathbf{K}\boldsymbol{\lambda} = \sigma_v^2 \tag{4.3}$$

where $\mathbf{k}$ is the simple kriging right member, σ_v^2 is the block variance and μ_1 and μ_2 are the Lagrange multipliers associated to constraints.

Upon a few simple manipulations and substitutions (see Appendix for details), the solution to the above system of equations is the following:

$$m_2 = 1 + \mu_2 = \left[\frac{\mathbf{k}'\boldsymbol{\lambda}_s - b^2/s}{\sigma_v^2 - 1/s}\right]^{1/2} \tag{4.4}$$

with $b = \mathbf{1}'\mathbf{K}^{-1}\mathbf{k} = \mathbf{1}'\boldsymbol{\lambda}_\mathbf{s}$, $s = \mathbf{1}'\mathbf{K}^{-1}\mathbf{1}$ and $\boldsymbol{\lambda}_s$ is the vector of simple kriging weights, i.e. $\boldsymbol{\lambda}_s = \mathbf{K}^{-1}\mathbf{k}$.

$$\mu_1 = \frac{b - m_2}{s} \tag{4.5}$$

$$\boldsymbol{\lambda} = \frac{1}{m_2}\mathbf{K}^{-1}\left(\mathbf{k} - \mu_1\mathbf{1}\right) \tag{4.6}$$

Eqs. 4.4 to 4.6 are identical, up to a change of notation, to expressions 3.11 to 3.13 of Cressie (1993). Recall that Eq. 4.4 involves terms that depend only on the covariance model. Once $m_2 = 1 + \mu_2$ is computed, it is straightforward to compute μ_1 and $\boldsymbol{\lambda}$ using Eqs. 4.5 and 4.6. Note that it can occur that CK does not have a real solution in Eq. 4.4, especially when the selected neighborhood is small in fields with relatively strong spatial correlation. In this case, OK can be used as a substitute predictor. A better option to simply increase the number of neighbors for these points.

Another instance where CK cannot be evaluated is when $\mathbf{k} = \mathbf{0}$. In this case, the simple kriging weights are all 0s, $b = 0, m_2 = 0$ so μ_1 in Eq. 4.5 is 0 and $\boldsymbol{\lambda}$ in Eq. 4.6 is indeterminate. Including a long range component with very small variance in the variogram model solves this problem.

CK prediction variance

Using the classical prediction variance formula the CK estimation error variance is:

$$\begin{aligned}\sigma_c^2 = Var(Z_v - Z_c^*) &= Var(Z_v) + Var(Z_c^*) - 2Cov(Z_v, Z_c^*) \\ &= 2(Var(Z_v) - \boldsymbol{\lambda}'\mathbf{k})\end{aligned} \tag{4.7}$$

where Z_c^* is the CK predictor. The simple kriging variance is $\sigma_k^2 = Var(Z_v) - \boldsymbol{\lambda}_s'\mathbf{k}$. It is known that the prediction variance of a conditional realization used as a predictor is $Var(Z_v - Z_v^{sc}) = 2\sigma_k^2 = 2(Var(Z_v) - \boldsymbol{\lambda}_s'\mathbf{k})$, which has the same form as σ_c^2. However, because $\boldsymbol{\lambda}$ minimizes the prediction variance and conditional simulation does not, one is ensured that $\sigma_k^2 \leq \sigma_c^2 \leq 2\sigma_k^2$.

4.3.2 Computational aspects

Computation of CK has similar complexity to OK (i.e., $O(n^3)$, n the number of neighbors) as the main step in Eq. 4.4 requires solving the simple kriging system. The notable difference with respect to OK is the computation of $s = \mathbf{1}'\mathbf{K}^{-1}\mathbf{1}$, which requires the explicit computation of the inverse of $\mathbf{K}$ to sum all its elements. For OK, the inverse does not need to be computed explicitly, and therefore, more efficient factorization methods may be used (Chilès & Delfiner, 2012, p. 170).

4.3.3 Kriging neighborhood analysis (KNA)

Defining a proper search neighborhood is crucial for the prediction of regionalized variables because it can improve precision and reduce the risk of introducing conditional bias within the predictions. A well-established method in the literature is the kriging neighborhood analysis (KNA), which considers that the spatial correlation model (variogram or covariance) is valid and the regression is linear (Vann et al., 2003). Five criteria were found in the literature: slope of regression (SR), over-smoothing ratio (OSR), kriging efficiency (KE), weight of the mean (WOM), and proportion of negative weights (NEG). This article focuses on the analysis of three determining criteria: SR, KE, and OSR. WOM and NEG are not considered herein since the former is highly correlated to KE, and the latter is rather unstable and more difficult to interpret.

The slope of regression (SR) linearly relates the true value with the predicted value through $\mathbb{E}[Z_v|Z_v^*] = a + bZ_v^*$, where b is the SR and Z_v^* is the predicted value for the volume v (Rivoirard, 1987). The slope is given by:

$$SR \equiv b = 1 + \frac{\mu}{Var(Z_v^*)} = 1 + \frac{\mu}{\sigma_v^2 - \sigma_{ok}^2 - 2\mu} \tag{4.8}$$

where μ is the Lagrange multiplier, σ_v^2 is the block variance and σ_{ok}^2 is the ordinary kriging variance and $(\sigma_v^2 - \sigma_{ok}^2 - 2\mu) = Var(Z_v^*)$. A slope $b = 1$ implies $a = 0$, therefore, no conditional bias occurs. BiGaussian distribution of Z_v and Z_v^* ensures that the conditional expectation is linearly related to the predictor. Most often μ is negative, thus, $b < 1$, which implies ore

grade overestimation at high cut-off.

Krige (1997) proposed the kriging efficiency (KE) as an indicator of the effectiveness of the block predictions. KE is calculated as:

$$KE = \frac{\sigma_v^2 - \sigma_{ok}^2}{\sigma_v^2} = \frac{Var(Z_v^*) + 2\mu}{\sigma_v^2} \tag{4.9}$$

High KE (i.e. close to 100 %) values correspond to small kriging variance (hence, small μ) and variance of the predictor close to the block variance, so the smoothing is limited.

Camus & Desharnais (2015) proposed to compute experimentally the level of smoothing from the estimates by comparing the theoretical block variance with the variance of the block estimates, which is the statistic known as over-smoothing ratio (OSR). An analogous theoretical definition that we introduce is:

$$OSR = \frac{\sigma_v^2 - (\sigma_v^2 - \sigma_{ok}^2 - 2\mu)}{\sigma_v^2} = \frac{\sigma_{ok}^2 + 2\mu}{\sigma_v^2} \tag{4.10}$$

A zero OSR value indicates absence of smoothing. With ordinary kriging, OSR is usually positive, but it can be negative for very small neighborhoods. When using a restricted neighborhood, the Lagrange multiplier can take non-negligible negative values reducing the OSR and providing a partial theoretical justification for the common practice of using restricted neighborhood (Rossi & Parker, 1994).

Note that the above definitions enable to compute one different theoretical value per predicted block for SR, KE, and OSR. We assume that their average over different blocks is meaningful and can be used as a comparison to the unique experimental equivalent.

4.4 Results

Three case studies are considered. The first dataset is obtained by simulation and is used to compare KNA results of OK and CK. Two real datasets, Walker lake data and data from a real gold deposit, are used to compare performances of OK, CK, and UC for both precision of estimates and quality of ore grade-tonnage curves.

4.4.1 Synthetic data

This section aims to perform the KNA for OK and CK using a marginal lognormal distribution. Samples are generated along vertical boreholes. In each borehole, the two closest

samples to the estimated block are retained. The prediction performance of OK and CK is compared with root mean square prediction error (RMSPE), correlation coefficient (R), and recovery functions obtained (ore grade, tonnage and conventional profit curves).

Figure 4.1a shows the marginal lognormal density function considered in this analysis. The Gaussian dataset is simulated using the Cholesky method, with an isotropic spherical covariance structure (range 20 m), and a nugget effect representing 30 % of the sill. Ten thousands blocks of size 5 m x 5 m x 5 m were individually simulated in the Gaussian domain along with five vertical boreholes per quadrant randomly located around and within the estimated block considering a rectangular window of size 40 m x 40 m centered on the block. Different neighborhood configurations were considered: 3 boreholes in total (6 samples), 1 borehole per quadrant (8 samples), 2 boreholes per quadrant (16 samples) and 3 boreholes per quadrant (24 samples). The large number of available boreholes (5 boreholes per quadrant of the rectangular window) would typically categorize resource estimates as measured in NI-43-101 reports.

Variogram analysis

After back-transformation, sets of boreholes and block grades compatible with the point lognormal marginal distribution are obtained. The grade variogram is also computed by back-transformation of the variogram used in Gaussian space. First, numerous pairs of points (n=100,000) separated by h m are simulated in Gaussian space through the Cholesky method. Second, the half mean square difference of the back-transformed pairs is computed. This is repeated for a series of different lag distance h m. The resulting “experimental" variogram is then automatically fitted using a nested model composed of a nugget, an exponential, and a spherical structure. The “experimental" and modeled variograms are illustrated in Fig. 4.1b.

KNA results

Figure 4.2 shows the SR, KE, and OSR statistics as a function of the number of boreholes used in OK and CK. Average theoretical values (solid lines) and experimental values (dashed lines) for SR and OSR are shown. The theoretical expressions for SR, KE and OSR match adequately the experimental values in this well-controlled experiment.

OK presents higher SR, KE, and OSR than CK in all cases. OK is almost conditionally unbiased (SR close to 90 %) when the sampling density is large enough (i.e., 3 boreholes per quadrant in the search area $\equiv$ 12 boreholes and 24 samples total). On the contrary, CK remains conditionally biased (SR close to 70 %) in all cases.

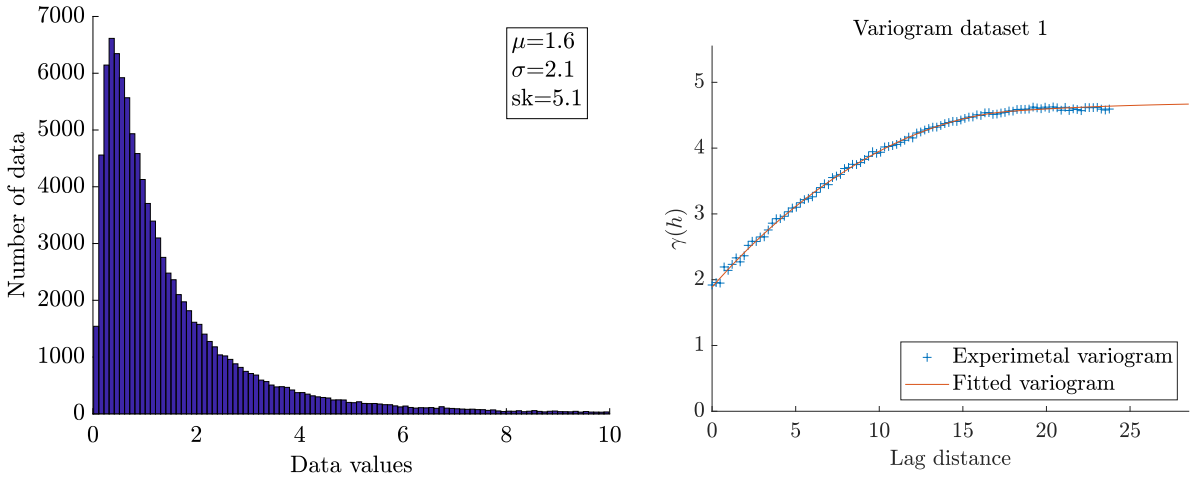

(a) Lognormal distribution

(b) Variogram

Figure 4.1 Histogram (a) and variogram (b) of synthetic dataset. Experimental variogram (blue crosses) and theoretical model (solid line): $\gamma(h) = 1.89\ nug + 1.36\ exp(h, a = 8.05) + 1.46\ sph(h, a = 17.88)$.

As expected, for a fixed number of boreholes, the KE is systematically larger for OK compared to CK. A larger sampling density is therefore required in CK to recover KE comparable to OK.

As imposed by construction, CK has no smoothing effect in none of the cases. In contrast, OK exhibits significant smoothing effect even when only one borehole per quadrant is considered. Hence, the common practice of using small neighborhoods for OK reduces SR and KE, and does not necessarily permit to reach the goal of completely removing the smoothing effect. In contrast, CK does not show smoothing for all choices of neighborhoods.

Table 4.1 compares the performance of OK and CK regarding the root mean square prediction error (RMSPE) and correlation coefficient (R) for different neighborhood sizes. As expected, MSPE is smaller for OK than for CK and both RMSPEs decrease with an increase of neighborhood size (differences for the same neighborhood between 2 % to 10 %). The correlation R shows little differences between OK and CK for all neighborhoods. OK with a small neighborhood (3 boreholes total) has similar MSPE and R to CK with a larger neighborhood (3 boreholes per quadrant). In that case, both OK and CK are not smoothed with, respectively, OSR of -5 % and 0 %.

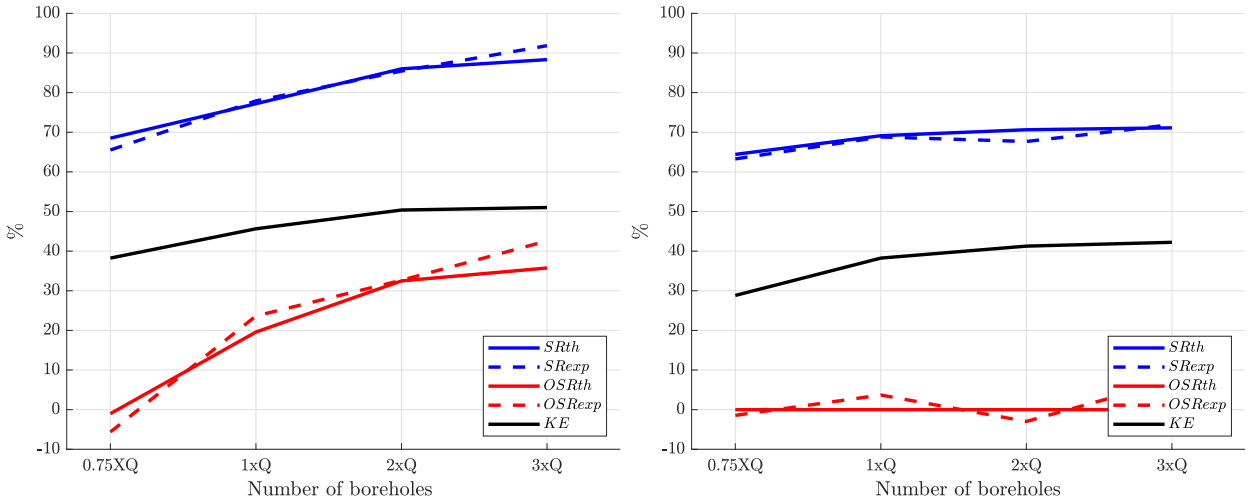

(a) OK (b) CK

Figure 4.2 KNA results for SR (blue), KE (black) and OSR (red) as a function of number of boreholes per quadrant, synthetic dataset. Theoretical values (solid lines) and experimental values (dashed lines).

Table 4.1 RMSPE and R results using OK and CK and different neighborhood sizes.

Number of neighbors	**MSPE**		**R**	
	OK	**CK**	**OK**	**CK**
6 (1 borehole in 3 quadrants)	1.12	1.14	0.67	0.67
8 (1 borehole per quadrant)	1.03	1.08	0.68	0.68
16 (2 boreholes per quadrant)	0.97	1.07	0.70	0.69
24 (3 boreholes per quadrant)	1.02	1.09	0.70	0.69

Recovery functions

Using the synthetic dataset, Figure 4.3 displays the recovery functions of tonnage, ore grade, and conventional profit obtained with OK and CK considering two neighborhood configurations: one with three boreholes in total (i.e., 6 samples; best results with OK) and the other with three boreholes per quadrant (i.e., 24 samples; best results for CK).

Based on Figure 4.3, CK satisfactorily reproduces the recovery functions at all cut-offs in both neighborhood configurations. In contrast, OK does not match the real curves when three boreholes per quadrant are used. In that case, the tonnage is overestimated at low cut-offs and underestimated at high cut-offs, whereas ore grades and conventional profits are underestimated at all cut-offs as a result of the smoothness of OK predictions. Hence, CK recovery curves appear quite robust to the exact choice of the neighborhood contrary to OK which appears to be more sensitive to this choice. In a sense, this justifies the practice of KNA for OK to select the “right" neighborhood for interim resource estimation if such a thing exists. As already discussed, this requires implicitly a strong homogeneity in sampling density. CK has the definite advantage of being able to adapt automatically to the sampling density available locally and still provide un-smoothed estimates.

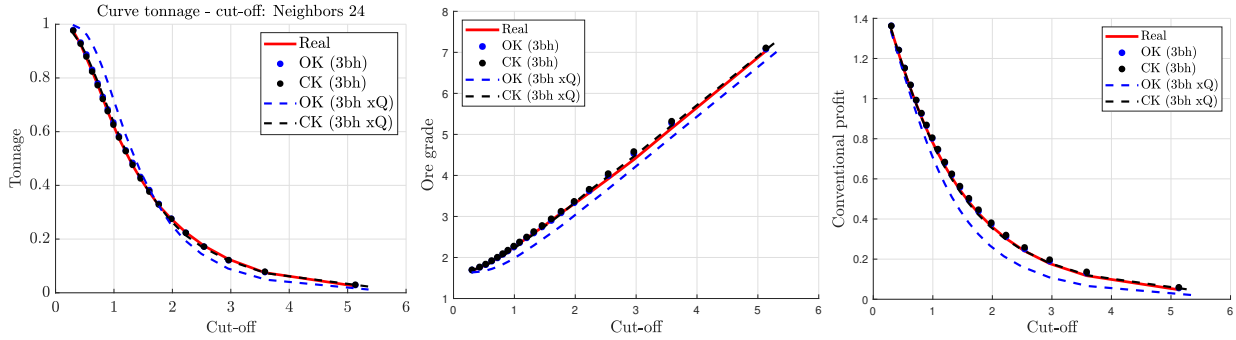

(a) Tonnage curve (b) Ore grade curve (c) Conventional profit curve

Figure 4.3 OK and CK recovery functions using one borehole in three quadrants (dots) and three boreholes per quadrant (dashed lines). Real recoveries with synthetic dataset (solid red line).

4.4.2 Real datasets

This section aims to compare the CK, OK and UC prediction performance and reproduction of recovery functions on two real datasets, the Walker Lake data and grade data from a gold mine (unidentified for confidentiality reasons).

Walker Lake

Walker Lake dataset (Isaaks & Srivastava, 1989) is a well-known public domain database constructed from the topography of the Walker Lake area in Nevada, US. The exhaustive dataset (considered as the reality) is preferentially sampled in the high-grade area to mimic real sampling patterns found in mining. Only the variable V of the Walker Lake dataset is analyzed.

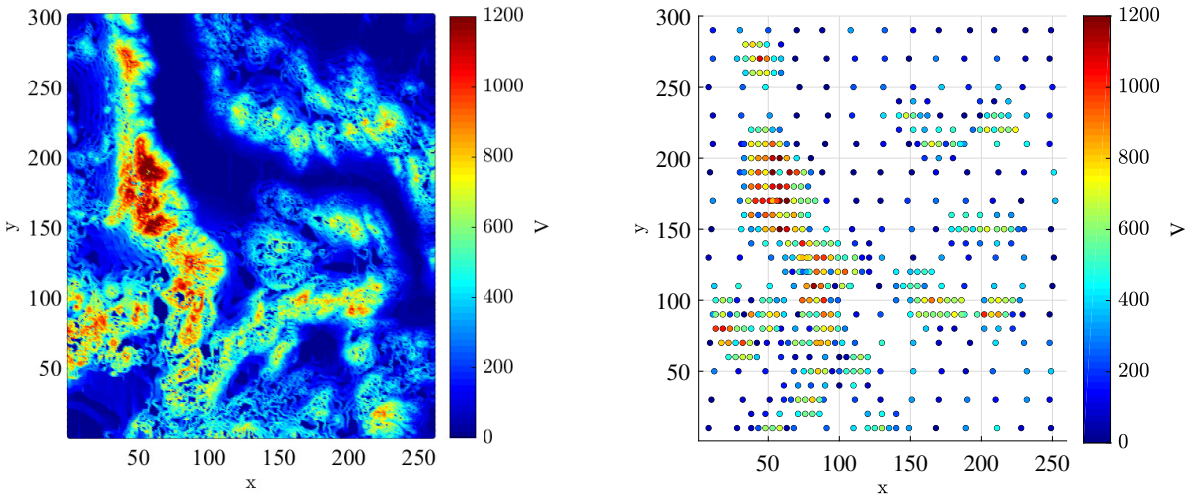

(a) Exhaustive dataset (b) Sample dataset

Figure 4.4 Location maps of variable V, Walker Lake. The exhaustive dataset (a) and the sample dataset (b).

The declustered experimental variogram is computed using the sample dataset. The fitted variogram model is: $\gamma(h) = 90,000\ exp(-h/14)$ where the range 14 is expressed in number of cells. OK and CK predictions are computed for a block model of 5×5 cells, using one neighbor per quadrant for OK and two neighbors per quadrant for CK as these neighborhoods were found to provide best results for each method. For UC, the prediction with OK is firstly performed at panel support (here 65 cells $\times$ 75 cells) with the 50 closest neighbors. A declustered histogram is used to define the required Gaussian transformation for UC.

Table 4.2 compares the performance of the three methods with the real values obtained from the exhaustive dataset. Note that UC does not localize results at the 5×5 scale, hence, it is not possible to compute RMSPE and R at this scale. The mean grade of OK is closer to the real value, but the OK variance of the estimated values (σ^2) indicates the presence of a smoothing effect even with the small neighborhood considered (one neighbor per quadrant). CK suitably describes the real variability of the studied variable as the real variance and CV

are well reproduced. Finally, the RMSPE is smaller for OK than for CK and R coefficients are similar.

Table 4.2 Comparison of statistics obtained with UC, OK, and CK methods for blocks 5×5, Walker Lake.

	μ	σ^2	CV	RMSPE	R
Real	277.98	52,304	0.82		
OK	277.81	44,089	0.76	112.57	0.87
CK	274.97	52,918	0.84	122.87	0.86
UC	280.07				

The experimental variogram of real block values is shown in Figure 4.5 along with the experimental variograms of OK and CK estimates. Note that even though both OK and CK estimates are non-stationary by construction (for example, their variances are location-dependent), the experimental variograms can be used as a descriptive measure of similarity between the fields. Hence, CK variogram appears to be more similar to the real block grade variogram than OK variogram.

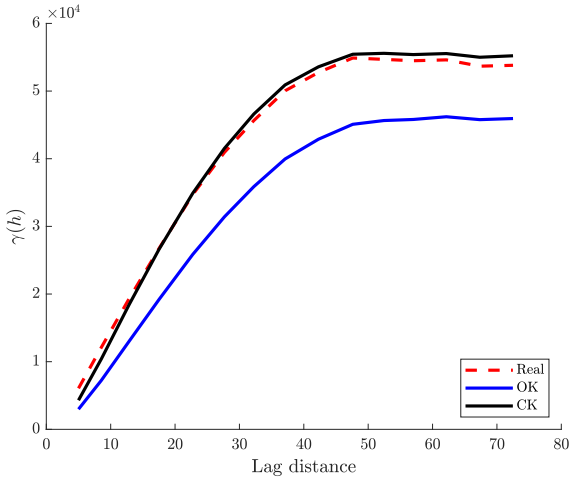

Figure 4.5 Experimental block variograms of OK (blue), CK (black) and real block values (red dashed). Walker Lake dataset.

Figure 4.6 shows the ore grade-tonnage curves for OK, CK and UC. Firstly CK properly fits the real recovery functions for the ore grade and tonnage. Secondly UC shows a good reproduction of the real tonnage, while the reproduction of the ore grade is not as good in this test case. On the other hand, OK generates an overestimation of tonnage at low cut-offs and an underestimation of tonnage at high cut-offs, a typical direct consequence of the smoothness of OK estimates. Ore grades are however well reproduced by OK in this test, especially at high cut-offs.

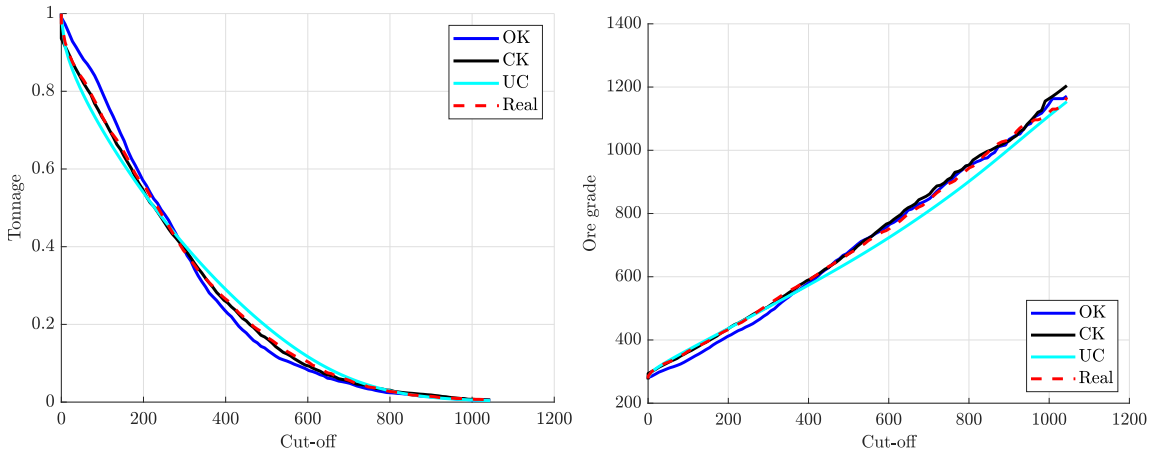

(a) Tonnage curve (b) Ore grade curve

Figure 4.6 Recovery functions for OK (blue), CK (black), UC (cyan) and real values (red dashed). Walker Lake dataset.

Swath plots of real values, as well as OK and CK estimates, are drawn along the two main directions: East-West (EW) and North-South (NS). Figure 4.7 indicates that OK and CK present similar swath plots even though CK estimates have slightly more variations. Both methods show larger discrepancies in the same locations when compared with the real field.

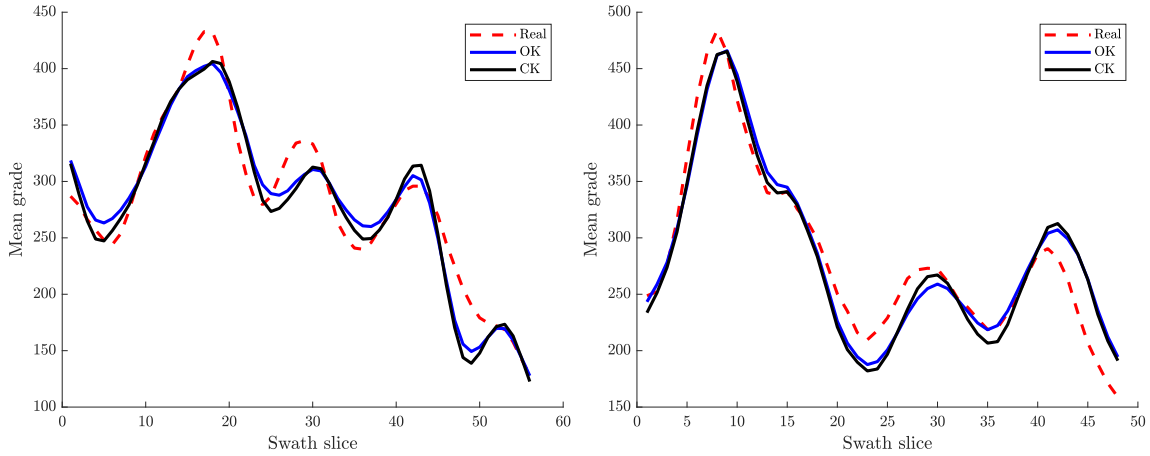

(a) East-west direction (b) North-south direction

Figure 4.7 Swath plots along east-west (a) and north-south (b) directions. Walker Lake dataset.

Sensitivity to variogram model

It can be difficult to define a variogram model unambiguously. The robustness of recovery functions obtained for OK, CK and UC is examined by repeating estimations with a significantly different model. To this end, the variogram model was modified to include a nugget effect of 30 % of the total sill (compared to 0 % in previous estimates), while keeping the range, the sill, and type of model.

Figure 4.8 shows the ore grade-tonnage curves for OK, CK and UC. OK and CK ore grade functions are slightly modified by the change in the variogram model. This is corroborated by the high correlation of new predicted values with former ones (0.994 and 0.989 for OK and CK respectively). However, UC grade curve appears farther from the real curve (compare Figs 4.8 to 4.6). The average relative differences between ore grade predictions with the original and modified variogram models are 0.6 %, 2.1 %, and 4.2 % for OK, CK and UC respectively. For tonnage, while OK seems little affected, both CK and UC present higher tonnages at low cut-offs with the modified variogram model. The average differences between the predicted tonnage using the original and the modified variogram models are 2.7 %, 6.6 %, and 15.1 % for OK, CK and UC respectively. This experiment shows that OK is most robust method followed by CK and then UC. However, even with the modified model, CK still globally performs better than OK for the tonnage and ore grade curves.

We repeated the experience this time modifying the original model by increasing in 50 % the variogram range. Differences in ore grade and tonnage curves were almost imperceptible for the three methods when compared to Fig. 4.6, so they are not further reported.

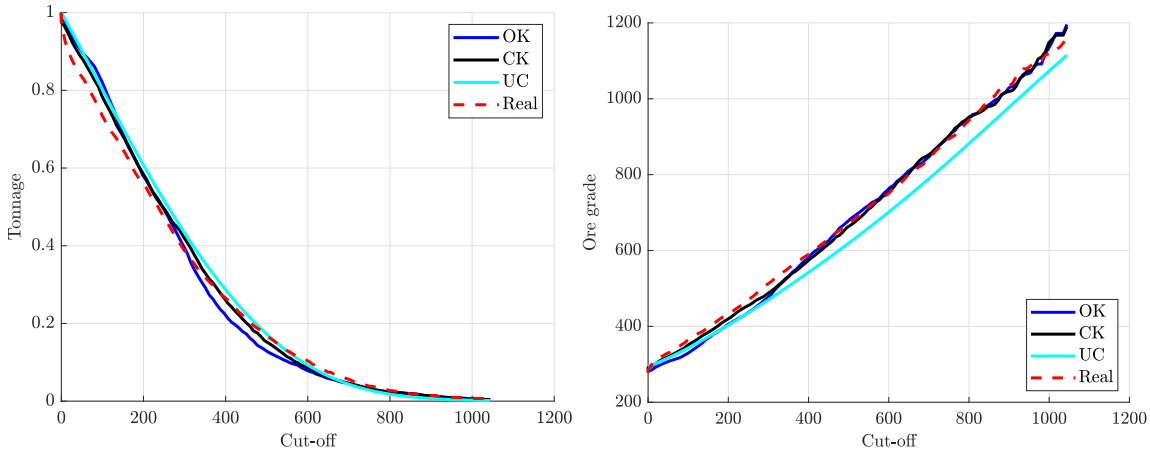

(a) Tonnage curve (b) Ore grade curve

Figure 4.8 Recovery functions for OK (blue), CK (black), UC (cyan) and real values (red dashed). Walker Lake dataset.

Gold deposit

The case study is a real gold deposit where fine-grained felsic volcanic units compose the main part of the stratigraphy. Most of the mineralization are gold-bearing quartz and quartz-carbonate shear, and tension veins hosted in the footwall of a reverse fault. The mineralogy in the ore zones includes 2 % to 7 % pyrite and some traces of pyrrhotite. A total of 91,104 diamond drill (DDH) core samples and 82,773 reverse circulations (RC) inclined drilling used for grade control (see Fig. 4.9) are available. The RC data are concentrated in a volume representing roughly 40 % of the volume covered by the DDH.

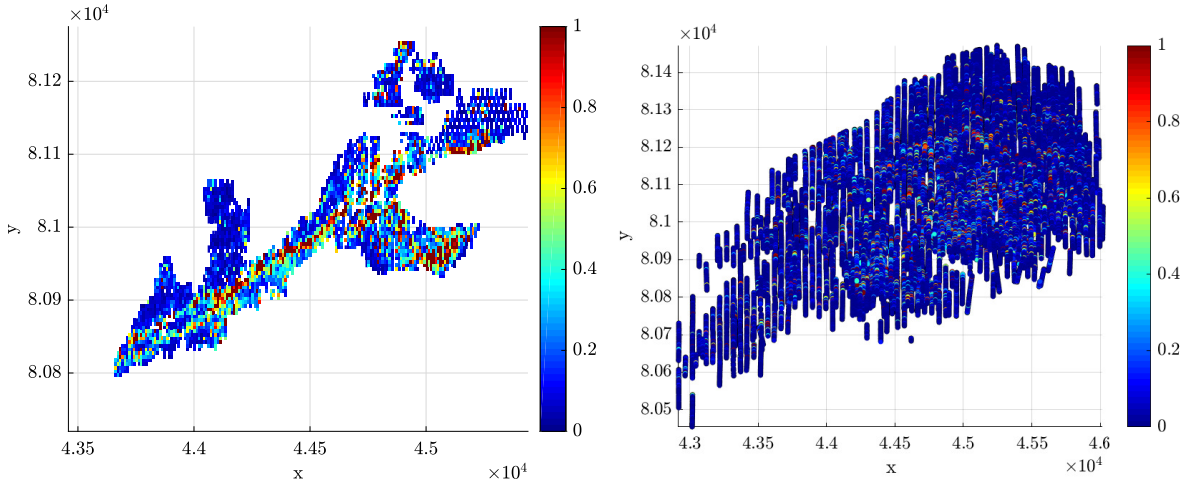

(a) RC (b) DDH

Figure 4.9 Plan views of gold variable. Reverse circulations drilling (a) and diamond drill samples (b) at level 443 m.

Table 4.3 shows the main statistics of uncapped and capped data (at 30 ppm) for DDH and RC. The capped value corresponds to a very high percentile of the distribution of both DDH (99.91 %) and RC (99.96 %) data. The capped mean is slightly smaller than the uncapped one. However, a substantial reduction in variance occurs for both distributions (27.7 % for DDH and 40.0 % for RC). Therefore, the capped value was applied hereafter.

Table 4.3 Declusterized capped (at 30 ppm) and uncapped statistics for DDH and RC

	μ	σ^2	skewness	Percentile at capped value
DDH uncapped	0.25	2.02	22.50	99.91 %
DDH capped	0.24	1.46	15.53	-
RC uncapped	0.39	2.59	30.53	99.96 %
RC capped	0.38	1.56	12.60	-

Given the high-density of RC drilling, it is assumed that one realization obtained by turning bands method over blocks of 5 m x 5 m x 5 m is representative of the block grade. Those DDH samples found within the RC domain were composited to a length of 3 m which was found to ensure DDH grade variance comparable to RC grade variance. A strong difference was nevertheless observed between the declusterized means of DDH and RC grades (the mean of DDH representing only 77 % of the RC mean). The causes of this difference are unknown. DDH grades were corrected by applying a quantile-quantile transformation so that DDH distribution matches the RC distribution. The experimental variogram on RC was fitted by cross-validation. The resulting variogram model is: $\gamma(h) = 1.2nug + 0.35\ sph(h, a = 25m) + 0.05\ sph(h, a = 60m)$ where nug and sph stands respectively for nugget effect and spherical model and a is the finite range. One neighbor per octant (i.e., a total of 8 samples) is used for CK and OK. This neighborhood was found best for both methods after KNA. For UC, the panel size used is 50 m x 50 m x 30 m.

Table 4.4 compares the statistics obtained with OK, CK and UC. UC shows a good reproduction of the global mean grade value. OK has the lower RMSPE value and the higher R but shows a lower variance than the variance of the blocks, contrary to CK which succeeds in reproducing the block variance exactly.

Table 4.4 Comparison of statistics obtained with UC, OK, and CK methods for blocks $5\times5\times5$ m, gold deposit.

	μ	σ^2	CV	RMSPE	R
Real	0.37	0.27	1.40		
OK	0.38	0.20	1.18	0.58	0.28
CK	0.39	0.27	1.35	0.63	0.27
UC	0.37				

To compare the spatial behavior of real values to OK and CK estimates, the experimental variograms of real block grades, CK and OK estimates are depicted in Fig. 4.10. As for Walker Lake data, CK variogram seems more similar to the real block grade variogram than OK variogram.

Figure 4.11 exhibits the ore grade-tonnage curves for OK, CK and UC predictions. UC tonnage curve indicates a suitable reproduction of the real curves. CK and OK slightly overstimate the tonnage at middle cut-off values. UC and CK properly reproduce the ore grade curves, while OK underestimates the ore grade at all cut-off values.

Figure 4.12 depicts a plan view of the predicted gold variable at 443 m level using OK (left) and CK (right). Despite the higher variance of CK estimates compared to OK, both figures

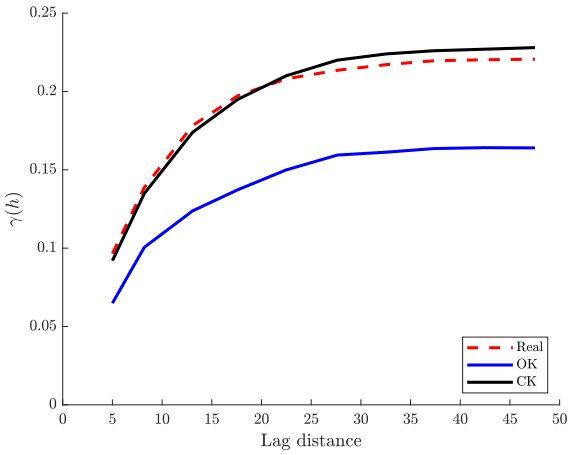

Figure 4.10 Experimental block variograms of OK (blue), CK (black) and real values (red dashed). Gold deposit dataset.

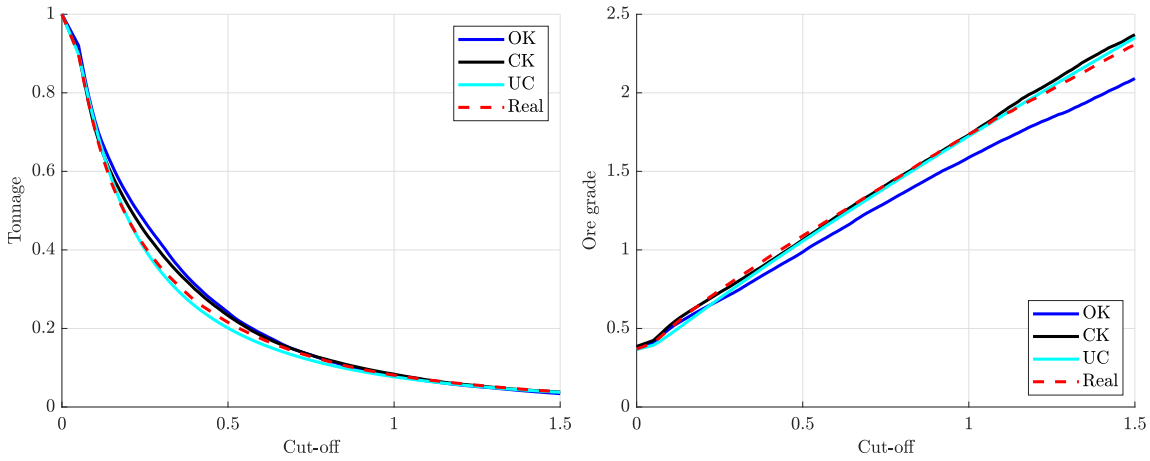

(a) Tonnage curve

(b) Ore grade curve

Figure 4.11 Recovery functions for OK (blue), CK (black), UC (cyan) and real values (red dashed). Gold deposit dataset.

appear quite similar visually.

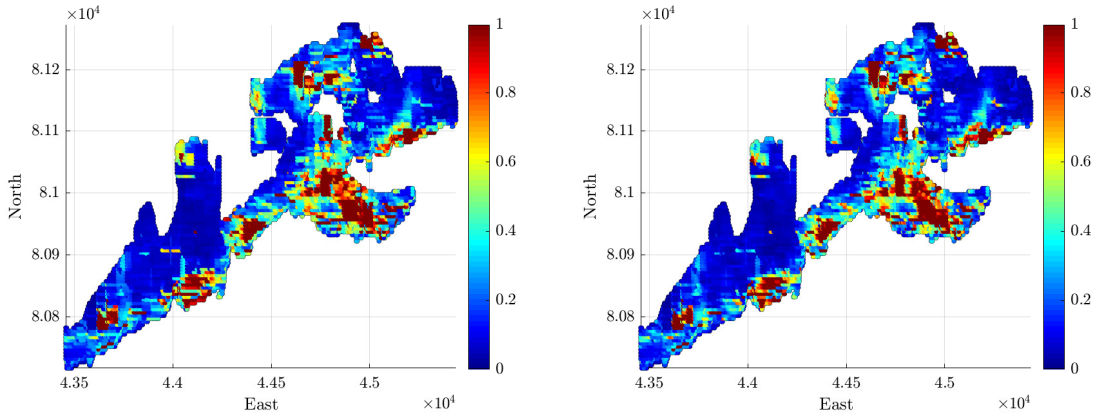

(a) OK (b) CK

Figure 4.12 Plan view (level 443 m) of predicted gold variable using OK (a) and CK (b).

The grade distribution along specific swaths are computed for the there main directions: East-West (EW), North-South (NS) and elevation. Swatch plots are illustrated in Fig. 4.13. As for Walker Lake data, CK and OK swaths are quite similar and they show globally similar discrepancies to the real swath. Certainly, CK cannot be considered as a panacea for those samples whose estimated grades do not represent well the real grades in some parts of the field.

4.5 Discussion

Predicting global resources on block support and simultaneously localizing the resources in a deposit is a challenge when only relatively sparse data are available for the prediction of interim resources. The localization is achievable to some extent with local change of support methods, conditional simulation, and other non-linear kriging approaches (e.g., disjunctive kriging, UC, multiGaussian, and biGaussian kriging). However, these approaches either permit the localization at the scale of large panels or depend on more restrictive multiGaussian hypothesis.

Block kriging is typically used in NI-43-101 resource assessments despite the known bias it introduces in recovery function estimation due to the smoothing effect. It is a common practice to shrink the neighborhood so as to reduce the smoothing effect. The question arises as how to determine a suitable neighborhood to diminish the bias on recovery functions and still precisely localize the resources. KNA based on SR, KE, and the newly introduced OSR statistics is useful for this purpose in domains homogeneously sampled. However, when the

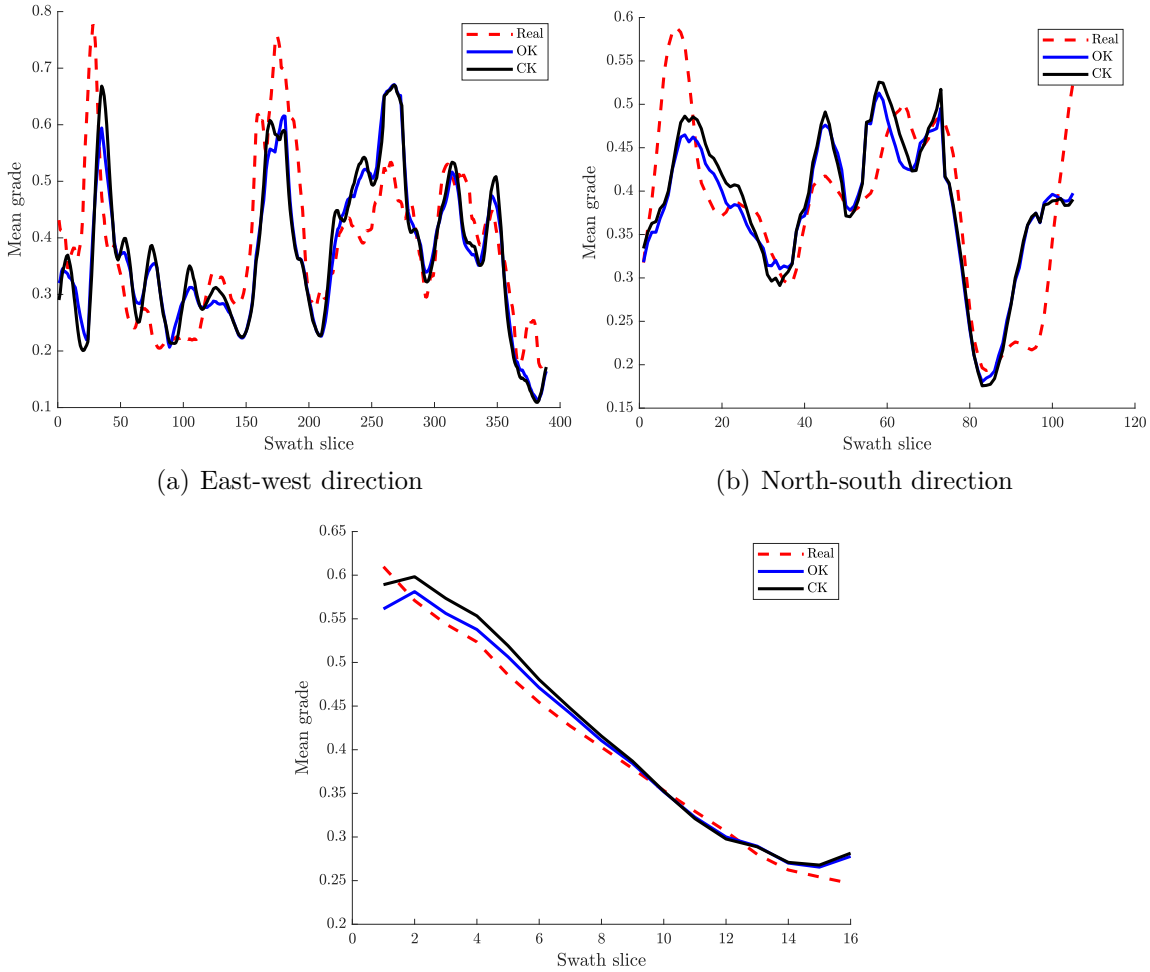

(a) East-west direction

(b) North-south direction

(c) Elevation

Figure 4.13 Swath plots along east-west (a), north-south directions (b) and elevation (c). Gold deposit.

sampling density varies in space, the KNA approach would require to subdivide the deposit in homogeneously sampled domains. A different and easier approach is to use non-smoothed CK predictions as proposed by Cressie (1993), which has the distinct advantage of self-adapting to varying sampling densities.

For the synthetic case, the KNA of OK shows that decreasing the neighborhood size reduces smoothing. This beneficial effect is obtained at the expense of a loss in KE and SR. In contrast, KNA of CK shows no smoothing for all choices of neighborhoods; hence, OSR is robust to this choice. The KE and SR statistics of CK slightly increase with the neighborhood size, suggesting that it might be better for precision to use CK with larger neighborhoods. Interestingly, the only configuration in OK that shows a small OSR (3 boreholes total) also shows similar SR and KE to those of CK with more boreholes. Recovery functions based on OK predictions (with 3 boreholes) and CK predictions (any number of boreholes) show an excellent agreement with the real recovery functions. However, recovery functions computed from OK predictions with 3 boreholes per quadrant are clearly impacted by the increased smoothing effect. These results support the current practice of the mining industry to work with limited neighborhoods for OK. However, the fact that CK is rather insensitive to the choice of the neighborhood constitutes a definite advantage when the sampling density is non-homogeneous or is insufficient to ensure local availability of boreholes in the restricted search area.

Both the Walker Lake and gold deposit case studies showed similar results. OK is more precise than CK but CK has less smoothing effect, which results in ore grade-tonnage curves closer to the real ones. In fact, CK reveals to be as good as the non-linear UC for recovery function estimation, a remarkable achievement considering UC is specifically designed for this task. Moreover, contrary to CK, UC necessitates a stronger biGaussian hypothesis of the transformed grades at block and panel scales and it assumes that the discrete Gaussian model applies for both. In addition, CK (like OK) allows to localize the predictions at the block scale compared to the panel scale for UC. An extension to UC, localized uniform conditioning (LUC) Abzalov (2006) has been proposed to localize UC estimates at the block scale, but this approach is known to generate discontinuities in the predicted grades at the panel boundaries, which is not the case for CK.

An alternative not examined in this paper is the use of conditional simulations. Contrary to CK, conditional simulation requires a stricter multiGaussian hypothesis. Moreover, the variogram of the Gaussian variable must be selected very carefully as mean grade after back-transformation can be strongly affected by a wrong choice of variogram parameters in the Gaussian space. Finally, the localization of resources is not as direct as with CK. One can

produce e-type maps (that will then be similar to OK), or probability maps to be above cut-off grades (similarly as with UC), but there is no direct equivalent to CK.

Some issues regarding CK have to be mentioned. One difficulty with CK is the absence of real solutions in few cases where too small neighborhood sizes are used. This problem is easily solved by using a larger neighborhood. A second problem is the higher proportion of (small) negative grade predictions obtained with CK compared to OK. The solution adopted here was simply to set to zero all negative estimates obtained by either CK or OK. Another problem is the absence of solutions when no data is found within the largest (finite) range of the variogram. In that case, $\mathbf{k} = 0$, hence simple kriging return all zero weights, b, m_2 and μ_1 in Eqs. 4.4 and 4.5 are also 0, hence λ in Eq. 4.6 is indeterminate. An easy solution is either to incorporate one variogram component with asymptotic sill (e.g. exponential, Gaussian or Matérn models), or include a component with large finite range (and eventually small variance contribution).

4.6 Conclusions

Constrained kriging represents a promising alternative to traditional approaches for block-support resources estimation, such as ordinary kriging and uniform conditioning, because of its capacity to simultaneously predict and localize geological resources. CK adopts common practices of OK (e.g., the use of search neighborhood) and avoids the main issues of UC and the strong multiGaussian hypothesis of conditional simulation. Despite the fact that CK predictor is less precise than OK, it generates non-smoothed predictions and it succeeded to properly reproduce the recovery functions in all study cases. One definite advantage of CK over OK is that it is by construction self-adaptive, i.e., the estimates are non-smoothed for all neighborhood configurations. Recovery functions obtained by CK in the two real case studies were at least as precisely estimated by CK than by UC, an interesting outcome considering that UC is a widely used non-linear method specifically targeted to estimate recovery functions.

4.7 Appendix

Recall the system of equations to solve for determining CK weights:

$$\mathbf{K}\boldsymbol{\lambda} + \mu_1\mathbf{1} + \mu_2\mathbf{K}\boldsymbol{\lambda} = \mathbf{k} \tag{4.11}$$

$$\mathbf{1}'\boldsymbol{\lambda} = 1 \tag{4.12}$$

$$\boldsymbol{\lambda}'\mathbf{K}\boldsymbol{\lambda} = \sigma_v^2 \tag{4.13}$$

Premultiplying Eq. 4.11 by $\mathbf{K^{-1}}$ and arranging the terms, it follows:

$$\boldsymbol{\lambda} = \frac{1}{1+\mu_2}\mathbf{K^{-1}}\left(\mathbf{k} - \mu_1\mathbf{1}\right) = \frac{1}{m_2}\mathbf{K^{-1}}\left(\mathbf{k} - \mu_1\mathbf{1}\right) \tag{4.14}$$

where $m_2 = 1 + \mu_2$. Premultiplying Eq. 4.11 by $\mathbf{1'K^{-1}}$, the following form is written:

$$m_2 + \mu_1 s = b \tag{4.15}$$

with $b = \mathbf{1'K^{-1}k} = \mathbf{1'\lambda_s}$ and $s = \mathbf{1'K^{-1}1}$. Premultiplying Eq. 4.11 by $\boldsymbol{\lambda}'$, the following expression is obtained:

$$m_2\sigma_v^2 + \mu_1 = \boldsymbol{\lambda}'\mathbf{k} \tag{4.16}$$

Substituting Eq. 4.14 in Eq. 4.16 leads to the following:

$$m_2\sigma_v^2 + \mu_1 = \frac{1}{m_2}\left(\mathbf{k}' - \mu_1\mathbf{1}'\right)\mathbf{K^{-1}k} \tag{4.17}$$

$$= \frac{1}{m_2}\left(\mathbf{k'\lambda}_s - \mu_1 b\right) \tag{4.18}$$

Substituting Eq. 4.15 in Eq. 4.18, one obtains:

$$m_2 = \left[\frac{\mathbf{k'\lambda}_s - b^2/s}{\sigma_v^2 - 1/s}\right]^{1/2} \tag{4.19}$$

which completes the proof.

CHAPTER 5 ARTICLE 2: QUANTIFYING MINERAL RESOURCES AND THEIR UNCERTAINTY USING TWO EXISTING MACHINE LEARNING METHODS

Nadia Mery and Denis Marcotte
Mathematical Geosciences 54(2), 363-387, DOI 10.1007/s11004-021-09971-9
Accepted: July 2021

5.1 Abstract

Mineral resources are typically quantified by estimating the grade-tonnage curve for different resource categories. Statutory resource assessment reports (e.g., NI-43-101), however, do not include a measure of uncertainty for the disclosed resources despite the major investments required for mining projects. Although conditional simulation can provide confidence intervals (CIs) for resource estimation, it requires a strong stationarity assumption and depends on the variogram model selected, which is often poorly defined with the available data. In order to avoid these limitations, this research proposes the use and comparison of two machine learning (ML) methods: multiple linear regression and multi-layer neural network to generate tonnage curves and their CIs directly from the data. The classical variogram modelling step is replaced by the specification of intervals for each parameter of the selected variogram model. The learning is carried out in a perfectly controlled environment using simulations with known variograms. Numerous reference deposits are sampled, and for each one, a series of conditional realizations define the mean tonnage and CI curves. Different statistics computed for the entire dataset are used as input to predict the tonnage and CI curves by the ML methods. The results indicate that there are no significant differences between the ML methods. In addition, ML resource predictions outperform those obtained with ordinary kriging, constrained kriging, uniform conditioning and indirect lognormal correction, being surpassed only by the discrete Gaussian model. Nevertheless, these predictors were favored by the use of true variogram models. Moreover, the coverage probabilities of different CIs reach the nominal levels indicating adequate resource uncertainty quantification. Finally, two case studies validate the effectiveness of the proposed approach for tonnage prediction and uncertainty quantification.

Keywords: machine learning - recovery curves - tonnage curve - confidence intervals - geological uncertainty

5.2 Introduction

A proper mineral resource assessment should quantify associated uncertainty. Financial investments and the failure/success of several mining projects are strongly influenced by the precision of resource assessment, which relies on relatively scarce data obtained from a limited number of boreholes (Roden & Smith, 2001; Dominy, 2007). Nevertheless, statutory resource assessment reports, such as NI-43-101, rarely include information on the uncertainty of the predicted values and mainly summarize the available resources using grade-tonnage curves (Owusu & Dagdelen, 2019).

Conditional simulation (CS) (Chilès & Delfiner, 2012) enables to quantify uncertainty on regionalized variables by generating multiple scenarios. However, CS relies on strong assumptions, such as stationarity and multi-Gaussian distribution. Moreover, CS requires that a variogram model be defined, which is typically fitted on experimental variograms. The latter are often erratic because of the highly skewed distribution of the data. Several authors have studied the effect of variogram model definition on resource predictions, providing tools to enhance variogram model selection (Armstrong, 1984; Olea, 1994; Gringarten & Deutsch, 2001; MacCormack et al., 2017). Nevertheless, variogram modelling may be considered a sensitive step since it requires subjective and interrelated decisions, such as defining statistically homogeneous domains where the stationarity hypothesis can be stated, determining parameters for computing experimental variograms and variogram model selection.

The most widely used geostatistical methods, such as ordinary kriging (OK) (Matheron, 1963) and uniform conditioning (UC) (Rivoirard, 1994), also rely on the variogram model definition to characterize the spatial behavior of regionalized variables. These predictors suffer from pitfalls, such as smoothed predicted values generated by kriging (Isaaks & Srivastava, 1989), the effect of the kriging neighborhood on the conditional bias of predictions (Rivoirard, 1987), and for UC, the inability to localize recoverable resources at a smaller scale than a large panel. Localized uniform conditioning (LUC) (Abzalov, 2006) has been proposed for this purpose, but this method generates discontinuities at panel boundaries. Change of support models are an alternative to directly compute global resources at volumetric support larger than point support. Several models have been developed to this end, such as affine correction, direct lognormal correction, indirect lognormal correction (IL) and discrete Gaussian model (DG) (Isaaks & Srivastava, 1989; Emery & Torres, 2005; Chilès & Delfiner, 2012). None of these methods make it possible to compute confidence intervals (CIs) on resource estimates.

Constrained kriging (CK) (Cressie, 1993; Mery et al., 2020) has shown promising results for resource prediction. Mery et al. (2020) completed a sensitivity analysis of the variogram

model definition to evaluate its impact on recovery curves obtained by OK, CK and UC. The authors indicate that UC is the method most affected by an incorrect variogram model definition, followed by OK and CK. Furthermore, CK provides more robust predictions than OK when analyzing the choice of kriging neighborhood. However, the most common weakness of OK, CK, UC and any other interpolation method is the lack of uncertainty quantification for grade-tonnage curves.

In recent years, machine learning (ML) methods have been applied in a variety of geoscientific contexts, including geothermal borehole optimization (Pasquier et al., 2018), earthquake predictions (Rouet-Leduc et al., 2017), geological domain classification (Balamurali et al., 2019; Halotel et al., 2020; Hasterok et al., 2019), landslide susceptibility mapping (Micheletti et al., 2014), mineral recognition (Maitre et al., 2019), spatial interpolation (Nwaila et al., 2020) and mineral exploration (Zuo & Xiong, 2020). The increased acceptance of artificial neural network (ANN) tools is due to their ability to find patterns or intrinsic relationships between a set of input variables and the corresponding dependent outputs without needing to generate an explicit model or knowing the process itself. This advantage makes it possible to solve complex problems (Zhang et al., 1998). To our best knowledge, ML methods has not been applied to predicting grade-tonnage curves and quantifying their uncertainty.

This research uses and compares two ML methods, namely multiple linear regression (MLR) and ANN, to learn rules that link a series of statistics computed directly from data with tonnage curves provided by geostatistical simulations. For a given dataset obtained from a reference realization, conditional simulations can be used to generate a series of potential tonnage curves. A large number of such reference fields are created, each with a different variogram and fixed sample locations. Therefore, the learning process takes place in a perfectly controlled environment where the true variogram models are known. This process seeks to identify features within the data that are best related to mean tonnage and quantile tonnage curves. Once the learning process is completed, the mean tonnage and its CI can be predicted directly from the data of a real deposit.

The proposed approach aims to quantify uncertainty on resource estimates within a fixed domain. The quantification of uncertainty may contribute in early stages to the decision to proceed or not with a mining project. ML methods are data-driven, as it provides the tonnage curves and CI directly from data, without having to specify a variogram model or a block variance. Although the studied domain is fixed, the proposed approach may be applied separately to any domain, such as geological subdomains or subdomains corresponding to resource categories for the ore deposit. The approach is global, and kriging is not required for the ML approach. Finally, only resources, not reserves, are considered in this work, as

defining reserves involves numerous additional factors and decisions far outside the scope of this research.

The paper is structured as follows. Sect. 5.3 describes the ML methods and the methodology used to predict the mean tonnage and quantile curves. Sect. 5.4 provides the results obtained from applying ML methods to predict tonnage curves and assess uncertainty for two synthetic cases showing different distributions. A comparison of using MLR, ANN, OK, CK, UC, IL and DG to predict tonnage curves is presented. Sect. 5.5 contains a series of non-Gaussian cases, including data from a real gold deposit to verify the effectiveness of the proposed method. Finally, Section 5.6 discusses the main findings of this research and the implications for current practices in mineral resource assessment and uncertainty quantification.

5.3 Methods

The research aims to predict ore tonnage and confidence intervals using ML algorithms on tonnage estimates at several cut-offs and for different confidence levels. First, assumptions and choices are clearly stated to clarify the range of applicability of the approach. Then, MLR, the architecture of ANN, output targets and input variables used in the learning are described in turn.

5.3.1 Assumptions

The main assumption of the research is that the boundaries of the domain under study are assumed to be fixed. This means that the confidence intervals obtained by ML methods do not account for uncertainty on domain boundaries. The domain can correspond to a geological domain or a particular resource category (e.g., measured, indicated) based on data availability, as is usually assessed in resource estimation using different estimation passes. It can also correspond to a period of exploitation (e.g., a year or more) for which resources and their uncertainty need to be assessed.

In the learning phase, thousands of different cases were considered. Each case corresponded to fixed sample locations, different variogram parameters and different sample Gaussian transform (defined from declusterized data histogram). However, following standard practice in geostatistical simulations, the Gaussian transform used to generate the reference deposit was kept fixed for each case.

Conditional simulations were used to generate 100 realizations per case using the variogram model of the case. However, the sample declusterized histogram was used to define the Gaussian transform. The conditional realizations provided the output variables. The input

variables were all computed directly from either the raw data or the Gaussian grades computed with the sample Gaussian transform. No model or result from the reference deposit or the conditional realizations were used on the input side. At last, sufficient statistical homogeneity within the studied domain is assumed as usual in resource assessment.

The variogram parameters are allowed to vary within intervals. This makes it possible to have a predictive model that has generalization capacity and is robust to variogram parameter specification. It also allows producing different sample Gaussian transforms to incorporate variability with respect to the initial Gaussian transform used to generate the reference deposit of each case.

Table 5.1 summarizes the assumptions of the proposed approach. Note that since domain and rock density are fixed, the proportion of resources, or normalized tonnage, at each cut-off is used instead of raw resource tonnages to facilitate the training. The normalized tonnages can be easily converted to real tonnages by simply multiplying by T_0, the rock tonnage in the studied domain at zero cut-off. Hereinafter, the term tonnage is used for normalized tonnage.

Table 5.1 Summary of assumptions and choices made for ML training.

Element	**Assumption**
Domain	Fixed
Rock density	Fixed
Gaussian transform (reference cases)	Fixed
Gaussian transform (input and output)	Variable (sample declusterized histogram)
Sampling location	Fixed
Nugget effect	Variable
Variogram range	Variable
Variogram model	Isotropic spherical (could be changed)

5.3.2 Machine Learning Algorithms

Two ML methods, classical multiple linear regression (MLR) and feed-forward artificial neural networks (FFANN), are used to compare the performance of predicting tonnage curves and the capability of accurately assessing the uncertainty defined by CIs. In FFANN, the information moves in one direction following a path from the input nodes towards hidden layers (multi-layer perceptron, MLP) until the output layer, with neither cycles nor loops in the process (Carvalho et al., 2011). Figure 5.1 portrays a scheme of an MLP with two hidden layers and an output layer displaying a single node. The input information is weighted and flows through several interconnected layers of neurons, while an activation function generates the output signal of each node. The network training is done by backpropagation, an iterative

process that adjusts the weights of the network so as to minimize a statistic of the prediction error. FFANNs are able to model any measurable function with low error when both a proper number of neurons is used within the hidden units and a relationship between the input and output information exists (Hornik et al., 1989). The success of the ML approach is highly related to the quality of the input and output data.

5.3.3 Output (target) Data

Output data is constituted of ore tonnage as a function of cut-offs. The function is discretely sampled at different cut-offs that encompass the main part of the grade distribution. To obtain a distribution of possible tonnages at each cut-off, conditional realizations are employed. Quantiles of tonnage distributions define tonnage CIs. Since the mean tonnage at each cut-off is considered the best tonnage predictor, the ML models are carried out on the mean at different cut-offs. Similarly, separate ML models are performed for each quantile of interest.

To obtain the numerous exemplars of mean tonnage and quantile curves necessary for ML trainings, several datasets are simulated over the same field, each considering the same *pdf* but a different variogram. Fixed samples locations are used in each dataset. For a given dataset, the sample Gaussian transform computed from the declusterized histogram and the true variogram model are used to generate conditional realizations. Mean tonnage and quantile curves are computed based on these conditional realizations.

5.3.4 Input Data

It is advisable to feed the ML models with meaningful data-derived features or statistics chosen based on the learning objective. These statistics should jointly reflect the point *pdf* and the effect of the change of support on grade distribution, and should account for the spatial correlation.

Nearest-neighbor (NN) interpolation is applied to the same grid used in the conditional simulation to define a declusterized histogram. Convolutions on previous NN interpolations for different block sizes are subsequently calculated to help in identifying short-scale correlation and change of support rules. The spatial correlation is also characterized by the first lags of an experimental variogram computed on Gaussian-transformed grades to reduce the variability of the values.

The steps of the proposed approach are summarized in Algorithm 1.

Algorithm 1 ML approach

1. Initialization
- Define the Gaussian anamorphosis
- Define the parameter interval and type for variograms
- Define the field size
- Define the number of samples and locations

2. for $i = 1$ **to** K (K the number of cases)
- Randomly select a set of variogram parameters
- Simulate reference deposit i
- Extract data from the reference deposit using fixed locations
- Perform NN interpolation on a regular grid to get declusterized point histogram
- Define a sample Gaussian transform based on declusterized histogram
- Compute N conditional realizations
- Compute selective mining units (SMUs) grade for the realizations and determine tonnage curves for each one
- Compute mean tonnage curve and quantile tonnage from realizations. Output variables are obtained for the three different trainings (mean, lower-bound (LB) and upper-bound (UB))
- Compute input statistics used in training ▷ see Section 5.4.2

3. Choice of ANN architecture

4. Training by MLR and ANN
- Perform the three trainings (mean, LB and UB) separately for each method

5. Prediction performance
- Compare predictions of the trained models with references using new cases

6. Quantification of uncertainty
- Compare nominal CI probability to the coverage probability of the CIs computed from the conditional realizations

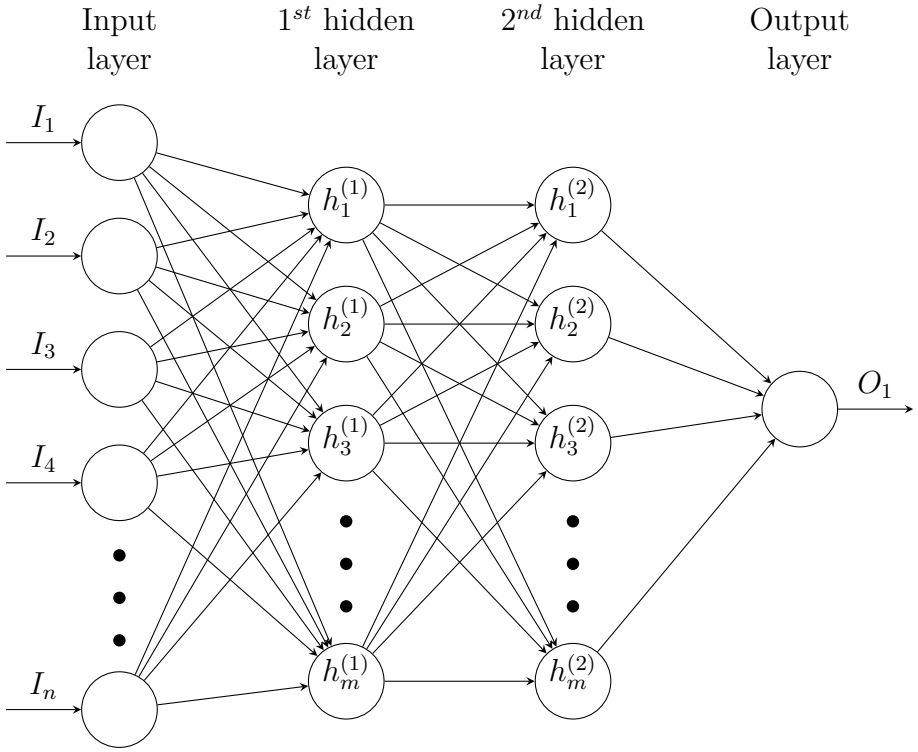

Figure 5.1 Neural network architecture schematic composed of two hidden layers.

5.3.5 Settings for the Synthetic Case

Table 5.2 summarizes the parameters used for the synthetic case. These parameters represent values that may be found in a typical gold deposit. They are sampled using a low-discrepancy Halton sequence (Halton, 1960) to ensure uniform sampling.

The mean tonnage curve and tonnage curves at different quantiles of the realizations (i.e., 2.5%, 5%, 10%, 15%, 20%, 25%, 30%, 35%, 40%, 45%, 55%, 60%, 65%, 70%, 75%, 80%, 85%, 90%, 95%, and 97.5%) are trained separately. Using these curves, ten CIs (95%, 90%, 80%, 70%, 60%, 50%, 40%, 30%, 20% and 10%) are generated to quantify uncertainty on the predicted mean tonnage curve. Each CI is defined by its lower and upper bounds. The CIs are not symmetric around the mean curve.

Once the input-output pairs are determined for the ANN method, different network architectures are tested and compared to establish an efficient network. This process includes analyzing the number of hidden layers and neurons, defining the activation function and choosing training algorithms, among other decisions. The main statistics considered to select the network architecture are the mean absolute error (MAE) and the root mean square error (RMSE) for the testing set. The shape of the predicted curves and the absence of

Table 5.2 Summary of parameters utilized to generate each of the $K = 5,000$ cases for training.

Parameter	Value and units
Sampling density	375 samples
Nugget effect	$\in$ [0, 0.7]
Variogram range	$\in$ [20, 100] m
Variogram model	Spherical
Number of conditional realizations N	100
Cut-off values	From 0.3 to 3.3 by step of 0.3 (any unit)
Domain size	500 $\times$ 500 m
SMU size	5 $\times$ 5 m
Capping value	30 ppm

inconsistencies for each curve independently and between curves are also examined by computing metrics, such as the difference between consecutive values for each curve and values of different tonnage curves at the same cut-offs to evaluate crossing between curves.

The predictions generated with the trained models are validated by the MAE and RMSE. The coverage probability (CP) is calculated and compared to the nominal CI probability. CP measures the proportion of cases (over all cut-offs) in which the real tonnage curve lies within the intervals defined by the CI curves. A similar analysis is also performed for each cut-off separately.

5.4 Results

In this section, numerous tonnage and CI curves are computed and subsequently used as output data in the training process for both MLR and ANN. In addition, two different distributions are considered: lognormal and bimodal. The corresponding input parameters and the network architecture of the ANN are defined to predict tonnage curves and quantify their uncertainty. Lastly, the prediction performance of the ML models is compared to the results obtained by OK, CK, UC, IL and DG.

5.4.1 Point Grade Distributions

Lognormal and bimodal distributions are considered (Fig. 5.2). All the steps described in Algorithm 1 are applied to each distribution independently in a perfectly controlled two-dimensional case.

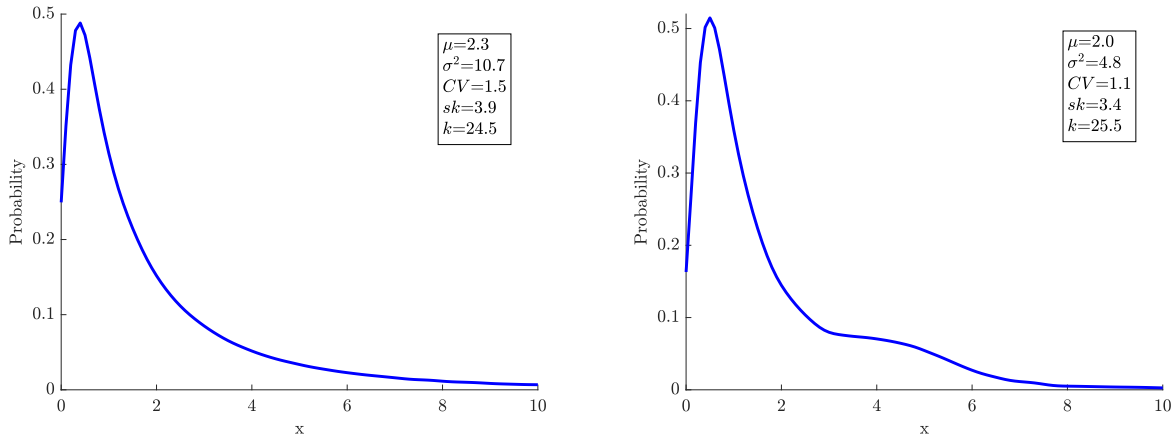

(a) Lognormal distribution

(b) Bimodal distribution

Figure 5.2 Probability density function of histogram values generated from defined Gaussian anamorphosis used in the synthetic controlled case. Lognormal (a) and bimodal (b) distributions.

5.4.2 Input Data

For each dataset, NN interpolation is used to obtain a declusterized histogram. Then, block values at SMU size are generated by applying a convolution operator on the interpolated grid. The first five bins of the experimental variogram at five lag distance (the SMU size) are used to describe the spatial correlation.

Table 5.3 describes the set of inputs used to result in 27 variables. Note that several other inputs were tested without success. For instance, variograms of different orders for raw or Gaussian-transformed values, indicator variograms and rank variograms were assessed, but based on the results, they were not retained. Nonetheless, the selection of input variables is not a critical issue, as ML adapts learning to the inputs provided. Hence, similar results were obtained with a variety of input variable combinations. The inputs selected in Table 5.3 represent variables that are relatively easy to compute, have a clear interpretation and provide more stable results overall for the cases analyzed.

5.4.3 Network Architecture of ANN

The Levenberg-Marquardt backpropagation algorithm is used in the training process because of its speed and efficiency (Hagan & Menhaj, 1994).

The number of layers and nodes is decided based on the performance of the testing dataset. Figure 5.3 shows the RMSE for different configurations. According to these results, two

Table 5.3 Summary of input variables.

Item	Variables	Number
Point recovery from NN interpolation	Tonnages at 11 cut-offs	11
NN SMUs recovery	Tonnages at 11 cut-offs	11
Experimental variogram of Gaussian transformed variable	$\gamma(h)$ for $h \in \{5, 10, ..., 25\}$	5
	Total	27

hidden layers with ten nodes are utilized in the network. For this configuration, several activation functions are tested (see Table 5.4). The sigmoid function is finally used as the activation function in the two hidden layers and a linear activation function is applied to the output layer. Moreover, input and output data are pre-processed and post-processed during the training process by normalizing the values between -1 and 1 since data normalization usually improves prediction performance (Kotsiantis et al., 2006).

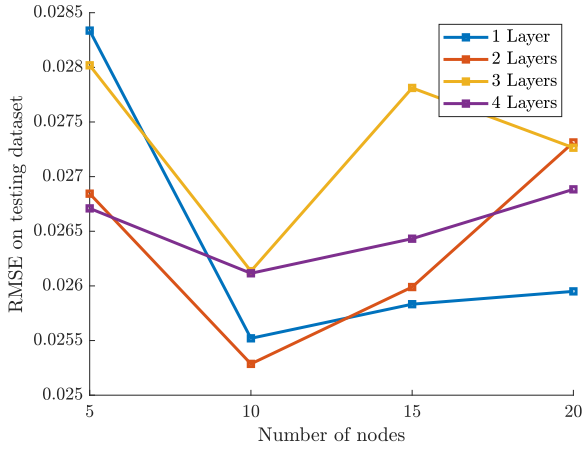

Figure 5.3 Sensitivity analysis of network architecture.

5.4.4 Tonnage Curve Prediction

Of the 5,000 cases considered, 4,000 were used for training while 1,000 were set aside as testing set. MAE and RMSE are computed on the testing datasets for all the resulting tonnage curves, including those generated at different quantile values (see Table 5.5). The errors in the testing datasets are just slightly larger than in the training dataset, indicating a good generalization capability. Results obtained with the bimodal distribution are similar to those obtained with the lognormal distribution, indicating good robustness to the Gaussian transform used. MLR and FFANN performed similarly on the test set.

Table 5.4 Sensitivity analysis of activation function.

Activation function	**RMSE**
Log-sigmoid	0.0264
Rectified linear	0.0278
Linear	0.0314
Radial basis	0.0277
Normalized radial basis	0.0267
Saturating linear	0.0264
Softmax	0.0271
Sigmoid	0.0263
Triangular basis	0.0271

Table 5.5 MAE and RMSE for training and testing datasets obtained by ANN and MLR.

ML method	**Dataset**	**Lognormal distribution**		**Bimodal distribution**	
		MAE	**RMSE**	**MAE**	**RMSE**
ANN	Training	0.0169 to 0.0287	0.0220 to 0.0343	0.0145 to 0.0261	0.0188 to 0.0306
	Testing	0.0169 to 0.0292	0.0220 to 0.0350	0.0145 to 0.0262	0.0188 to 0.0307
MLR	Training	0.0169 to 0.0287	0.0220 to 0.0343	0.0144 to 0.0261	0.0187 to 0.0306
	Testing	0.0169 to 0.0295	0.0220 to 0.0350	0.0145 to 0.0261	0.0187 to 0.0308

Figure 5.4 depicts an example of the results for the testing dataset obtained by MLR. One of the realizations is plotted alongside the predicted mean tonnage curve and the corresponding 95% CI, defined by the predicted LB 2.5% and UB 97.5% quantile curves. The predicted 95% CI entirely includes the real tonnage curve for both distributions. Note that all CI curves monotonically decrease despite the fact that this constraint could not be explicitly imposed in ML modelling.

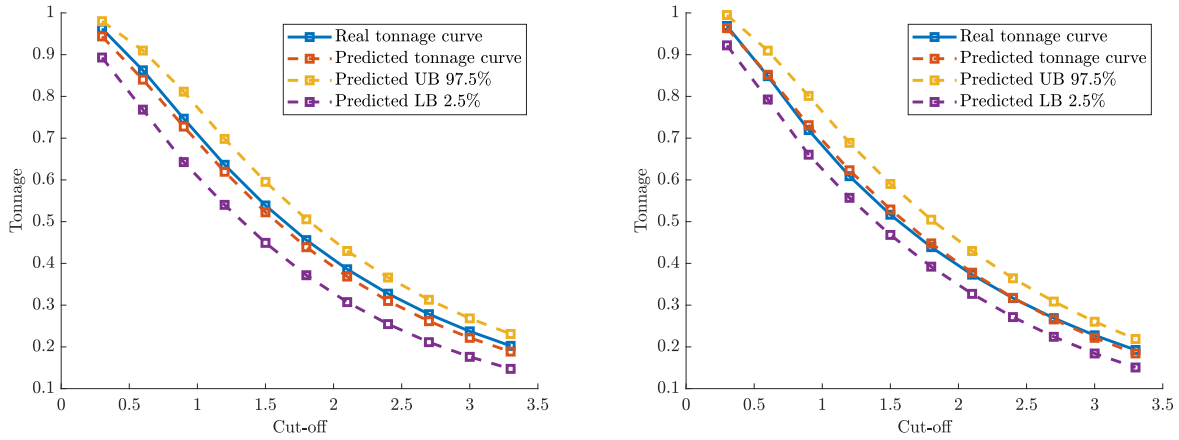

(a) Lognormal distribution (b) Bimodal distribution

Figure 5.4 Real and predicted tonnage by MLR, predicted upper-bound (UB 97.5%) and lower-bound (LB 2.5%) defining 95% CI. Lognormal (a) and bimodal (b) distributions.

5.4.5 Assessment of Uncertainty over Resource Predictions

The coverage probability of each CI is computed to assess prediction performance based on the uncertainty quantification of tonnage curves. Each interval is compared to all the $N \times K = 100 \times 5,000$ tonnage curves generated by CS. Thus, the proportion of times the curves lie within the CI is counted separately for each cut-off. The mean proportion over different cut-offs is considered the CP.

The initial coverages obtained for both ML methods are systematically lower than the nominal CI probability (see Fig. 5.5, blue squares). Self-correction of the confidence interval was learned in the MLR training by optimizing the following correction function

$$w(c) = \alpha \; exp(-|c - \beta|/\delta) \text{ with } c \geq 0, \delta > 0, \tag{5.1}$$

where c is the cut-off, whereas α, β and δ are parameters of the function chosen such that the difference between the coverage and the nominal CI probability, after setting $UB_{corr} = UB + w$

and $LB_{corr} = LB - w$, is minimized considering all cut-offs. Note that the same $w(c)$ function is applied to all cases as well as to UB and LB, but a different function is computed for each CI. The correction function allows the continuous modification of the UB and LB. After correction, the resulting CPs are close to the diagonal for the *testing* set (see Fig. 5.5).

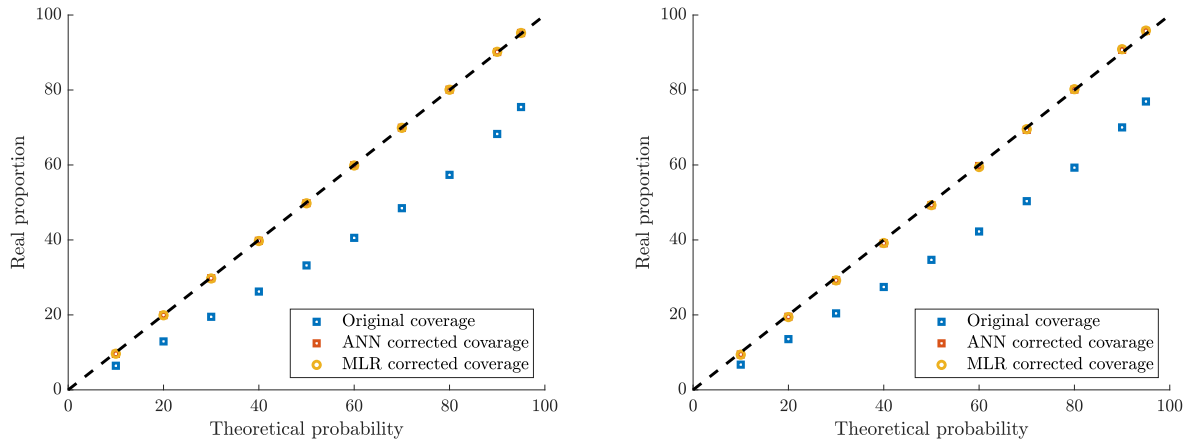

(a) Lognormal distribution

(b) Bimodal distribution

Figure 5.5 Coverage probability vs CI width in testing dataset: Original coverage (blue squares), ANN (red squares) and MLR (yellow circles). Lognormal (a) and bimodal (b) distributions.

Figure 5.6 displays the initial and corrected CP for the nominal 95% CI at different cut-offs. When the additive correction $w(c)$ is applied, CP is enhanced at all cut-offs.

5.4.6 Comparison between Curves Predicted by ML Methods and Traditional Geostatistical Methods

This section compares the prediction performance of tonnage curves obtained by ML methods to those obtained by CK, UC, OK, IL and DG. For OK, small neighborhoods of one neighbor per quadrant are selected to reduce the smoothing effect of kriging. More samples are used for CK (two per quadrant), as CK has no smoothing effect by construction, whatever the neighborhood size (Mery et al., 2020). In the case of UC, a panel size of 50 × 50 is chosen and 50 neighbors are considered. CK, UC, OK, IL and DG were favored, compared to ML methods, by using the same variogram models as were used in the simulations to generate the reference deposits.

The results are summarized in Table 5.6. The success rate is computed as the percentage of times a method outperforms the other ones over the 5,000 cases × 11 cut-offs. On this criterion, DG ranks first, followed by MLR for both distributions. Similar results are obtained

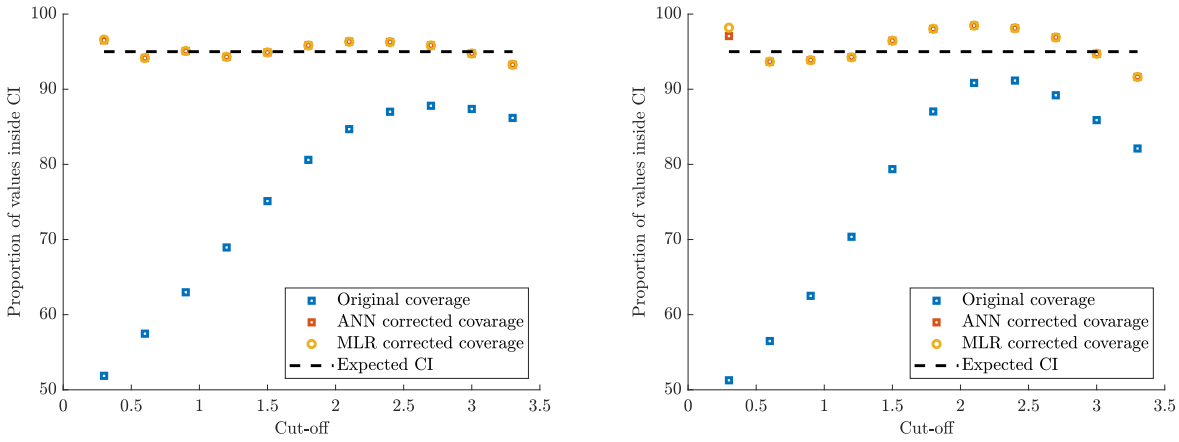

(a) Lognormal distribution

(b) Bimodal distribution

Figure 5.6 Coverage probabilities for 95% CI at different cut-off values in testing dataset. Original coverage (blue squares), ANN (red squares) and MLR (yellow circles). Lognormal (a) and bimodal (b) distributions.

based on the MAE and the RMSE. DG appears best, followed by MLR, ANN and CK with similar performances. The fact that ML methods perform well is interesting, considering that DG and CK were favored by using the true variogram.

Table 5.6 Summary of MAE and RMSE of tonnage curves and success rate of different prediction methods: ANN, MLR, CK, UC, OK, IL and DG.

Method	**Lognormal distribution**			**Bimodal distribution**		
	MAE	**RMSE**	**Success rate**	**MAE**	**RMSE**	**Success rate**
ANN	0.0173	0.0225	13.0%	0.0154	0.0199	13.0%
MLR	0.0170	0.0220	13.5%	0.0145	0.0187	15.0%
CK	0.0191	0.0236	11.6%	0.0144	0.0182	14.5%
UC	0.0336	0.0383	6.4%	0.0256	0.0297	6.6%
OK	0.0332	0.0404	9.2%	0.0310	0.0376	8.1%
IL	0.0159	0.0208	14.4%	0.0196	0.0243	10.0%
DG	0.0094	0.0134	31.9%	0.0088	0.0133	32.8%

Table 5.7 shows the pairwise comparison results for the different methods. Each row indicates the percentage of times, the method corresponding to the row beat the methods indicated in columns, also computed over the 5,000 cases $\times$ 11 cut-offs. This analysis verifies that for both distributions, DG is the best method compared with the geostatistical predictors studied. ANN, MLR and CK are contenders as the second-best approach, followed by IL, OK and UC in descending order.

Table 5.7 Pairwise comparison between prediction methods.

	Lognormal distribution							**Bimodal distribution**						
	ANN	MLR	CK	UC	OK	IL	DG	ANN	MLR	CK	UC	OK	IL	DG
ANN	-	48.8%	54.3%	69.7%	66.3%	48.4%	30.3%	-	46.9%	49.5%	67.6%	69.6%	60.2%	31.3%
MLR	51.2%	-	55.3%	71.7%	68.0%	49.3%	30.8%	53.1%	-	52.0%	70.8%	72.3%	62.6%	34.3%
CK	45.7%	44.7%	-	67.7%	64.5%	43.8%	25.9%	50.5%	48.0%	-	70.1%	71.2%	61.3%	31.2%
UC	30.3%	29.3%	32.3%	-	51.3%	30.2%	15.5%	32.4%	29.2%	29.9%	-	56.9%	45.1%	17.5%
OK	33.7%	32.0%	35.5%	48.7%	-	33.3%	21.0%	30.4%	27.7%	28.8%	43.1%	-	40.5%	20.0%
IL	51.6%	50.7%	56.2%	69.8%	66.7%	-	28.8%	39.8%	37.4%	38.7%	54.9%	59.5%	-	21.8%
DG	69.7%	69.2%	74.1%	84.5%	79.0%	71.2%	-	68.7%	65.7%	68.8%	82.5%	80.0%	78.2%	-

Since MLR and ANN provided similar performance, only MLR is considered hereinafter because of its simplicity.

Sensitivity to the Variogram Model for DG Predictions

DG (and all the other methods) were favored by specifying the same variogram model used to obtain the reference simulated deposits. In practice, only the experimental variogram is available, which is often erratic and noisy. Defining the right variogram model can therefore be difficult. To evaluate the impact of variogram uncertainty on DG predicted curves, the true block variance s_v^2 is varied by a multiplicative factor between 0.7 and 1.3. New predicted curves are obtained by using the modified block variance on DG.

Figure 5.7 shows the success rate of MLR compared with DG and the MAE ratio of DG to MLR. DG appears quite sensitive to the selection of the right block variance. MLR outperforms DG in both studied distributions when the error on block variance exceeds 20%.

5.4.7 Computational Aspects

Given the large amount of information required in the training process, different strategies are applied to maintain a reasonable computation time for the generation of the data used in the training phase. Conditional simulations are carried out using the fast Fourier transform moving average (FFT-MA) method (Le Ravalec et al., 2000), post-conditioning is conducted with global dual kriging, and parallel computing is performed on the graphics processor unit (GPU). Once the training is completed, expected grade-tonnage curve and confidence interval predictions are rapidly computed for a new dataset.

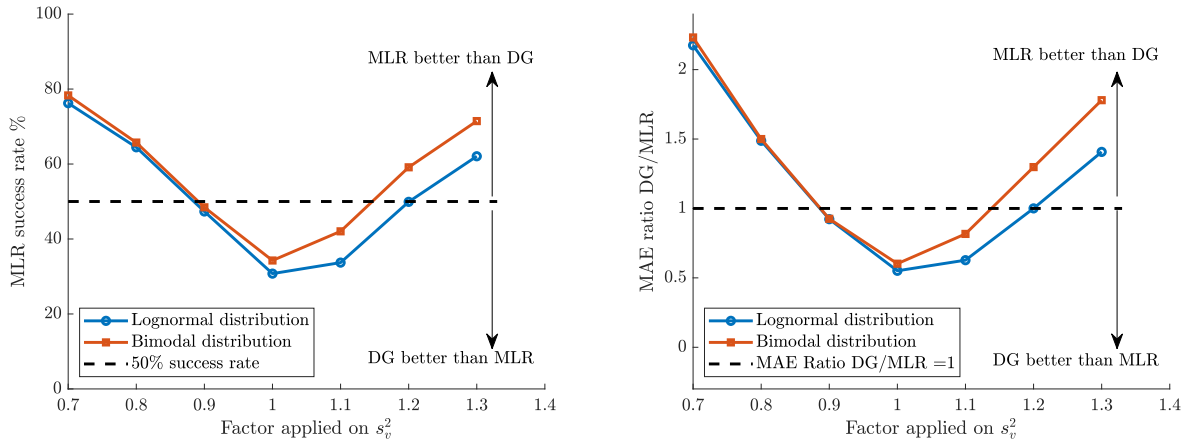

(a) MLR success rate % compared with DG

(b) MAE ratio DG/MLR

Figure 5.7 Sensitivity analysis of varying block variance s_v^2 by a factor, lognormal and bimodal distributions. Success rate of MLR (a) and MAE ratio DG/MLR (b).

5.5 Case Studies

Two different case studies are used to test the applicability of the method to non-Gaussian and less-controlled cases. The first case study concerns a series of ten satellite images randomly selected from the Internet. The second case study pertains to a two-dimensional section of a real gold deposit (unidentified for confidentiality reasons) that has been extensively sampled by blast holes and reverse circulation (RC) holes.

5.5.1 Synthetic Data of non-Gaussian Fields

A new training is performed for the satellite images using parameters of Table 5.8. The training of MLR is done with 5,000 new cases, each involving 100 realizations. For each image, samples are selected at fixed locations to obtain the dataset. Input statistics for MLR prediction are computed using the dataset and used to predict the mean, 5% and 95% tonnage curves for each image individually. Real SMU (i.e., 5×5) tonnage curves are also computed on each backtransformed image and compared with the prediction curves. The backtransformed images utilized in this case study are shown in Fig. 5.8 for the two distributions studied (lognormal and bimodal).

When the comparison between predicted and real tonnage curves is considered, the MAE and RMSE values computed over all cut-offs and the ten images, are 0.0258 and 0.0305, respectively, for the lognormal distribution and 0.0270 and 0.0329, respectively, for the bimodal distribution. The CI encompasses most of the real curves. Exceptions are found in

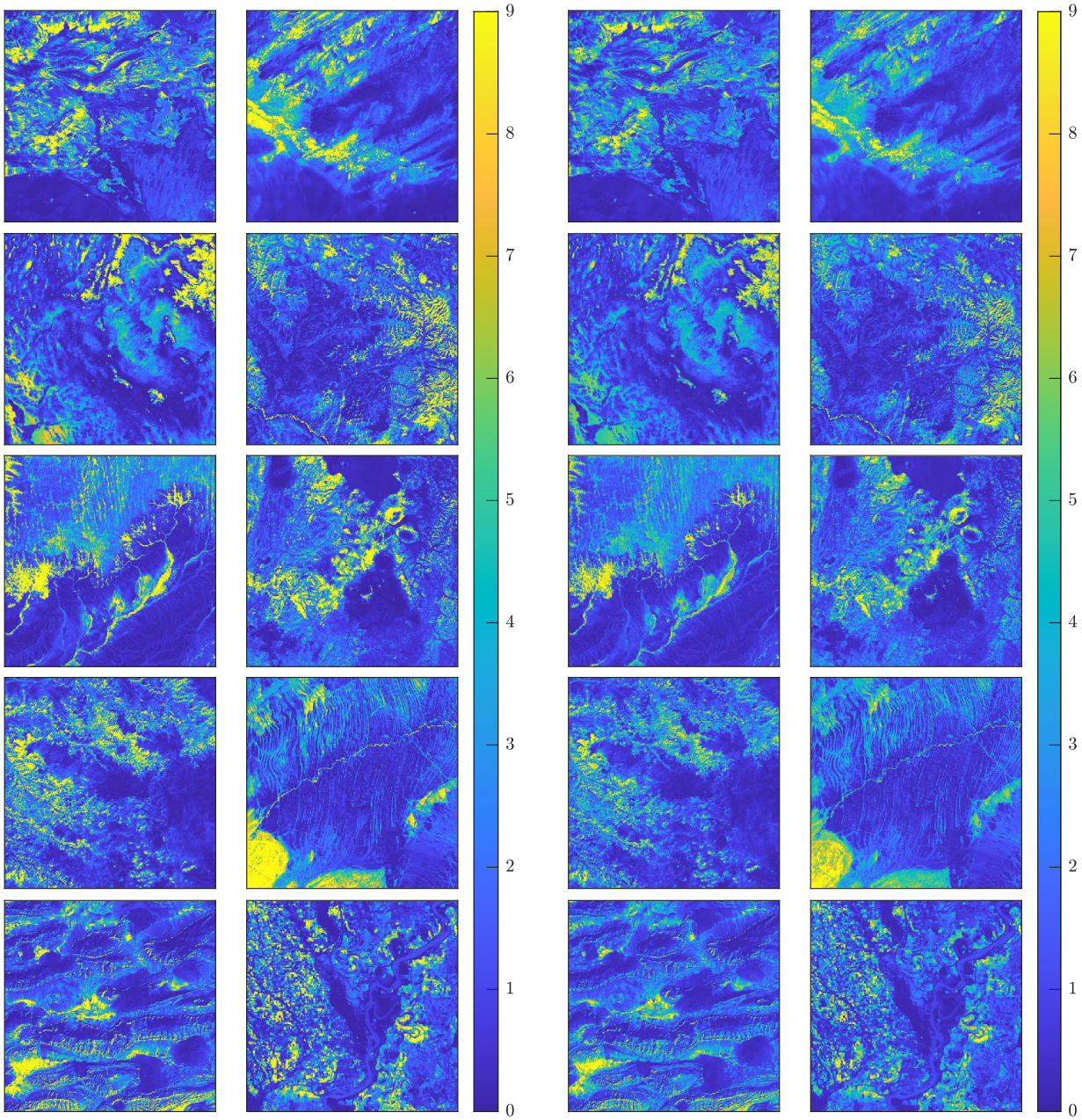

(a) Lognormal distribution (b) Bimodal distribution

Figure 5.8 Images used in the synthetic non-Gaussian case. Lognormal (a) and bimodal (b) distributions.

Table 5.8 Summary of parameters utilized to generate each of the $K = 5,000$ cases for training. Synthetic non-Gaussian case.

Parameter	Value and units
Sampling density	375 samples
Nugget effect	$\in$ [0.05, 0.6]
Variogram range	$\in$ [90, 190] m
Variogram model	Spherical
Number of conditional realizations N	100
Cut-off values	From 0.3 to 3.3 by step of 0.3 (any unit)
Domain size	500 $\times$ 500 m
SMU size	5 $\times$ 5 m
Capping value	30 ppm

images 5 and 10 for both distributions, where the tonnage curves appear slightly outside the computed CI for certain cut-offs (see Fig. 5.9).

Real and predicted tonnage curves are then averaged over the ten images to represent the case of a deposit with different geological domains. The average tonnage curves are presented in Fig. 5.10, which indicates an excellent overall prediction performance for the ML models, as the real curve is entirely contained in the CI.

Finally, the proposed ML approach is compared with CK, UC, OK, IL and DG using the methodology and parameters discussed in Section 5.4.6. Based on the MAE and RMSE (Table 5.9), the predicted MLR curves outperform those obtained using traditional methods for both distributions. In this case, the variogram models are unknown and the variogram model parameters of CK, UC, OK, IL and DG are thus inferred from the available data of each image. MLR is the best method in four out of ten images for both distributions, followed by DG, CK, IL, OK and UC.

Table 5.9 MAE and RMSE of tonnage curves and success rate of prediction methods MLR, CK, UC, OK, IL and DG. Training on synthetic Gaussian case, prediction for images of Fig. 5.8.

Method	Lognormal distribution			Bimodal distribution		
	MAE	RMSE	Success rate	MAE	RMSE	Success rate
MLR	0.0258	0.0305	40%	0.0270	0.0329	40%
CK	0.0299	0.0391	30%	0.0278	0.0333	20%
UC	0.0409	0.0484	0%	0.0318	0.0396	0%
OK	0.0404	0.0465	0%	0.0340	0.0395	0%
IL	0.0326	0.0401	0%	0.0338	0.0398	20%
DG	0.0290	0.0350	30%	0.0288	0.0349	20%

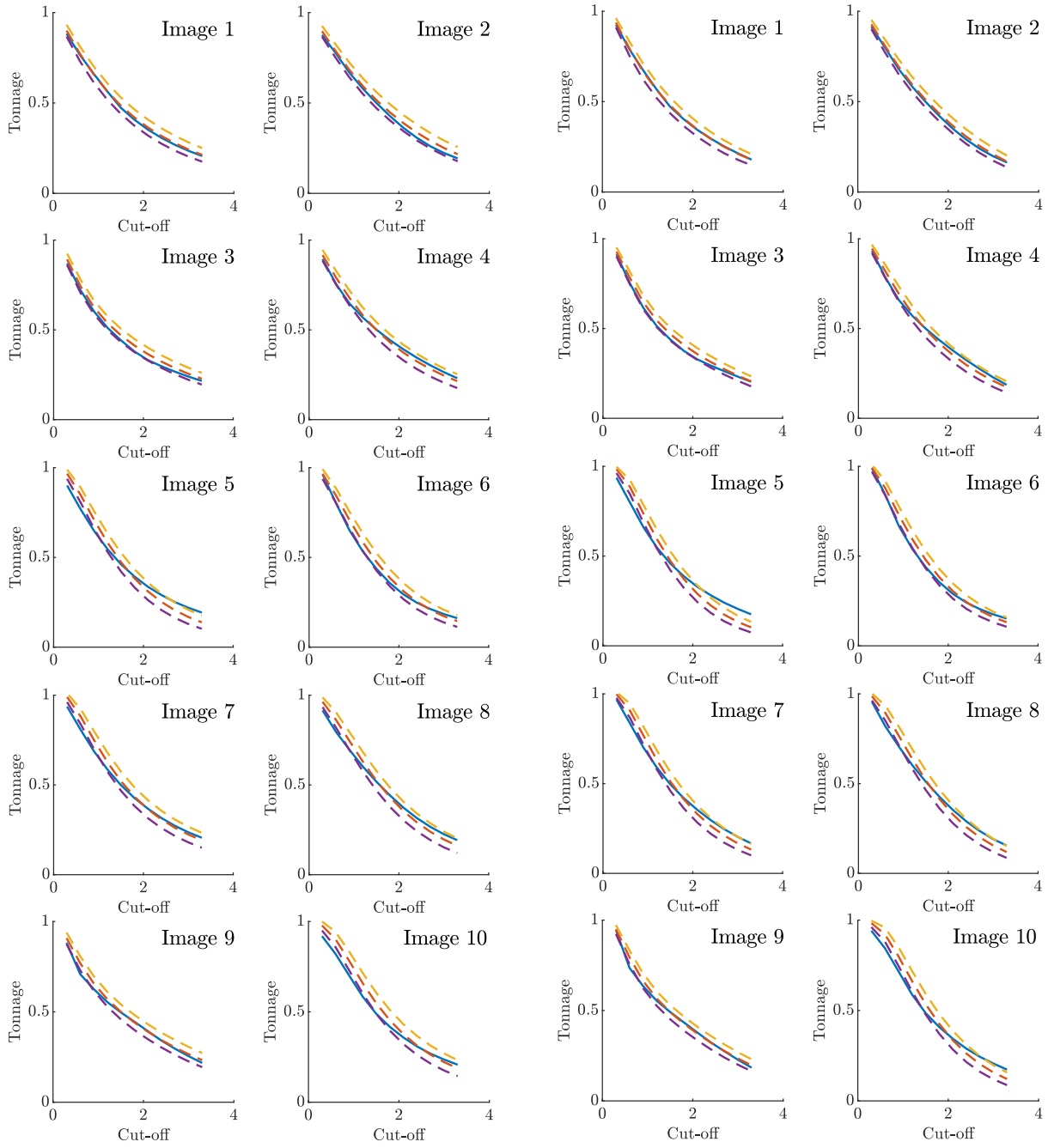

(a) Lognormal distribution

(b) Bimodal distribution

Figure 5.9 Real (solid blue) and predicted (dashed red) tonnage curves with predicted upper-bound 95% and lower-bound 5%, for the images of Fig. 5.8. Lognormal (a) and bimodal (b) distributions.

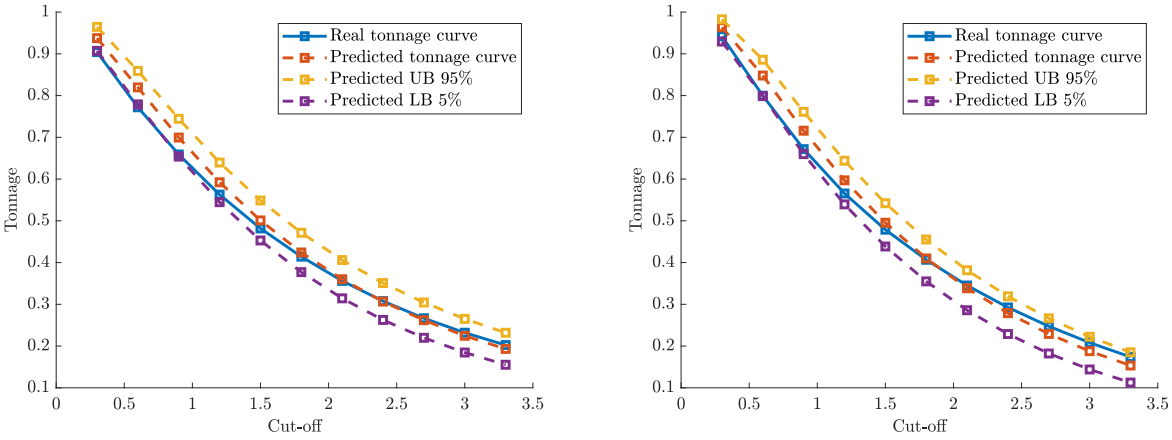

(a) Lognormal distribution (b) Bimodal distribution

Figure 5.10 Real and predicted tonnage curves and 90% CI for the amalgam of the ten images of Fig. 5.8. Lognormal (a) and bimodal (b) distributions.

5.5.2 Gold Deposit

The gold mineralization is mainly composed of pyrite (2% to 7%) and pyrrhotite. Several reverse circulation drilling data are available as they are used for grade control. From this dataset, a level is selected for the case study. The main statistics of the case study are summarized in Table 5.10.

Table 5.10 Basic statistics of RC data.

Mean	**Variance**	**Median**	**CV**	**Skewness**	**Kurtosis**	**# samples**
0.38	1.77	0.11	3.49	12.16	205.97	2,268

A new training process is carried out for this case study considering the gold deposit histogram, domain size and variogram model parameters. In order to generate the input-output pairs for the learning process, the parameters have to be adapted to the information gathered from the real dataset. The intervals of the variogram model parameters are determined from quick examination of the real RC experimental variogram, and cut-off values are adjusted to the gold grade distribution of the RC dataset. Table 5.11 summarizes the parameters used in the case study.

The training process is performed with unconditional simulation in a perfectly controlled Gaussian case. The predictive model obtained from training is used on the real deposit (i.e., 200 samples from the RC dataset) to predict the tonnage curve. This curve is subsequently

Table 5.11 Summary of the parameters utilized to generate each of the $K = 3,000$ cases for training. Gold deposit dataset.

Parameter	Value and units
Sampling density	200 samples
Nugget effect	$\in [0.4, 0.8]$
Variogram range	$\in [20, 65]$ m
Variogram model	Spherical
Number of conditional realizations N	100
Cut-off values	From 0.05 to 0.75 by step of 0.05 ppm
SMU size	5×5 m
Capping value	30 ppm
Surface covered by RC	$1{,}775 \times 448$ m^2

compared with the 'real' tonnage curve generated from a turning bands (TB) conditional simulation using all RC data on the defined domain. Note that the TB realization can be considered a close approximation to reality because of the initial large number of RC data. Figure 5.11 shows the real and predicted tonnage curves alongside 95% CI. The MAE and RMSE are 0.0147 and 0.0185, respectively. An excellent prediction performance is observed, and the real tonnage curve lies mostly within the 95% CI.

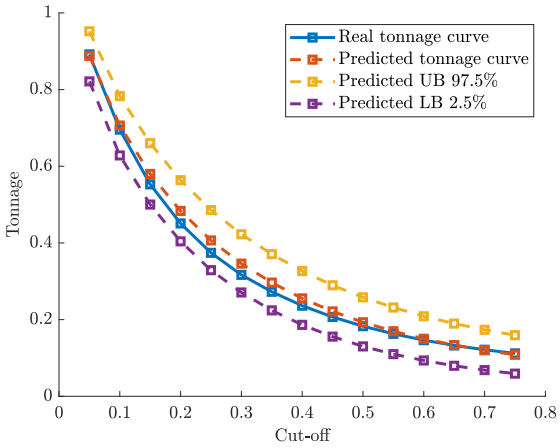

Figure 5.11 Real and predicted tonnage curves and 95% CI obtained with samples taken from RC data.

Finally, the ML model is compared with OK, CK, UC, IL and DG for real tonnage curve prediction. OK, CK, UC, IL and DG used the same variogram model to generate the real tonnage curve with TB simulation. The results are summarized in Table 5.12. MLR is the best method in terms of errors, followed by DG, CK, IL, OK and UC in decreasing order.

Table 5.12 Summary of MAE and RMSE for tonnage curves computed using different prediction methods: MLR, CK, UC, OK, IL and DG. Gold deposit dataset.

Method	MAE	RMSE
MLR	0.0197	0.0207
CK	0.0295	0.0351
UC	0.0356	0.0468
OK	0.0318	0.0423
IL	0.0303	0.0406
DG	0.0272	0.0338

5.6 Discussion

Quantifying recoverable resources and their corresponding uncertainty is a complex task. Current geostatistical approaches, such as CK, UC, OK, IL and DG are not able to generate confidence intervals on predictions. For this purpose, conditional simulations are more appropriate. However, the quality of CS results depends entirely on the choice of variogram model parameters and the validity of the stationarity hypothesis. The variogram model may be challenging to obtain when data are sparse, erratic or not representative of the entire domain under study. CS is particularly sensitive to the variogram model and the stationarity assumption, as its parameters are defined in the Gaussian scale.

The proposed ML approach does not rely directly on this sensitive modelling feature and instead uses multiple sets of conditional simulations in the training phase. Each set considers different variogram parameters and sample data. The output recoveries are computed on each conditional realization for a given dataset. The recoveries at each cut-off are averaged over different sets (mean recovery) and ranked to define quantile curves. Recoveries are then paired to data input statistics using two different ML methods: MLR and ANN that learn the key relationships in the input stream to predict the recoveries (with a separate training phase for each desired curve).

The performance of the ML methods was similar for the prediction of tonnage curves, reproducing the CP at different CIs. Being simpler to apply, the MLR technique was preferred over FFANN for application to case studies. Other ML methods, such as random forest and support vector machine, were tested but provided similar results to MLR for this particular problem. The results suggest that features extracted from the data (i.e., input variables) are well correlated with the tonnage (i.e., output values). Hence, the MLR approach suffices to capture the useful information without recurring to evolved ML methods. Despite this, more complex problems could require deep learning methods able to deal with stronger non-linearity than the problem addressed in this research.

Although the proposed approach is general, a new training phase has to always be rerun based on the parameters of each case, such as the histogram of the studied field or the intervals for variogram model parameters.

According to the MAE and RMSE values for lognormal and bimodal distributions, ML models exhibit excellent prediction performance for mean and quantile tonnage curves. The results are similar for both training and testing datasets. The quantification of uncertainty by CIs provides coverage probabilities on the test set close to the nominal CI level. As expected, the CIs generated are asymmetrical around the mean grade-tonnage curve. CPs at different cut-offs are stable and close to CI level.

For the lognormal distribution, DG is the best predictor in 31% of cases compared to 15% for MLR and 12% for CK. The results are similar for the bimodal distribution. All methods but ML methods were favored by utilizing the same variogram model used in the simulation of the reference deposits. A sensitivity analysis of the block variance used to compute DG tonnage curves showed significant variations in the performance of DG. MLR has the advantage of not requiring a variogram model to predict tonnage after training is completed. CK, which is a local estimator, like OK, showed good overall performance due to the absence of smoothing effect, confirming the findings of Mery et al. (2020). However, only ML methods provide CIs on the tonnage curves. The coverage probabilities of the CIs were shown to reproduce the nominal probabilities, especially after applying an additive correction function that is easily determined by optimization during the training phase.

Two case studies were carried out to further test the effectiveness of the proposed methodology. First, non-Gaussian images were analyzed where the predicted tonnage curves are precise (i.e., small MAE and RMSE values). The predictive models are capable of predicting local (i.e., each image separately) and global uncertainties (i.e., based on the juxtaposition of the ten images). The second case study is of a two-dimensional section of a real gold deposit. Prediction performance, uncertainty quantification and comparison with traditional methods lead to the same conclusions as for the other case. Therefore, the ML approach is a suitable alternative to reproduce tonnage curves and quantify uncertainty while providing acceptable predictions, compared to geostatistical methods such as OK, CK, UC, IL and DG.

The proposed ML approach is trained in an ideal environment where stationarity is guaranteed. The combined analysis of ten satellite images, emulating a deposit with different domains, suggests that the method is robust to some forms of non-stationarity. However, further studies are required to define and quantify the extent of non-stationarity that the model can tolerate. These studies could lead to revisions of the input statistics or how the tonnage curves are parameterized. The method was applied to two different distributions,

lognormal and bimodal. These distributions are analogous to those found in several deposits. However, they represent only a small range of possibilities. Further research is needed to assess changes in the ML approach to incorporate other probability distributions, for instance, a stronger bimodal distribution.

The set of input variables was selected after several analyses of a wide variety of variables, such as variograms of various orders for both the raw and the Gaussian grade, and other histogram and sampling density statistics. The variables used provide acceptable results, but they do not necessarily represent an optimal subset. In some cases, adding more variables can deteriorate the results, especially when the variables are noisy or very erratic. Similarly, numerous tests were conducted for the output variables. For instance, the parameterization of the curves with dual kriging added complexity without improving the results. Attempts to model the tonnage curve using a mixture of different $cdfs$ also failed to enhance the predictions.

The field extent was not considered as a parameter in this research. This assumes that the limits of the deposit (or part of the deposit) are known. The sample locations were fixed within the domain studied to reproduce a real case where data samples are available, and therefore, their location are known. Note that the model can be applied to a particular sub-zone (or domain) of the deposit. For instance, the proposed approach may be used first for a well-sampled zone considered as measured, then in a less sampled zone considered as indicated. Thus, training for each zone separately makes it possible to provide tonnage estimates and CIs by resource category.

This research explores the capacity of ML to predict mean grade-tonnage and CI curves in a two-dimensional stationary case. Additional research has to be carried out to assess the robustness of the method for non-homogeneous deposits. The possibility of extending the results to 3D cases is also of great importance and to be addressed in further studies.

The ML approach aimed to quantify the uncertainty (i.e., the CI) on resources in preliminary assessments to enhance the decision-making process of mining projects. Although the uncertainty on histogram and variogram models is accounted for in the training phase, the uncertainty on deposit boundaries is not included, as the training pertains to a specified domain. As is customary in geostatistics, a single (population) Gaussian transform was used to simulate the reference deposits. Each sample declusterized histogram defines a different sample Gaussian transform for the conditional realizations used to generate output variables. ML training is completely data-driven, as the input side relies entirely on statistics computed directly from raw or Gaussian-transformed data. No kriging and no variogram or histogram modelling are needed to obtain predictions for a new case.

5.7 Conclusions

Machine learning is a reliable alternative to quantify mineral resources (tonnage curves) without needing to perform complex variogram modelling. The proposed approach showed outcomes comparable to the best results obtained with geostatistical methods on reference deposits, even though the latter were favored by using the known variogram model. Moreover, the ML models allow for the uncertainty on resulting tonnage curves to be quantified by predicting the CI tonnage curves at different confidence levels. Coverage probability results indicate that ML models are able to adequately reproduce nominal values. Simulation and case studies conducted on a series of satellite images and data from a real gold deposit demonstrate the effectiveness of the method at predicting grade-tonnage curves and quantifying resource uncertainty.

5.8 Amendment

Addendum to Figure 5.8: x and y axis are respectively Easting and Northing given in pixels. The length of each pixel along each direction varies from one satellite image to the other.

CHAPTER 6 ARTICLE 3: ASSESSMENT OF RECOVERABLE RESOURCES UNCERTAINTY IN MULTIVARIATE DEPOSITS THROUGH A SIMPLE MACHINE LEARNING TECHNIQUE TRAINED USING GEOSTATISTICAL SIMULATIONS

Nadia Mery and Denis Marcotte

Natural Resources Research 31(2), 767-783, DOI 10.1007/s11053-022-10028-9
Accepted: February 2022

6.1 Abstract

Mine design, mine production planning and the economic evaluation of multivariate ore deposits are based on the mineral resources that are recoverable after applying cutoffs to the grades of selective mining units. Being able to reliably assess the recoverable resource uncertainty of more than one element is key for the economic evaluation of mining projects. Multivariate geostatistical models are difficult to fit and strongly influence the resources reported. The proposed approach avoids the delicate modeling step by directly estimating multivariate tonnages and their associated confidence intervals from a reduced set of features extracted from data. The predictive models are obtained by training with conditional simulations. For each case considered in the training phase, the coregionalization parameters are drawn randomly from within specified intervals and multiple realizations make it possible to obtain deposits conditional to the simulated data sets. Multiple linear regression training is carried out using input-output data to generate predictive models that relate the input variables calculated from the simulated data sets and the output variables (i.e., mean tonnage and tonnage quantiles) computed from the simulated deposits. The results from a synthetic bivariate case indicate excellent tonnage prediction and credible uncertainty quantification. A lateritic nickel deposit subject to a constraint on the maximum silica/magnesia ratio shows the applicability of this approach in a real-world context. The resulting tonnage surface and the associated uncertainty quantification provide an essential tool to help assess the economic value of the mine project.

Keywords: recoverable resources - resources uncertainty - data-driven technique - multivariate modeling - tonnage surfaces - machine learning

6.2 Introduction

Recoverable resource assessment significantly impacts the downstream stages of mining projects, such as mine planning, mine design and financial forecasting. Resource uncertainty, which stems from our partial knowledge of the deposit, is critical for correctly valuing a mining project in preliminary studies. Incorrect uncertainty quantification can have severe effects on the life and profitability of the mine (Dominy et al., 2002).

There is increasing interest in the current mining practices for predicting not only the main products, but also the by-products and contaminants in ore deposits. For instance, in copper-molybdenum deposits, the ore definition includes both elements (Hosseini et al., 2017). In iron deposits, it is desirable to predict the alumina content conditional to the iron content (Boucher & Dimitrakopoulos, 2012). In lateritic deposits, the nickel content is usually subject to a constraint on the maximum admissible silica (SiO_2) / magnesium oxide or magnesia (MgO) ratio, with the latter having a determinant influence on the performance of the ferronickel smelting process (Keskinkilic, 2019).

The study of multi-element ore deposits poses a particular challenge for resource evaluation. Several studies conclude that multivariate geostatistical techniques outperform approaches that model the variables independently. For instance, cokriging outperforms kriging in polymetallic copper deposits (Pan et al., 1993; Yalçin, 2005; Dhaher & Lee, 2013; Vergara & Emery, 2013) and a synthetic case study (Minnitt & Deutsch, 2014). In addition, Montoya et al. (2012), Battalgazy & Madani (2019) and Eze et al. (2019) contrast univariate and multivariate simulations in different ore deposits and applications. For example, Montoya et al. (2012) display ore grade variability as a function of time using all the realizations obtained by conditional simulation (CS) in a porphyry copper-silver deposit. Eze et al. (2019) use CS to generate probability maps and quantify the spatial uncertainty of lead in a copper-nickel deposit, where lead is considered a contaminant. The multivariate approaches require specifying a coregionalization model that is usually difficult to determine and strongly influences the resources estimated (Faria et al., 2021). Alternative methods based on factorization techniques can be also utilized to simulate the multiple variables of interest, such as principal component analysis (Goovaerts, 1993b), maximum minimum autocorrelation factors (Desbarats & Dimitrakopoulos, 2000), stepwise transformation (Leuangthong & Deutsch, 2003), projection pursuit multivariate transform (Barnett et al., 2014), flow anamorphosis (van den Boogaart et al., 2017) and independent component analysis (Tercan & Sohrabian, 2013). Most applications either do not report any measure of uncertainty for the predicted resources or provide one that is model-dependent, i.e., valid when all the assumptions are strictly met. Moreover, the validity of the uncertainty quantification is not evaluated in the

latter applications. Hence, there is a need for a resource uncertainty assessment methodology that is more data-driven and less dependent on the tricky adjustment of a particular geostatistical model.

Machine learning (ML) methods include multiple linear regression (MLR), logistic regression, support vector machine, random forest and artificial neural network (ANN), among others. They are data-driven methods that have been widely applied in the geosciences, including for resource evaluation (Zhang et al., 2021b; Mery & Marcotte, 2022), subsurface mineralization modeling using lithogeochemical data (Granian et al., 2015), rock type prediction and hydrothermal alteration detection (Bérubé et al., 2018), mineral prospectivity mapping (McKay & Harris, 2015; Karbalaei Ramezanali et al., 2020; Ghezelbash et al., 2021; Zhang et al., 2021a), low-salinity waterflooding performance prediction (Kalam et al., 2021) and geochemical exploration (O'Brien et al., 2015).

Mery & Marcotte (2022) study recoverable resource assessment and uncertainty quantification in a gold deposit utilizing ML. ML uses multiple ensembles of conditional simulations, each having its own set of parameters and data. Experimental statistics data on the input side are related to tonnages computed on the simulated deposits on the output side. The authors compare the performance of two ML techniques, MLR and ANN, and conclude that both methods perform similarly, although MLR is ultimately chosen as the preferred technique for its robustness, simplicity and fast learning. The authors also apply their approach to a series of simulated deposits, demonstrating the validity of their proposed uncertainty assessment approach.

This research aims to extend the recoverable resource assessment and uncertainty quantification methodology proposed by Mery & Marcotte (2022) to multi-element deposits. The additional elements can be either economic by-products or costly contaminants to avoid or control. The approach accommodates non-additive element functions, such as the silica/magnesia ratio in nickel deposits.

As in Mery & Marcotte (2022), the method uses an MLR training phase where input and output variables are obtained from conditional simulations. The outcomes of this approach include tonnage resources of a primary variable subject to a critical value of a secondary variable (e.g., a contaminant) or tonnage surfaces describing the joint distribution of two variables. Moreover, the confidence intervals (CIs) on constrained tonnages or tonnage surfaces are obtained simultaneously by an MLR training. The coverage probability (CP) of the CIs is studied and compared to the nominal level.

This paper is organized as follows. Section 6.3 explains the proposed approach and the methodology used to predict multivariate recoverable resources and their uncertainty. Sec-

tion 6.4 shows the application of the MLR approach on a three-dimensional (3D) bivariate synthetic case where the predictive performance and uncertainty quantification is validated on simulated deposits. Moreover, univariate and bivariate predictive models obtained by MLR are contrasted. Section 6.5 illustrates the efficiency of the proposed approach on a nickel deposit. Finally, Section 6.6 addresses the main findings, highlighting the impacts of the research on the practice of recoverable resources assessment.

6.3 Methods

In this section, an ML algorithm for multivariate recoverable resource prediction is detailed along with the main parameters required for its proper implementation.

6.3.1 General assumptions

The proposed approach is an extension of Mery & Marcotte (2022). The assumptions stated therein are replicated in this research, i.e., the geological domain is fixed, hence, the uncertainty quantification does not include uncertainty about geological boundary delimitation. Even though the approach is said to be data-driven, some parameters have to be defined to generate the data for MLR training, especially to perform the CSs that are the source of the training data. As is commonly done in mineral resource assessment, statistical homogeneity is assumed in the defined domain. The term “tonnage" refers, with a slight abuse of language, to the *fraction* of rock tonnage that is above the cutoff grade in the domain studied. Since the domain and rock density are considered fixed, the reverse transformation to mass tonnage is direct.

6.3.2 MLR for multivariate recoverable resource prediction and uncertainty quantification

The approach involves applying MLR to predict multivariate recoverable resources based on sample data following the methodology used in Mery & Marcotte (2022). Consequently, a set of feature (input) and target (output) variables have to be generated for the learning process. Without loss of generality, only a case with two variables is presented for simplicity. However, the approach is straightforwardly generalizable to more than two variables.

The input-output pairs are obtained from multivariate CSs using linear coregionalization models (LCMs) and the turning bands (TB) algorithm (details about this algorithm can be found in Brooker (1985) and Emery et al. (2006)). Note that any simulation algorithm may be used for this purpose. The simulation requires that the conditioning data, the domain

to simulate and the Gaussian anamorphosis be specified and that the LCM parameters be defined. The location of the conditioning data and the domain to simulate are assumed to be known. The Gaussian anamorphosis can be obtained from the declusterized sample data. The LCM parameters are only loosely specified by providing wide intervals of possible values for the nugget effect components, the distance of correlation, and the collocated correlation. These intervals are determined from the data after a quick examination of variograms and cross-variogram. There is no need to define a unique LCM as is usually done; the LCM is used only for the training phase, not for the prediction phase.

Numerous sets of LCM parameters are drawn using a quasi-random Halton sequence. Each set is checked to provide an admissible coregionalization model. As routinely used in Bayesian analysis, the sampling scheme assumes a non-informative prior uniformly and independently distributed over the selected parameter intervals. A reference deposit is simulated for each set. Simulated data are extracted from data locations and used as conditioning data for a series of CSs. The input variables for training are computed from the set of conditioning data, whereas the output variables are obtained from the multiple conditional realizations of the set. This is repeated for each set to provide as many inputs and outputs as there are sets of parameters.

MLR training is carried out on a per-cutoff-pair basis. The cutoff pairs sweep the range of values for both variables (e.g., at regular intervals or at every decile of the point distribution for each variable). Then, a distinct MLR is done for each cutoff pair. The ensemble of MLR models makes it possible to predict a discretized version of the bivariate tonnage surface. Note that the training at each cutoff can be performed for different outputs, such as the mean tonnage recovered from the CSs or a given quantile. For example, if one wants to predict the mean tonnage along with the upper bound (UB) and lower bound (LB) at level α, three distinct MLR training phases have to be conducted at each cutoff. Clearly, this might become computationally heavy unless a fast training method like MLR is employed.

For comparison purposes, separate univariate training phases are also conducted utilizing the same multivariate simulations. In this case, the univariate training passes incorporate the distribution of each variable considered separately. On the input side, only univariate statistics are used (i.e., no experimental cross-variogram is considered). Also, the tonnage curve of a primary variable subject to the constraint value of a secondary variable can be obtained under the independence assumption.

The algorithm proposed for 3D multivariate predictions is described in Algorithm 2 and shown schematically in Fig. 6.1.

Algorithm 2 : ML multivariate approach

1. **Define parameters from available sample data**
   - 1.1. Sample data locations
   - 1.2. Domain size for prediction
   - 1.3. Initial Gaussian anamorphosis for each variable, which is used to obtain a reference deposit and conditioning data values
   - 1.4. Interval of LCM parameters (range, nugget, correlation coefficient and model type). For an LCM to be admissible, the coefficient matrices have to be symmetric positive semi-definite
2. **Obtain k conditional multivariate LCMs**
   For each CS from $i = 1, ..., k$
   - 2.1. Randomly select a set of LCM parameters
   - 2.2. Simulate the reference deposit i
   - 2.3. Define and store simulated pseudo-data values from the reference deposit at the real data locations
   - 2.4. Perform nearest-neighbor (NN) interpolation on a fine grid to get a declustered point histogram
   - 2.5. Compute pseudo-selective mining unit (SMU) distribution by convoluting previous interpolated values
   - 2.6. Compute input variables ▷ see Section 6.3.3
   - 2.7. Obtain a sample Gaussian anamorphosis based on the declustered data histogram
   - 2.8. Simulate n conditional realizations using TB, conditional to the simulated pseudo-data at real data locations
   - 2.9. Compute simulated grades at SMU support for the n realizations
   - 2.10. Calculate and store the mean and quantile tonnage curves and surfaces from the n realizations, which will define the output variables. Note that all tonnage curves are normalized by T_0, the total tonnage of the domain studied ▷ see Section 6.3.4
3. **Bivariate MLR learning**
   Using the tonnage surfaces as target variables
   - 3.1. Randomly divide the k cases to generate training and testing sets
   - 3.2. Perform separate training phases at each cutoff pair for each output variable (i.e., mean, quantile 2.5% and quantile 97.5% tonnage surfaces)

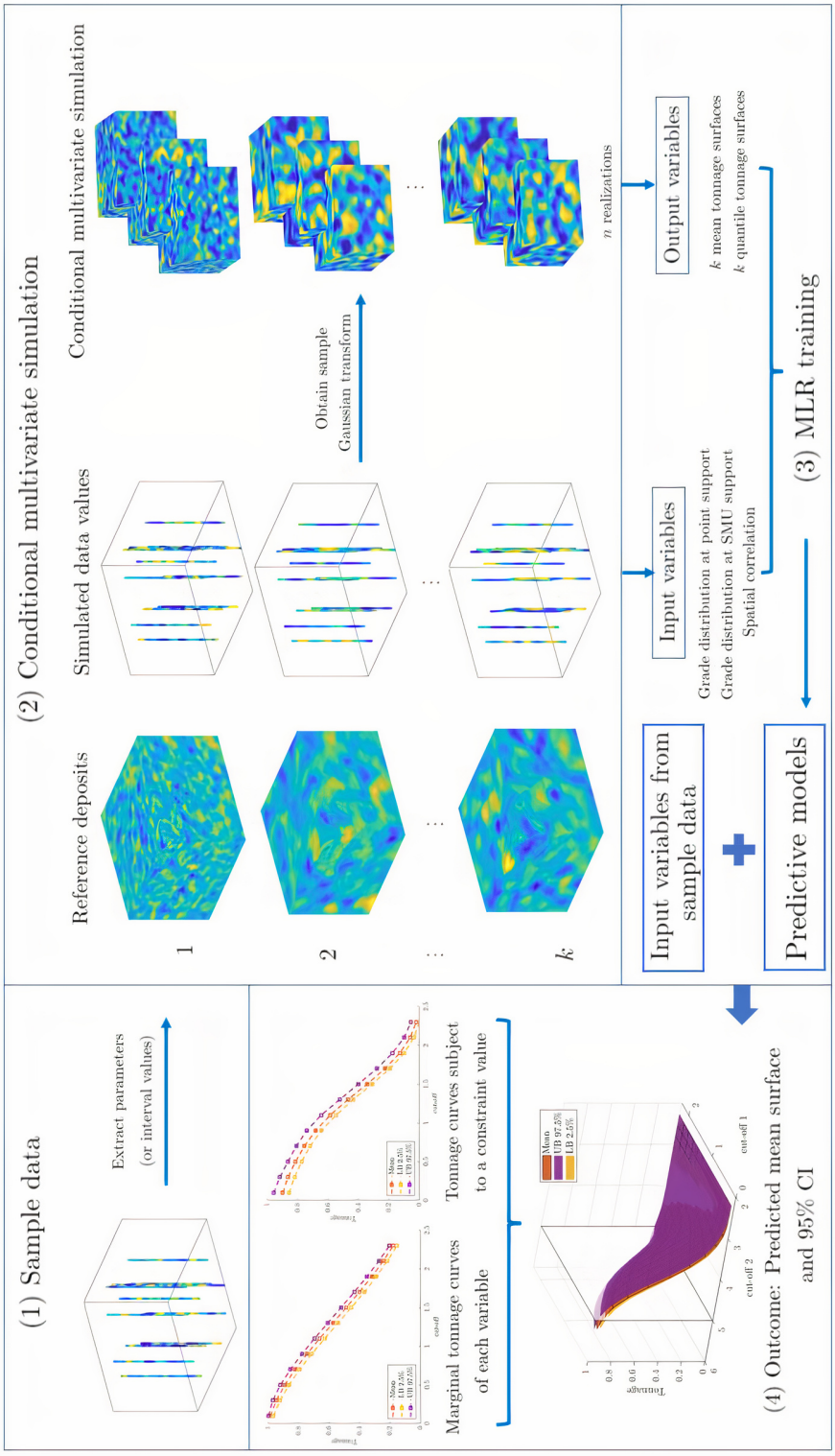

Figure 6.1 Scheme of the proposed multivariate ML algorithm

Algorithm 2 : ML multivariate approach (continued)

4. **Prediction performance assessment**

   4.1. Calculate metrics to evaluate performance on the training and testing sets, such as the root mean square error (RMSE), mean absolute error (MAE) and coefficient of determination (R^2)

   4.2. Compute the marginal tonnage curve for each variable using the predicted surfaces

   4.3. Define a constraint value for the secondary variable and apply it to the predicted surfaces to define a tonnage curve subject to this value

   4.4. Use the sample data to evaluate the predictive models by computing the RMSE

5. **Uncertainty quantification**

   5.1. Use the symmetric predicted quantiles (2.5% and 97.5%) from step 3.2 to define the 95% CI

   5.2. Compute the CP of the predicted CI using the n conditional realizations from step 2.8

   5.3. Compare the CP against the nominal CI probability (95%)

   5.4. If necessary, apply a correction function in the MLR training (step 3.2) to ensure the CP is close to the nominal CI probability ▷ see Section 6.3.5

Definition of interval parameters for LCM

An initial LCM is fitted to the Gaussian transform values of the variables studied. The parameters are allowed to vary for the training. The LCM is parameterized as

$$\mathbf{C}(\mathbf{h}) = \begin{bmatrix} C^0_{xx} & C^0_{xy} \\ C^0_{xy} & C^0_{yy} \end{bmatrix} + \begin{bmatrix} 1 - C^0_{xx} & \rho_{xy} - C^0_{xy} \\ \rho_{xy} - C^0_{xy} & 1 - C^0_{yy} \end{bmatrix} Sph(a; \mathbf{h}) \tag{6.1}$$

where the first matrix on the right describes the nugget components (all ≤ 1) on the direct variograms and cross-variograms, ρ_{xy} is the collocated correlation, Sph indicates the spherical model, a is the correlation range, and $\mathbf{h}$ is the separation vector between two points. The determinants of the two coefficient matrices must be ≥ 0 for the LCM model to be admissible.

6.3.3 Definition of input variables

Three key aspects are considered when defining the input variables: (i) the grade distribution at the point support (see Algorithm 2, step 2.4), (ii) the grade distribution at the SMU support to take into account the change of support (see Algorithm 2, step 2.5), and (iii) the spatial correlation of the grades. The first distribution is obtained from declustered

data by NN interpolation on a dense grid. The second distribution is obtained by averaging the NN interpolated values over the SMU support. The experimental direct variograms and cross-variograms of the Gaussian-transform values describe the spatial correlation and cross-correlation of the grades.

For univariate training, the spatial correlation is solely characterized by the experimental variogram. The input variables for univariate and bivariate training are summarized in Table 6.1.

Table 6.1 Summary of the input variables for univariate and bivariate training

	Variable	**Quantity**
Inputs - Univariate training	Tonnage at point support	As many as cutoff values
	Tonnage at SMU support	As many as cutoff values
	Experimental variogram of Gaussian transform values computed along the borehole (down-the-hole variogram). The lag value is equal to the composite length, and the number of lags is between five and eight	Number of lags
Inputs - Bivariate training	Tonnage surface at point support	Cutoff values of variable 1 $\times$ cutoff values of variable 2
	Tonnage surface at SMU support	Cutoff values of variable 1 $\times$ cutoff values of variable 2
	Experimental direct variograms and cross-variograms of Gaussian transform values computed along the borehole (down-the-hole variogram). The lag value is equal to the composite length, and the number of lags is between five and eight	3 $\times$ number of lags

6.3.4 Definition of target variables

As n conditional realizations are simulated for each case, mean and quantile tonnage surfaces are computed at defined cutoff values. The quantile values are defined according to the uncertainty level desired. For instance, if a 95% CI is required, then quantiles 2.5% and

97.5% have to be calculated. These tonnage values correspond to the target variables used in the bivariate training.

The output variables for univariate and bivariate training are summarized in Table 6.2.

Table 6.2 Summary of the output variables for univariate and bivariate training

	Variable	**Quantity**
Outputs - Univariate training	Mean tonnage curve	As many as cutoff values
	Quantile tonnage curve	As many as cutoff values × number of quantiles defined
Outputs - Bivariate training	Mean tonnage surface	Cutoff values of variable 1 × cutoff values of variable 2
	Quantile tonnage surface	(Cutoff values of variable 1 × cutoff values of variable 2) × number of quantiles defined

6.3.5 Uncertainty quantification

The predicted quantile surfaces are renamed the LB and UB of the CI they define. These surfaces are used to quantify the uncertainty of the predictive models. The indicator function is defined as

$$I_{ij}(c_1, c_2) = \begin{cases} 1 & \text{when LB} \leq T_{ij}(c_1, c_2) \leq \text{UB} \\ 0 & \text{otherwise} \end{cases} \tag{6.2}$$

where $T_{ij}(c_1, c_2)$ is the tonnage for realization i in case j at the corresponding cutoff values c_1 and c_2 of variables 1 and 2, respectively.

Then, the CP as a function of the cutoffs is computed using Eq. 6.3

$$\text{CP}(c_1, c_2) = \frac{1}{nk} \sum_{j=1}^{k} \sum_{i=1}^{n} I_{ij}(c_1, c_2) \tag{6.3}$$

where k is the number of cases used for bivariate MLR training and n is the number of realizations of each case.

The overall CP is then calculated by averaging $\text{CP}(c_1, c_2)$ over all the cutoff values.

The CP values are expected to be similar to the nominal CI probabilities at every cutoff. Since this does not usually happen, a simple correction function is proposed to bring the CP

values closer to the nominal CI values at every cutoff pair, as follows

$$f(c_1, c_2) = \alpha \exp\left(-\sqrt{(\mathbf{c} - \beta)\mathbf{R}\mathbf{A}\mathbf{R}'(\mathbf{c} - \beta)'}\right) \tag{6.4}$$

where $\mathbf{c} = [\mathbf{c_1}, \mathbf{c_2}]$, $\beta = [\beta_1, \beta_2]$, $\mathbf{A} = [\mathbf{1/\delta_1^2} \;\; \mathbf{0}\; ;\; \mathbf{0} \;\; \mathbf{1/\delta_2^2}]$, $\mathbf{R}$ is a rotation matrix defined by an angle, and c_1 and c_2 are the known cutoffs. Parameter α is real and controls the amplitude of the correction, parameters β_1 and β_2 are real and determine where to apply maximum correction, and parameters δ_1 and δ_2 are real positive scale factors. Variable $\mathbf{A}$ is the scaling matrix along each rotated axis. Note that six free parameters define the correction function.

The parameters that define $f(c_1, c_2)$ in Eq. 6.4 are obtained by minimizing the weighted squared differences between the corrected CP($f(c_1, c_2)$) and the nominal CI value, as follows

$$\hat{f}(c_1, c_2) = \arg\min_f \sum_{c_1} \sum_{c_2} w(c_1, c_2) \times [\mathrm{CP}(f(c_1, c_2)) - \mathrm{CI}]^2 \tag{6.5}$$

where CP($f(c_1, c_2)$) is determined by $\mathrm{LB_{corr}}(\mathrm{c_1}, \mathrm{c_2}) = \mathrm{LB}(\mathrm{c_1}, \mathrm{c_2}) - f(c_1, c_2)$, $\mathrm{UB_{corr}}(\mathrm{c_1}, \mathrm{c_2}) = \mathrm{UB}(\mathrm{c_1}, \mathrm{c_2}) + f(c_1, c_2)$, $w(c_1, c_2)$ is a weight function taken as the probability density function evaluated numerically at cutoffs c_1 and c_2 using all the cases considered during training. The weights favor good coverage for grades with highest probability density.

A unique correction function $f(c_1, c_2)$ is obtained for each nominal CI and remains the same for the LB and UB that defined the CI, and for all the cutoff values considered. The optimization described in Eq. 6.5 is a fast process carried out during MLR training.

6.3.6 Model evaluation

The following metrics are used to evaluate the performance of the predictive models on the training and testing sets: root mean square error (RMSE), mean absolute error (MAE), and coefficient of determination (R^2). For the uncertainty quantification assessment, the coverage probability (CP) defined in Eq. 6.3 is computed for each set. Moreover, a heat map with the CP values as a function of the cutoffs for the variables of interest in the testing sets is analyzed to evaluate whether the uncertainty quantification is properly reached at each cutoff pair. To show that approximately 5% of the realizations fall outside the corresponding 95% CI in the testing set, the differences between a few randomly selected realization tonnage curves and the predicted UB and LB are displayed.

6.4 Results

The proposed approach is applied to two different case studies. The first is a synthetic case in which two continuous variables are created from data representing voids in a small cube. The second is a nickel deposit subject to a constraint on the SiO_2/MgO ratio.

6.4.1 3D synthetic bivariate deposit

A synthetic model (Fig. 6.2) is created as follows. First, X-ray 3D microphotogrammetry of a small ceramic cube identifies voids in the solid matrix (coded as 0-1). Then, variable v_1 is computed proportionally to the amount of voids found in a sphere of radius 25 voxels centered at every voxel. Variable v_2 is similar to v_1 except that a large amount of noise (random voids and solid) is added to the original cube. Note that this is a physical model not obtained by geostatistical simulation. A priori, there is no Gaussian signature in this field, contrary to the geostatistical simulations used to train the MLR model.

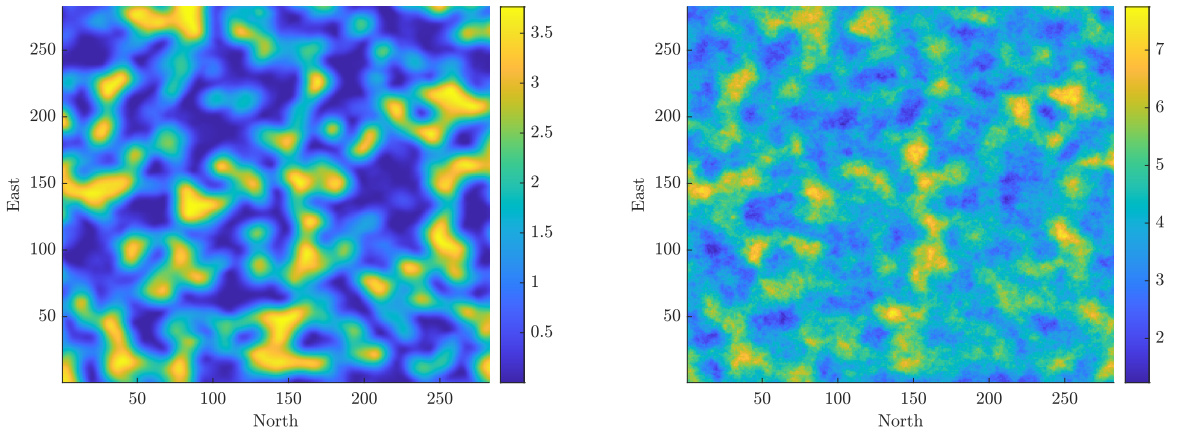

(a) v_1 (b) v_2

Figure 6.2 Section view at elevation 120 (a) v_1 and (b) v_2

The main statistics of both variables are shown in Table 6.3. Variable v_1 has a right-skewed distribution, while v_2 follows a close-to-normal distribution.

Data are extracted from the cube along vertical profiles mimicking boreholes located on a pseudo-regular grid and spaced approximately 100 units apart. Variables v_1 and v_2 are sampled at every point along the “boreholes" (Fig. 6.3).

Table 6.3 Basic statistics

	Mean	Min	Max	Std. dev.	CV	Skewness	Kurtosis	Correlation ρ
$\mathbf{v_1}$	1.5	0	3.8	1.0	0.7	0.3	2.1	0.76
$\mathbf{v_2}$	4.3	0	8.5	1.0	0.2	0.1	2.7	

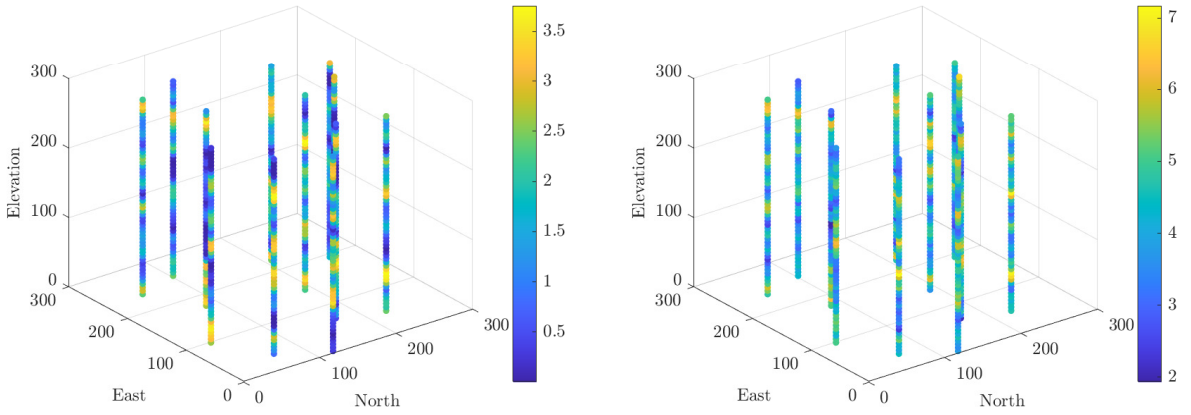

(a) v_1 (b) v_2

Figure 6.3 Samples from (a) v_1 and (b) v_2

6.4.2 MLR training

The training parameters and intervals of possible values for the various LCMs are given in Table 5.2. The LCM parameter intervals are chosen after a quick examination of the experimental variograms and the cross-variogram.

MLR learning is carried out using 70% of the input-output pairs as the training set and the remaining 30% as the testing set.

Table 6.5 presents the metrics used to evaluate the bivariate MLR approach's performance on the training and testing sets. As expected, the metrics are slightly better for the training sets than for the testing sets. The average CPs are 95.3% and 94.1% for the training and testing sets, respectively, which are close to the nominal 95% level and thus demonstrate that the proposed correction function generalizes adequately from the training set to the testing set. Note that the metrics are slightly better for the mean curve than for the UB and LB curves as the latter two are intrinsically more variable. Note also the very high R^2 values obtained for both the training and testing sets on the three curves, which indicate good performance and good generalization of the MLR training.

Table 6.4 Summary of the parameters utilized to generate the $k = 3,000$ cases used for MLR training. 3D synthetic bivariate analysis

Parameter	**Values**
Number of conditional realizations n	100
Cutoff values of v_1	From 0.1 to 2.3 in steps of 0.2
Cutoff values of v_2	From 2.8 to 5.3 in steps of 0.25
Domain size	$282 \times 282 \times 282$
SMU size	$15 \times 15 \times 15$
LCM initial fitting	**Variation for MLR training**
Nugget matrix $\begin{bmatrix} 0 & 0 \\ 0 & 0 \end{bmatrix}$	$\in$ [0, 0.1] for the diagonal terms
Correlation matrix $\begin{bmatrix} 1 & 0.76 \\ 0.76 & 1 \end{bmatrix}$	$\pm$ 0.15 on the off-diagonal terms
Sill matrix $\begin{bmatrix} 1 & 0.76 \\ 0.76 & 1 \end{bmatrix}$	As described in Section 6.3.2
Range	$\in$ [16, 48]
Variogram model	Cubic

Fig. 6.4(a) shows a map of CP as a function of cutoffs for v_1 and v_2. CP is close to 95% for most cutoff pairs. The values that are farther from the nominal CI are found mostly at cutoff combinations corresponding to rare events (e.g., a small c_1 combined with a large c_2, which is an unlikely event considering the strong positive correlation between v_1 and v_2). The differences between a few randomly selected realization tonnage curves and the predicted UB and LB are displayed in Fig. 6.4(b). In both cases, around 5% of the realizations lie outside the CI defined by the LB/UB at each cutoff, which is in line with Fig. 6.4(a).

Additionally, the CP is calculated and compared to the nominal CI probability for ten CIs from 10% to 95% in order to validate the uncertainty quantification of the approach. This is performed as explained for the 95% CI in Algorithm 2 step 5. Figure 6.5 shows that the resulting CPs are close to the diagonal for the testing set, which indicates a correct uncertainty assessment.

6.4.3 Tonnage curves predicted by bivariate MLR training

Once training is completed, the data is used to compute the input variables described in Table 6.1. These input variables then make it possible to predict the tonnage at each cutoff pair.

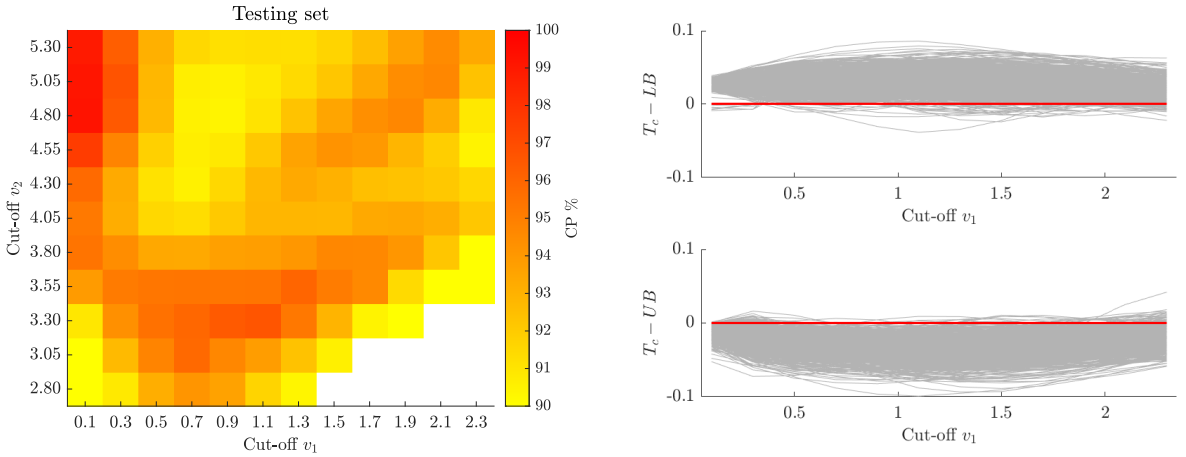

(a) CP (b) Difference between tonnage and LB/UB

Figure 6.4 (a) Heat map of mean CP as a function of cutoff values for the testing set and (b) difference between real tonnage curve and predicted LB/UB as a function of the cutoff on v_1 for the testing set

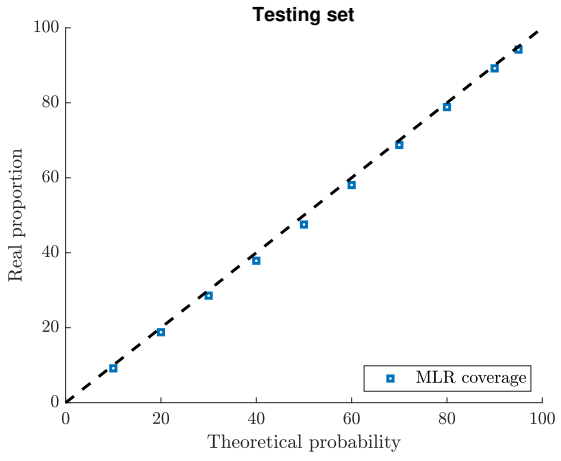

Figure 6.5 Coverage probability vs nominal CI in testing dataset

Table 6.5 Metrics to evaluate MLR learning for the training and testing sets. 3D synthetic bivariate analysis

		MAE	RMSE	R^2	CP
Training set	LB	0.0056	0.0072	0.987	95.3%
	Mean	0.0045	0.0057	0.995	
	UB	0.0075	0.0087	0.985	
Testing set	LB	0.0068	0.0083	0.984	94.1%
	Mean	0.0056	0.0064	0.993	
	UB	0.0082	0.0092	0.983	

Figure 6.6 shows the predicted mean, LB and UB tonnage curves for v_1 and v_2 along with the real tonnage curves. The latter are within the predicted CI at all cutoffs.

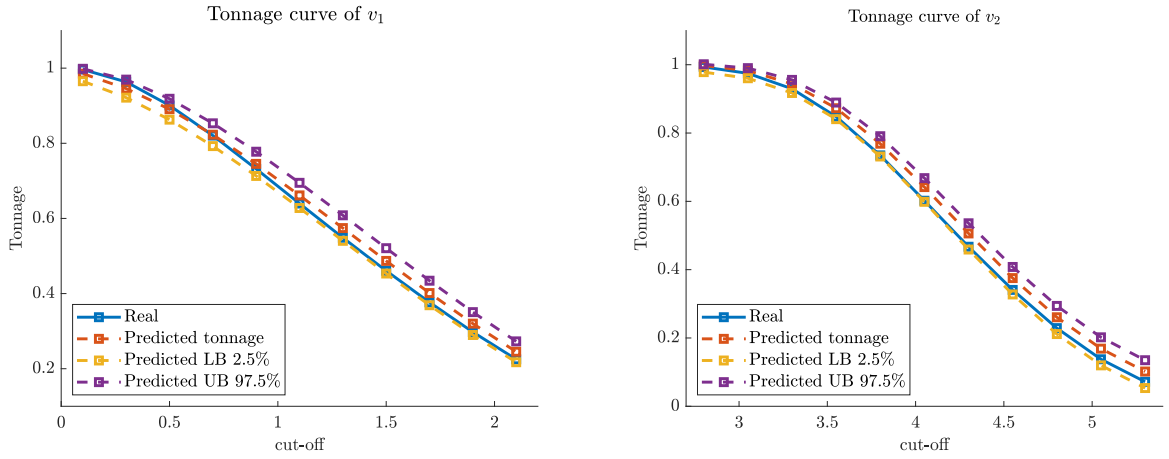

(a) v_1 (b) v_2

Figure 6.6 Predicted mean tonnage curve (orange dashed line) and its 95% CI (yellow and purple dashed lines) along with the real tonnage curve (blue line) for (a) v_1 and (b) v_2. Bivariate predictions

6.4.4 Comparison of univariate and bivariate MLR training for constrained tonnage curves

The tonnage curves of v_1 subject to a constraint on the value of v_2 are computed to mimic the case of a contaminant affecting the recoverability of the primary variable. The bivariate predictions of the tonnage curves are derived from the surfaces obtained through bivariate MLR training. These curves are compared against the predictions obtained using univariate

MLR training and assuming independence between v_1 and v_2, i.e., $P(v_1 > c_1 \cap v_2 < 5) = P(v_1 > c_1) \times P(v_2 < 5)$.

Figure 6.7 displays important differences between the two cases. The real constrained tonnage curve is better reproduced by the bivariate MLR approach, while the univariate predictive model has a significant bias at high cutoff values. Moreover, the real curve is entirely within the predicted bivariate 95% CI, which is not the case for the univariate 95% CI. Note that the width of the predicted CI is significantly narrower for the bivariate MLR training than for the univariate training. This is due to the strong positive correlation (0.76) between the variables, which is accounted for in the bivariate training but ignored in the univariate training.

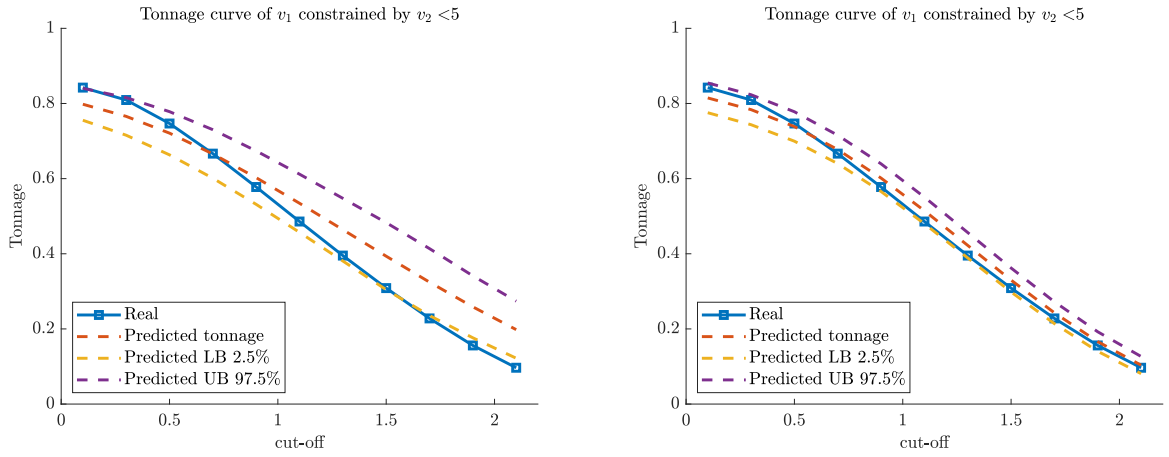

(a) Univariate predictions

(b) Bivariate predictions

Figure 6.7 Predicted constrained tonnage curve (orange dashed line) and its 95% CI (yellow and purple dashed lines) along with the real constrained tonnage curve (blue line). (a) Univariate MLR training and (b) bivariate MLR training

6.5 Case study: Multi-element nickel deposit

For Ni deposits, the SiO_2/MgO ratio typically plays a key role in metallurgical processing and can result in downgrading ore tonnages. The mining operation has to provide the mill with ore that is sufficiently rich in Ni while controlling the SiO_2/MgO ratio (Sagadin et al., 2016). The maximum ratio that is accepted before downgrading the ore can vary from mine to mine but is typically close to 2. Note that the non-additivity of the SiO_2/MgO ratio makes it necessary to simulate SiO_2 and MgO on point support and then compute the ratio of averages over SMU support.

6.5.1 Reference deposit

The lateritic profile is formed by a superficial iron-rich layer over a limonite layer that follows a transition zone to finish in a saprolite zone. The nickel enrichment can be explained by the weathering of ultramafic rock. Other elements of interest are present, such as iron, cobalt, silica and magnesia.

A densely sampled sub-domain of the deposit contains 1,597 samples from 137 vertical drill holes composited at 1 m lengths for Ni, SiO_2 and MgO grades. Figure 6.8 shows the sample data and grades distribution for nickel. An LCM is fitted to the data (see Table 6.7) and used to produce the reference deposit by multivariate CS. A total of 1,054 samples are extracted from the reference deposit along vertical pseudo-boreholes, and this data is used to apply the proposed approach.

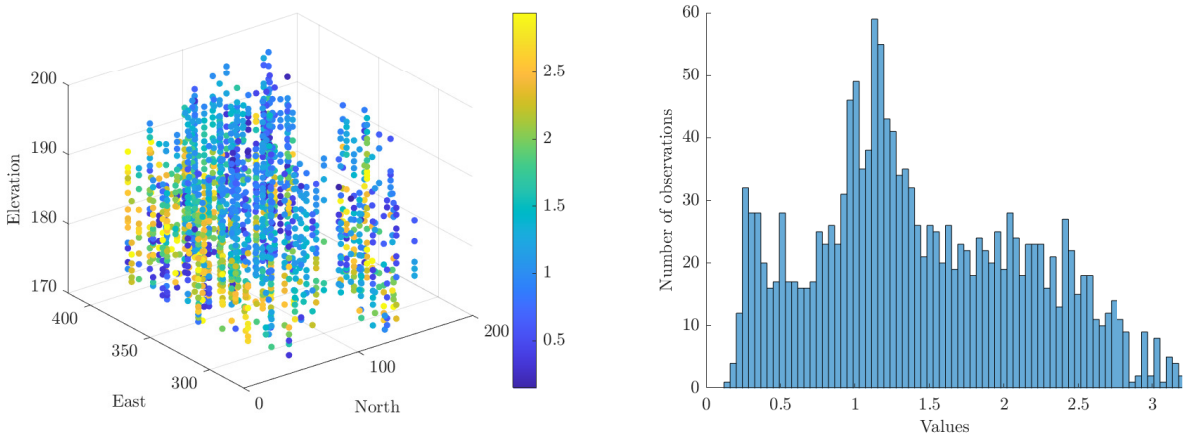

(a) Nickel sample data

(b) Nickel histogram

Figure 6.8 (a) Isometric view of nickel samples and (b) histogram of nickel grades

The main statistics of the 1,054 samples of the reference deposit are summarized in Table 6.6.

6.5.2 MLR training

The LCM parameter intervals used for training are given in Table 6.7. For each case, candidate LCM parameters are randomly drawn from these intervals and the LCM admissibility is checked. When a model is found non-admissible, new parameters are drawn. The input and output variables of each case are computed as described in Table 6.8. MLR training of the mean, UB (97.5 %) and LB (2.5 %) surfaces is conducted using a random subset of 70% of the admissible LCMs. The remaining 30% of admissible LCMs form the testing set.

Table 6.6 Basic statistics of the 1,054 samples of the reference deposit

	Mean	Min	Max	Std. dev.	CV	Skewness	Kurtosis
Ni	1.5	0.14	4.2	0.7	0.5	0.4	2.4
MgO	18.9	0.42	42.2	14.7	0.8	-0.1	1.3
SiO_2	26.8	0.7	77.8	18.1	0.7	-0.3	1.5

The MAE and RMSE values shown in Table 6.9 demonstrate both excellent prediction performance on the training set and adequate generalizability on the testing set. CP reaches the desired 95% CI on the training set and 94.1% on the testing set. The analysis of CP on the testing set at every cutoff pair (see Fig. 6.9(a)) shows almost perfect reproduction of the 95% CI in areas corresponding to most likely grade combinations. Fig. 6.9(b) displays the differences between a few randomly selected realizations (one out of every 100 realizations per LCM in the testing set) and the predicted UB and LB as a function of the nickel cutoff grades. These results illustrate that most of the curves lie within the predicted 95% CI.

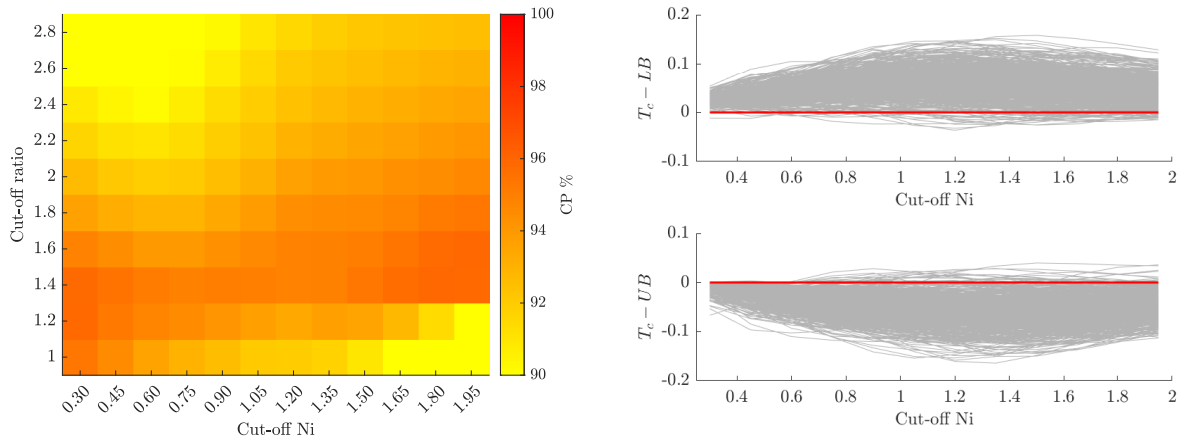

(a) CP

(b) difference between tonnage and LB-UB

Figure 6.9 (a) Heat map of mean CP as a function of cutoff values for the testing set and (b) difference between real tonnage curve and predicted LB/UB as a function of the nickel cutoff for the testing set

Table 6.7 Summary of the parameters utilized to generate the k =3,000 cases used for MLR training. Nickel deposit

Parameter	**Value and units**
Sampling density	1,054 samples
Cutoff values of Ni	From 0.3% to 2% in steps of 0.15%
Cutoff ratios	From 1 to 2.8 in steps of 0.2
Capping value of Ni	2.95%
Capping value of MgO	39.98%
Capping value of SiO_2	50.71%
Number of conditional realizations, n	100
Domain size	150 × 150 × 25 m
SMU size	5 × 5 × 5 m

LCM initial fitting	**Variation for MLR training**
Nugget matrix $\begin{bmatrix} 0.2 & -0.1 & 0 \\ -0.1 & 0.22 & 0 \\ 0 & 0 & 0.2 \end{bmatrix}$	± 0.2 on all the terms
Correlation matrix $\begin{bmatrix} 1 & -0.1 & 0.4 \\ -0.1 & 1 & 0.63 \\ 0.4 & 0.63 & 1 \end{bmatrix}$	± 0.2 on the off-diagonal terms
Sill matrix $\begin{bmatrix} 0.8 & 0 & 0.4 \\ 0 & 0.78 & 0.63 \\ 0.4 & 0.63 & 0.8 \end{bmatrix}$	As described in Section 6.3.2
Range	$\in$ [30, 70] m
Variogram model	Spherical

6.5.3 Nickel tonnage curve prediction

The input variables given in Table 6.8 are computed for the sample data extracted from the reference deposit. The surface models predicted by bivariate MLR training (see Fig. 6.10(a)) make it possible to compute the predicted mean and 95% CI for tonnage resources of nickel and compare them to the recoveries obtained from the reference deposit, as illustrated in Fig. 6.10(b).

6.5.4 Comparison of univariate and bivariate predictions for nickel tonnage curves constrained to the SiO_2/MgO ratio

Given the operational requirement to control the SiO_2/MgO ratio, it is necessary to determine the Ni resources that are subject to this constraint. On one hand, the nickel resources

Table 6.8 Summary of the input and output variables for tonnage surface prediction. Nickel deposit

	Variable	**Details**	**Quantity**
Inputs	Point tonnage surface from declustered sample data (NN interpolation)	Tonnage surface at 12 Ni cutoffs and 10 ratio cutoffs	12×10
	Tonnage surface from SMU grades computed from point NN interpolation	Tonnage surface at 12 Ni cutoffs and 10 ratio cutoffs	12×10
	Experimental cross-variograms of Gaussian transform for Ni and ratio values computed along the borehole	$\gamma_{\text{Ni}}(h)$, $\gamma_{\text{ratio}}(h)$ and $\gamma_{\text{Ni-ratio}}(h)$ for $h \in \{5, 10, ..., 25\}$	15
		Total	255
Outputs	Mean tonnage surface	Tonnage surface at 12 Ni cutoffs and 10 ratio cutoffs	12×10
	2.5% quantile tonnage surface	Tonnage surface at 12 Ni cutoffs and 10 ratio cutoffs	12×10
	97.5% quantile tonnage surface	Tonnage surface at 12 Ni cutoffs and 10 ratio cutoffs	12×10
		Total	360

with $SiO_2/MgO<2$ can be derived from the tonnage surfaces (see the cross-section in Fig. 6.10(a)). On the other hand, the univariate prediction of these resources can be determined with separate training for Ni and the SiO_2/MgO ratio, under the independence assumption, using $P(\text{Ni} > c_1 \cap\ SiO_2/MgO < 2) = P(\text{Ni} > c_1) \times P(SiO_2/MgO < 2)$.

Figure 6.11 illustrates the predictions obtained using univariate and bivariate MLR training. Both predictions reproduce the real nickel resources constrained to ratio<2 appropriately. Nevertheless, the width of the predicted 95% CIs of univariate and multivariate MLR training phases are significantly different. Accounting for the joint distribution of Ni and the SiO_2/MgO ratio makes it possible to reduce the uncertainty on the predicted tonnage curves.

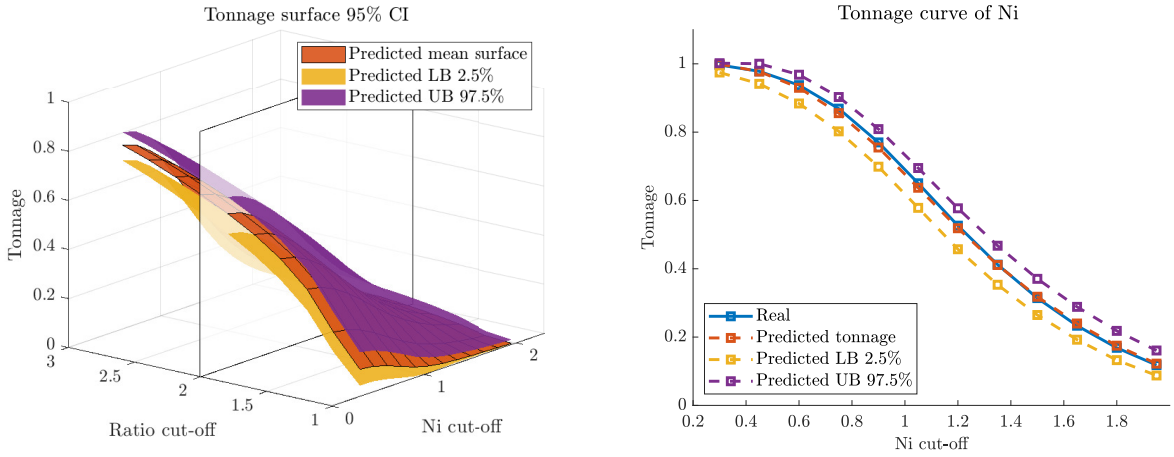

(a) Tonnage surface prediction

(b) Nickel resources

Figure 6.10 (a) Predicted tonnage surface (orange surface) and its 95% CI (yellow and purple surfaces) along with a cross-section at ratio<2 (white) and (b) predicted mean tonnage curve (orange dashed line) and its 95% CI (yellow and purple dashed lines) along with the real tonnage curve (blue line) for nickel resources

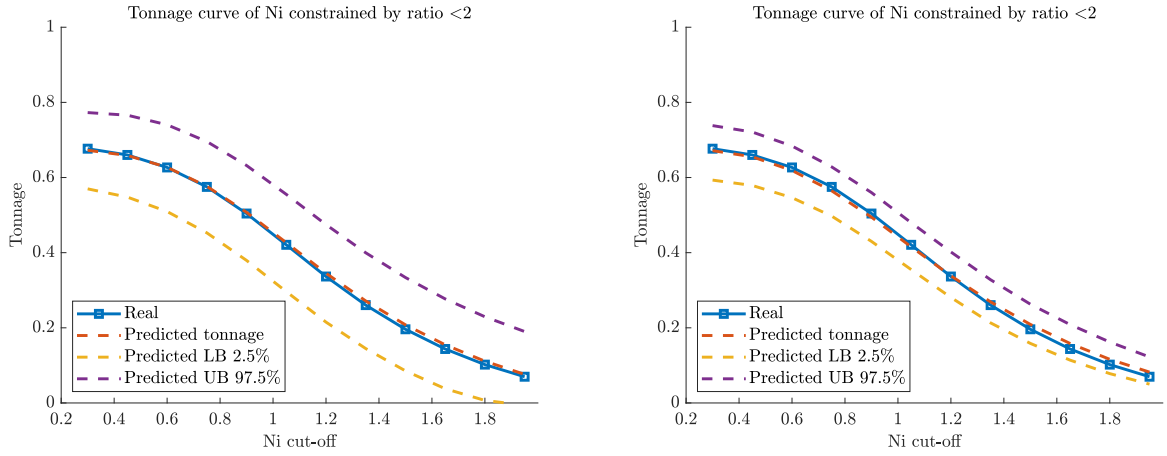

(a) Univariate predictions

(b) Multivariate predictions

Figure 6.11 Predicted mean tonnage curve (orange dashed line) and its 95% CI (yellow and purple dashed lines) along with the real tonnage curve (blue line) for nickel grades constrained by SiO_2/MgO<2. (a) Univariate MLR training and (b) multivariate MLR training

Table 6.9 Metrics to evaluate MLR learning for the training and testing sets. Nickel deposit

	Curve	MAE	RMSE	R^2	CP
Training set	LB	0.0195	0.0215	0.987	95%
	mean	0.0064	0.0077	0.993	
	UB	0.0111	0.0125	0.988	
Testing set	LB	0.0180	0.0195	0.985	94.1%
	mean	0.0084	0.0104	0.991	
	UB	0.0207	0.0225	0.985	

6.6 Discussion

The adequate assessment of recoverable resources and their associated uncertainty in the early stages of a mining project is essential for project success. Mineral deposits commonly host several variables of interest that should be jointly quantified to properly assess mineral resources. The multivariate conditional simulation is one tool that can be used to assess resource uncertainty. However, it relies on strong stationarity assumptions and requires the correct identification of parameters of the coregionalization model. Errors of the coregionalization model parameters definition (LCM herein for simplicity) directly impact the predicted recoverable resources and, above all, the uncertainty quantification. On the contrary, data-driven techniques do not require the problematic fitting of an LCM because several LCMs are used in the training phase considering parameters randomly selected within a large interval of possible values. The predicted recoverable resources are directly obtained from statistics based on the data. Admittedly, the proposed approach is computationally more demanding than the traditional CS in the training phase. However, it is shown that the approach provides an adequate uncertainty assessment on the resources (i.e., a right coverage of the real tonnage curves). A similar result could be obtained with CS only when the true underlying coregionalization model is used. Since fitting a coregionalization model relies on scarce and erratic data, the fitted model would most likely differ from the true one; therefore, CS would provide incorrect uncertainty quantification results. Thus, the additional computational time of the proposed approach is deemed justified.

Despite their increased usage, data-driven methods have not been used to predict multivariate recoverable resources to our knowledge. This research develops a multivariate extension of the studies carried out by Mery et al. (2020) and Mery & Marcotte (2022), one that focuses on predicting recoverable resources (i.e., tonnage curves) and their uncertainty.

A synthetic bivariate case obtained from a physical model is analyzed to validate the proposed methodology. The metrics on the training and testing sets (see Table 6.5) show excellent prediction performance since MAE and RMSE are lower than 0.01 for both sets and R^2 is close to one. The average CP is 95% for the training set and 94% for the testing set, which is close to the CI imposed by the correction function. Moreover, for most cutoff pairs the coverage in the testing set is close to the nominal 95% level, indicating the CIs are credible. We stress that the testing set is not used in the learning phase, so this suggests good generalizability of the MLR model obtained using the proposed training approach.

A comparison of univariate and bivariate MLR training is also performed on the synthetic deposit. As compared to the univariate learning approach, the bivariate approach simultaneously better estimates the real tonnage curve and produces a narrower CI while maintaining the right coverage. It should be noted that no inconsistencies such as crossing of the predicted tonnage curves or non-monotonicity of the tonnage functions are observed, despite these constraints not being explicitly incorporated in the training.

Regarding the lateritic nickel deposit, the MLR approach is used to predict the nickel tonnage curves subject to $SiO_2/MgO<2$ on simulated SMU grades. The non-additivity of the SiO_2/MgO ratio is resolved by simulating each variable separately and computing the ratio of averages at SMU support. The recoverable resources and their uncertainty are precisely estimated (refer to Fig. 6.11(a)). However, the univariate predictive models exhibit greater uncertainty on the predicted resources (Fig. 6.11(b)), confirming that the incorporation of correlation between highly correlated variables improves the predicted tonnages obtained.

A correction function is introduced to correct coverage bias observed when MLR is applied to raw CS quantiles. The results shown in Figs. 6.4 and 6.9 validate the proposed correction function, as the CP reaches the desired 95% in the area of most likely values for the variables studied. The correction function is defined by six parameters (in the bivariate case) that have to be optimized (see Eq. 6.5). The objective function includes a weighting function so as to give more weight to the most likely values of the joint distribution. The weight function is proportional to the norm of the gradient vector of the tonnage surface.

One of the main possible drawbacks of the proposed approach is that MLR training is still based on the multiGaussian model when jointly simulating the variables of interest, which might be unsuitable in some cases. This drawback is shared by the usual CS approach and its LCM fitting. However, in the proposed approach, the final predictions are obtained using only statistics extracted from data, which may confer some robustness to the results as suggested by the synthetic case where good results are obtained using variables computed from a physical model in which Gaussianity is not expected a priori.

The proposed MLR approach involves CSs using an LCM for the sake of simplicity. Recent works propose a series of multivariate models that are more general than the LCM used and could easily be used in its place. Some examples include hypergeometric covariance kernels (Emery & Alegría, 2021), Matérn covariance (Emery et al., 2021) and the possible adaptation of the twenty-two parametric isotropic multivariate covariance kernels defined in spheres proposed by Emery et al. (2021).

A final note about the computational aspects: a different training is done at each cutoff pair and for each curve. The cutoffs selected in the two case studies represent a total of 396 different training phases for the synthetic case and 360 training phases for the lateritic deposit. Moreover, the optimization of the six parameters of the coverage correction function involves retraining the LB and UB surfaces for each iteration. Despite this quite large number of training phases, the efficiency of MLR and the reduced size of each training make the computing time of the training step almost negligible compared to the time spent producing the CSs required to obtain the input and output data for training.

6.7 Conclusions

Data-driven methods, such as multiple linear regression, can provide a reliable alternative approach to predict recoverable resources and assess their geological uncertainty for univariate and multivariate ore deposits. The results obtained on a synthetic bivariate deposit and a lateritic nickel deposit demonstrate the proposed approach's capacity to assess tonnage resources and their uncertainty. The confidence intervals obtained present close-to-nominal-level coverage, indicating they are credible. A comparison of univariate and bivariate MLR predictions emphasizes the importance of including existing dependence between variables for adequate mineral resource quantification, especially when conditioning constraints are applied.

CHAPTER 7 COMPLEMENTARY RESULTS

Four additional analyses are carried out to enhance the results of the proposed ML approach. These complementary results corroborate the applicability of the ML approach in two different non-Gaussian cases, studying the effect of the sampling density on uncertainty quantification, analyzing the ML approach under a resource category definition (i.e., measured and indicated), and extending this method to the conventional benefit assessment.

7.1 3D synthetic non-Gaussian deposits

The additional synthetic cases are further analysed to complement the results presented in Section 6.4.1, following the same procedure.

The synthetic models correspond to X-ray 3D microphotogrammetry of small carbonate and sand cubes (Fig. 7.1 (a) and (b), respectively). Univariate analyses are carried out. It should be noted that there is no Gaussian signature in any of these cases, and also, they are significantly different.

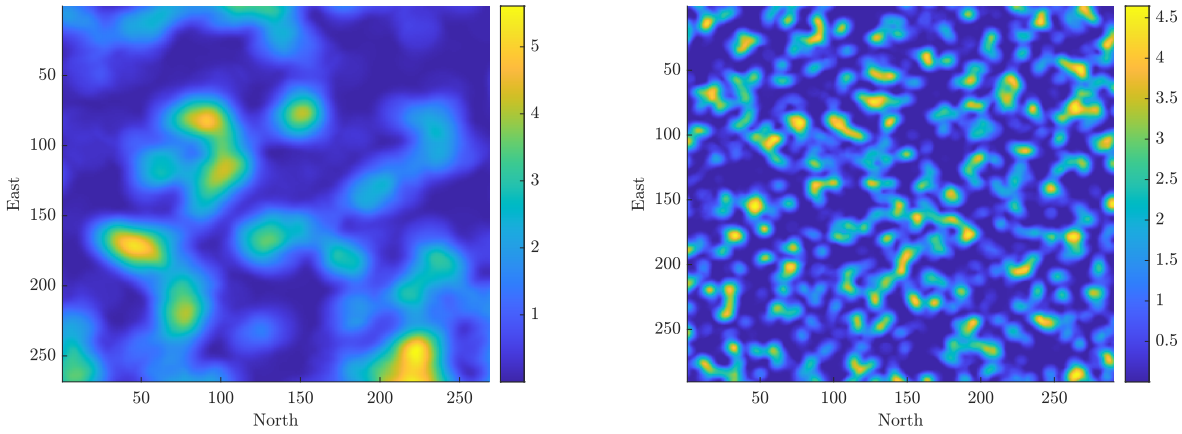

(a) Carbonate cube (b) Sand cube

Figure 7.1 Section view at elevation 120 (a) carbonate cube and (b) sand cube

The main statistics of each case are presented in Table 7.1.

Boreholes are sampled on a pseudo-regular grid on each case considering different locations (see Fig. 7.2 (a) and (b)).

The training parameter intervals of each case are given in Table 7.2.

Table 7.1 Basic statistics

	Mean	Min	Max	Std. dev.	CV	Skewness	Kurtosis
Carbonate cube	0.98	0	6.25	1	1.02	1.49	5.05
Sand cube	0.94	0	4.64	1	1.08	1.22	3.78

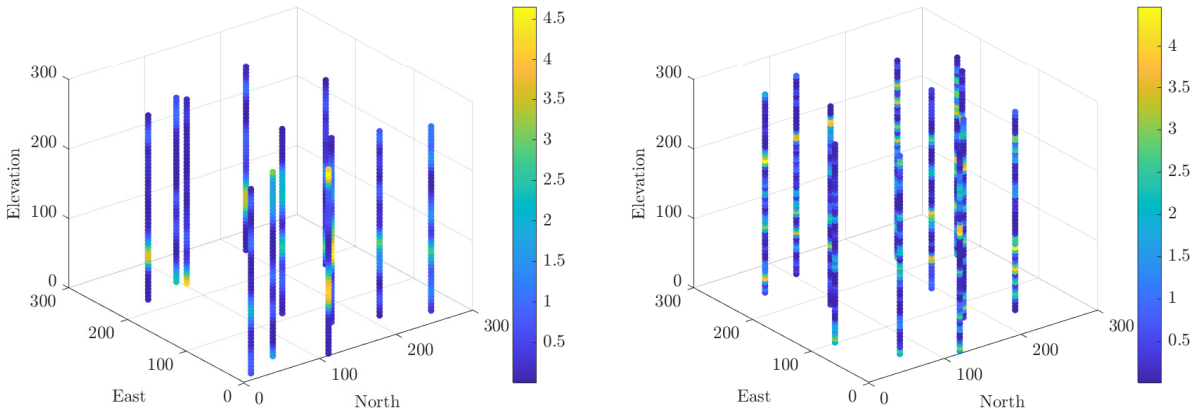

(a) Carbonate cube (b) Sand cube

Figure 7.2 Samples of (a) carbonate cube and (b) sand cube

Then, 70% of the input-output pairs (defined in Tables 6.1 and 6.2) are used as training set in the MLR training, while the testing set is composed of the remaining 30%. Three predictive models for each case are generated, representing the mean, 2.5% and 97.5% quantiles. Using the boreholes defined in Fig. 7.2, the mean tonnages are predicted, as well as the 95% CI curves for the carbonate (Fig. 7.3 (a)) and the sand cases (Fig. 7.3 (b)).

This result supports the conclusion that cases exhibiting dissimilar textures with different spatial continuities and sample locations can generate results able to reproduce the real tonnage curve. This is due to the low MAE for both the carbonate case (0.0105) and the sand case (0.0283). Moreover, the predicted CIs provide a measure of the uncertainty on the tonnage resources as the real tonnage curves lie completely within the defined CIs. Therefore, the approach appears robust to the particularities of the studied field.

Table 7.2 Summary of the parameters to generate the $k = 3,000$ cases used for each MLR training. 3D synthetic carbonate and sand cases

Parameters carbonate case	**Values**
Number of conditional realizations	100
Cutoff values	From 0.1 to 1 in steps of 0.1
SMU size	$15 \times 15 \times 15$
Domain size	$268 \times 268 \times 268$
Nugget	$\in$ [0,0.2]
Sill	1 - Nugget
Range	$\in$ [35,100]
Variogram model	Cubic
Parameters sand case	**Values**
Number of conditional realizations	100
Cutoff values	From 0 to 1.2 in steps of 0.1
SMU size	$15 \times 15 \times 15$
Domain size	$282 \times 282 \times 282$
Nugget	$\in$ [0,0.2]
Sill	1 - Nugget
Range	$\in$ [10,24]
Variogram model	Cubic

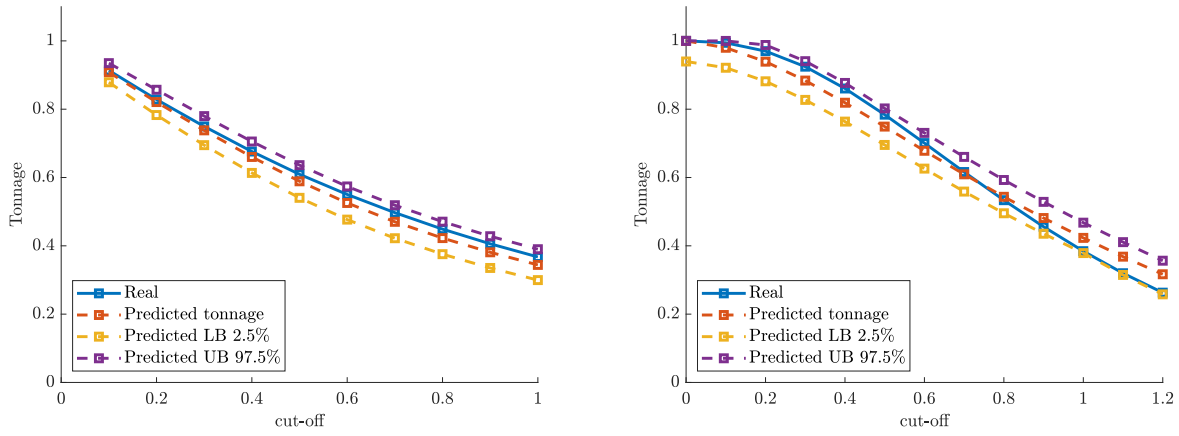

(a) Carbonate cube

(b) Sand cube

Figure 7.3 Predicted mean tonnage curve (orange dashed line) and its 95% CI (yellow and purple dashed lines) along with the real tonnage curve (blue line) for (a) carbonate cube and (b) sand cube

7.2 Influence of the sampling density

The effect of the amount of data (i.e., the number of boreholes used as conditioning data) is tested to evaluate whether the additional information of sample data can have a considerable impact on the prediction performance of the real curve and the uncertainty assessment by evaluating the width of the 95% CI. The synthetic variable v_1 defined in Section 6.4.1 is employed to carry out the analysis. Three configurations are defined (i.e., three, six, and twelve boreholes), where the smallest boreholes configurations are included in the definition of the subsequent configurations. Figure 7.4 shows the defined boreholes configurations.

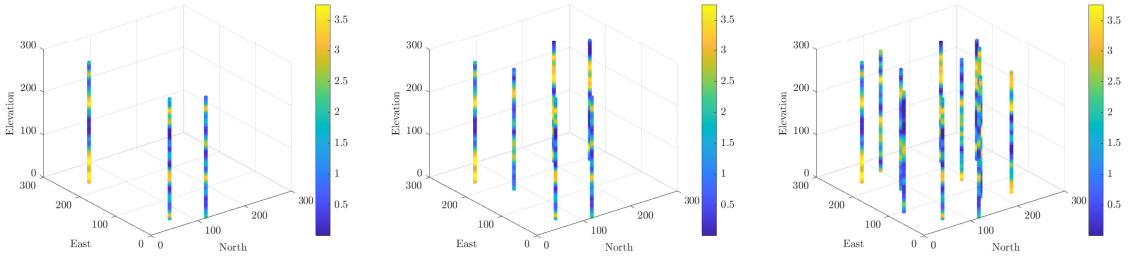

(a) 3 boreholes (b) 6 boreholes (c) 12 boreholes

Figure 7.4 Sample configurations. (a) 3 boreholes, (b) 6 boreholes, and (c) 12 boreholes

An univariate adaptation of the procedure detailed in Algorithm 2 is performed for each boreholes configuration, using the same parameters and input-output variables described in Section 6.4.1. After each MLR training is performed, each boreholes configuration displayed in Fig. 7.4 is used to obtain the predicted mean and 95% CI (see Fig. 7.5).

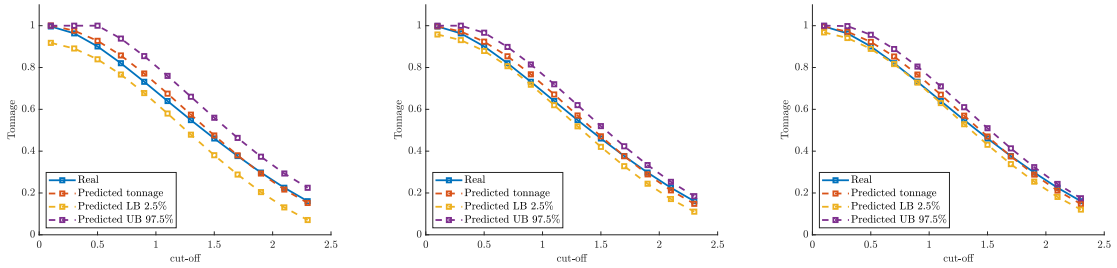

(a) 3 boreholes (b) 6 boreholes (c) 12 boreholes

Figure 7.5 Predicted mean tonnage curve (orange dashed line) and its 95% CI (yellow and purple dashed lines) along with the real tonnage curve (blue line) using as conditioning data (a) 3 boreholes, (b) 6 boreholes, and (c) 12 boreholes

Based on Fig. 7.5, there are no significant differences between the prediction performance of

each borehole configuration compared with the real tonnage curve, as the MAE is close to 0.015 for the three sampling densities. In addition, all the predicted 95% CI contain the real tonnage curve. Nonetheless, the uncertainty associated with each case clearly changes as the width of the predicted 95% CI decreases, as expected, when the number of conditioning data increases.

7.3 Application using mineral resources categories

The synthetic variable v_1 introduced in Section 6.4.1 is utilized to study whether the proposed MLR approach can predict the tonnage curves and their uncertainty on different mineral resource categories. To this end, a new set of vertical boreholes is defined on the physical cube (Fig. 6.2 (a)) to compute the predicted values and their associated variance through ordinary kriging (See Fig. 7.6 (a) for the kriging variance map at level 120m). The kriging variance is employed to determine the kriging efficiency (KE), which allows the mineral resources to be classified as

$$\text{Category} = \begin{cases} \text{Measured} & \text{when KE} \geq 0.8 \\ \text{Indicated} & \text{when } 0.5 \leq \text{KE} < 0.8 \\ \text{Inferred} & \text{otherwise} \end{cases} \tag{7.1}$$

The final definition of the resource categories (Fig. 7.6 (b)) is obtained after morphological operators that consider a disk as a structuring element of radius 2 for the closing and radius 1 for the opening operations. It is of great importance to note that no inferred resources are defined due to the high amount of sampling data. Moreover, the sample locations have a noticeable effect on the resources category definition since the kriging efficiency is related to the kriging variance.

For each defined category, the samples within the category domain are used to choose the parameters needed to carry out the MLR training independently. As a result, the predicted tonnage and 95% CI for the measured and indicated resources are shown in Fig. 7.7 (a) and (b), respectively. Higher uncertainty (i.e., wider CI) is observed for the indicated resources compared with the measured resources. Therefore, the MLR approach reproduces the level of confidence of the mineral resources classification.

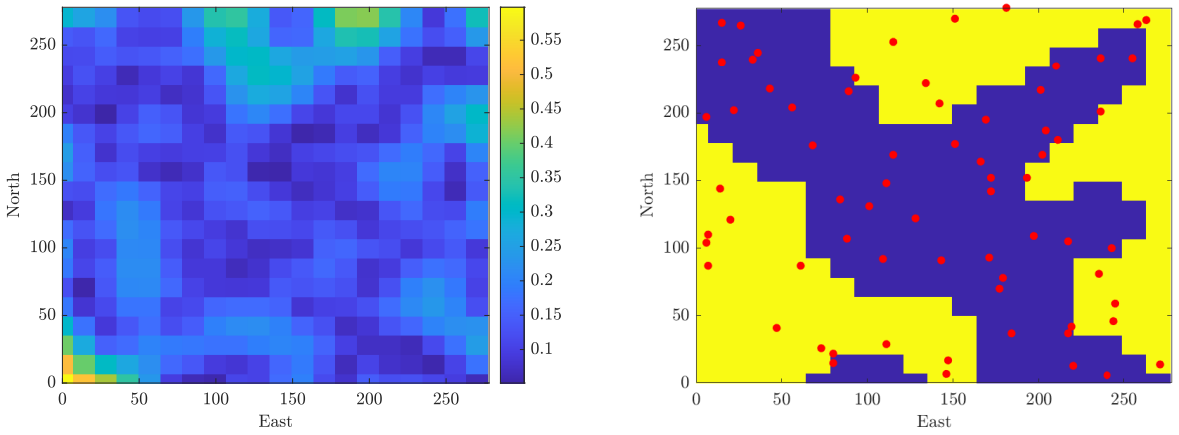

(a) Kriging variance

(b) Resources categories

Figure 7.6 (a) Section view of the kriging variance at elevation 120. (b) Resources categories obtained using the kriging efficiency. Measured resources (blue) and indicated resources (yellow) along with sampling data (red dots)

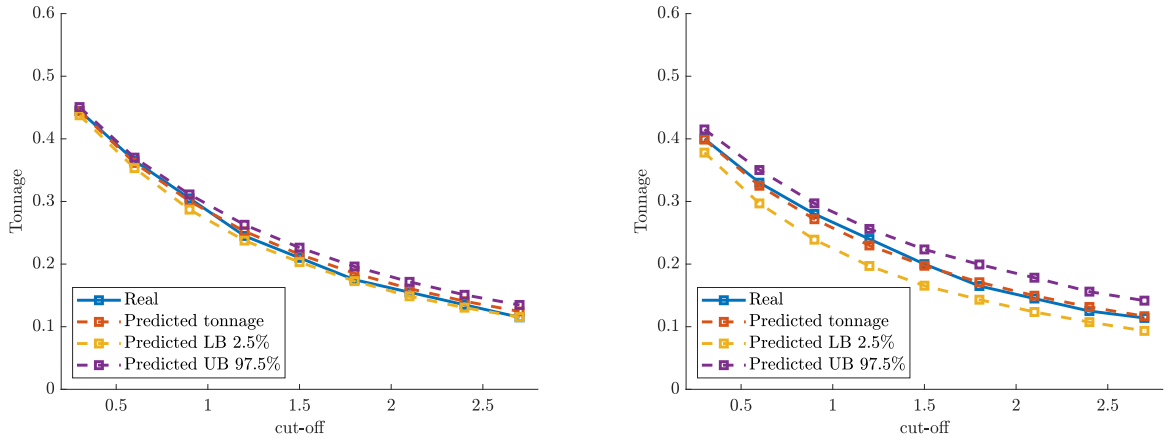

(a) Measured resources

(b) Indicated resources

Figure 7.7 Predicted mean tonnage curve (orange dashed line) and its 95% CI (yellow and purple dashed lines) along with the real tonnage curve (blue line). (a) Measured resources and (b) indicated resources

7.4 Another recovery function: the conventional benefit

A new recovery function (i.e., conventional benefit) is predicted to extend the proposed ML approach. The same methodology described in Algorithm 2 of Section 6.3 is applied, where step 2.10 does no longer calculate the tonnage curves, but instead computes the conventional benefits $B(z)$, i.e., the difference between real recovered metal quantity and the minimum quantity that is supposed to be recovered above the cut-off grade. Quantifying the conventional benefit provides a general idea of profit estimation from exploiting an ore deposit, even when no discount rates are considered. The benefit integrates the tonnage and ore grade, and therefore, it is a valuable tool to characterize the available recoverable resources.

The carbonate cube introduced in Section 7.1 is used considering v_1 and its parameters to perform the MLR training. The result indicates an excellent reproduction of the real conventional benefit curve from the full carbonate cube and the associated 95% CI (see Fig. 7.8). The predicted 95% CI of the conventional benefit is wider than the predicted 95% CI of the tonnage curves in Fig. 7.3 (a). This can be explained by the higher variability of the benefit values compared with the tonnage values, which are defined in a [0-1] range, whereas the conventional benefit involves both the tonnage and the grade, each with its own uncertainty.

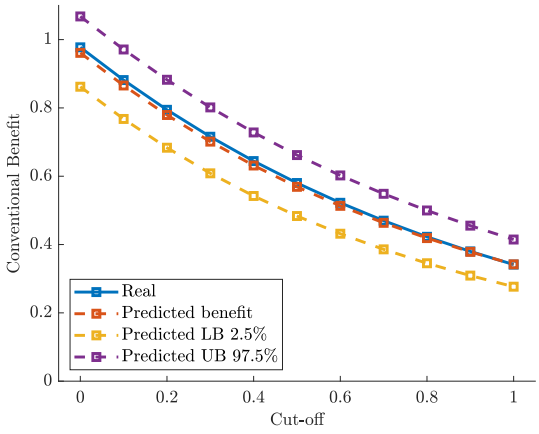

Figure 7.8 Predicted mean conventional benefit curve (orange dashed line) and its 95% CI (yellow and purple dashed lines) along with the real conventional benefit curve (blue line)

CHAPTER 8 GENERAL DISCUSSION

Three techniques have been proposed for the recoverable resources assessment and their uncertainty quantification. The research encompasses the use of geostatistics and machine learning techniques to predict resources considering change of support, providing non-smoothed estimates, properly characterizing the resource uncertainty, and extending their applicability to multi-elements ore deposits. The findings allow adequate fulfilment of the gaps of knowledge found in the state-of-the-art for the recoverable resource prediction, which is discussed in the following paragraphs.

CK is proposed to avoid the smoothness of traditional geostatistical approaches such as OK (refer to Chapter 4). This technique is able to predict recoverable resources taking into account the change-of-support in a univariate setting. The results enrich knowledge on CK since its applicability is extended beyond the environment field by predicting recoverable resources in the mining field by using synthetic cases and two real case studies (including a gold deposit). Moreover, the robustness of CK is studied considering several kriging neighborhood configurations, demonstrating the advantages over traditional methods such as UC. The major strength of CK is the reproduction of the grade variability, which is guaranteed as the method is designed to accomplish this property. CK also allows local and global predictions to be obtained within the studied ore deposits. The application of CK is straightforward and avoids the assumptions of non-linear predictors (e.g., DGM and UC). However, its main drawbacks are the possibility to get some imaginary predicted values when using small neighborhoods (e.g., no imaginary values were obtained for neighborhoods of at least one sample per quadrant in the case studies) and the inability to provide a measure of uncertainty on the predictions. The former issue can be dealt with a large neighborhood definition because the method is not affected by the smoothing effect (therefore, there is no need to restrict the neighborhood to attenuate this effect), while the use of CK variance can partially address the latter. It is important to note that this variance depends on the data configuration without accounting for the data values, so it is a measure of the neighborhood adequacy (same as for kriging variance). It does not provide a measure of precision on recoverable resources. Despite these drawbacks, the method is still better than traditional geostatistical predictors for recoverable resources prediction. The predicted negative values obtained by CK can be problematic if this proportion is high compared to the total predicted values; nevertheless, the case studies did not exhibit a proportion greater than 1%, where a straightforward solution is to set the negative values to zero.

Since CK is unable to quantify the uncertainty on both predicted values (beyond an error variance) and non-linear functions of the predicted values (such as, the recovery functions), there is a need to provide alternative approaches to address this challenge. CS, which is a possible option, is highly sensitive to model parameters definition and relies on strong assumptions. Considering that data-driven methods can avoid specifying the model parameters, ML techniques arise as promising tools to deal with the uncertainty assessment in mineral resource evaluation. The research carries out the recoverable resources assessment and the corresponding uncertainty quantification under a supervised learning environment, utilizing geostatistical simulations to obtain the input-output variables for the ML training (refer to Chapter 5). The outcomes of this thesis significantly improve current knowledge toward ML applications in mineral resources prediction. A comparison between ML techniques reveals that MLR is the most suitable method for the objective because it provides similar results faster than other alternative techniques, such as ANN. This can be explained by the strong correlation between input and output variables used in the training. The usability of MLR is demonstrated by the excellent prediction performance and an adequate generalization capability to predict recoverable mineral resources. The results obtained using the testing sets exhibit almost the same precision and coverage compared with the training sets. The MLR training time is negligible compared to the generation of the input-output variables required to perform the training. The predicted tonnage curves do not exhibit inconsistencies, for instance, non-monotonic behavior or crossing, even when no constraints are imposed on the training. ML techniques enable uncertainty to be assessed on recoverable resources as successfully confirmed by applying MLR and a correction function. This function is needed to adjust the initial ensued coverage through a straightforward and fast implementation. This correction is not applied with ANN due to its complexity and slowness. Consequently, the research suitably addresses the question that emerged during the literature review, concluding that ML techniques can predict recoverable mineral resources and perform their uncertainty evaluation. A novel finding from the application of the ML approaches is the new paradigm provided for assessing mineral resources since there is no need to define specific parameters. Furthermore, ML techniques may be suitable for preliminary studies in mining projects when there is insufficient available data to fit a variogram model and to make hypotheses on their distribution. Therefore, ML techniques become a promising alternative to traditional geostatistical methods; for example, CS, which is the most similar approach but is highly sensitive to the chosen variogram model.

A multivariate ML approach is proposed to predict the recoverable resources and their uncertainty for multiple elements of interest (refer to Chapter 6), based on the work of Mery & Marcotte (2022). The application of multivariate ML techniques helps to deepen knowledge

on how ML techniques perform on the mineral resources evaluation of multi-element ore deposits and on uncertainty quantification in multivariate contexts. Moreover, this research confirms the idea that carrying out the joint prediction of mineral resources is more beneficial when spatially correlated variables are analyzed. The principal drawback of this approach is the application of geostatistical simulations to generate the feature and target variables that still need LCMs to characterize the spatial continuity of the regionalized variables. Some attempts to fit the LCMs using the Bayesian inference were unsuccessful as this method is sensitive to the underlying Gaussian hypothesis. Projection pursuit multivariate transform (PPMT) was also tested as an option to avoid the fitting of a LCM; nonetheless, the results show a poorer prediction performance and therefore are not presented in the thesis. Another disadvantage of the ML approach is the necessity to update the predicted curves by new training when additional data is available (e.g., data gathered from production drill holes during the exploitation of the mine). It is expected that the mean tonnage curve does not significantly change if this information is incorporated; however, the width of the CIs can be substantially modified as shown in Section 7.2. This limitation can be handled by the efficiency of the MLR training and the simple definition of the input-output variables, where both maintain the regular update of the predicted models tractable if efficient CS algorithms are used. The multivariate ML approach has the potential to circumvent not only the definition of unique parameters but also the heavy reliance on assumptions usually accepted in traditional geostatistical multivariate approaches. Ultimately, the method allows for the assessment of multiple elements of interest and their geological uncertainty. This prediction can be conducted on either a primary variable or resources of a primary variable constrained by the values of a contaminant, which are typical scenarios that occur in mining projects.

Four complementary analyses (refer to Chapter 7) are performed to verify the robustness and suitability of the proposed ML approach. First, two additional cases (sand and carbonate cubes) confirm the results obtained with the ceramic cube presented in Chapter 6, as they validate the ability of MLR to reproduce the mean tonnage curves and characterize their uncertainty. These case studies are 3D physical models where Gaussianity is not visually exhibited, and therefore, the robustness of the approach under non-Gaussian fields is confirmed. The second study analyzes the influence of the amount of data on the uncertainty assessment. The width of the CI is reduced when additional data is provided to the MLR training. This finding confirms the idea that uncertainty on the tonnage resources can be diminished when more information is included, as typically occurs throughout mining exploitation. The third analysis is carried out to predict the tonnage resources within two domains classified as measured and indicated. A tonnage prediction is obtained for each resource category, where a higher uncertainty is observed for indicated resources compared to measured resources.

This outcome is expected since the resource classification is defined based on the kriging variance, which considers the sample configuration. As a result, a thinner CI is predicted within the measured resources area as more samples are available. Finally, the conventional benefit is predicted by the proposed approach. An excellent prediction of the mean benefit and uncertainty quantification is observed. This result extends the applicability of the ML approach, which has been tested herein only for tonnage resources.

Some assumptions of the ML approach should be stated. The uncertainty on the domain boundaries is not considered, and therefore, they are assumed to be fixed. These boundaries can be defined, for instance, by using an implicit geological model, a geological interpretation from boreholes in cross-sections, blocks that define the classical three passes of kriging employed in NI-43-101 reports, from the blocks that correspond to the amount of production in specific years, among others. The use of both a known Gaussian transform to generate the reference deposits and the multiGaussian model are also assumed. This is not exclusive to the proposed approach as CS has the same limitation.

The research provides three meaningful proposals that deal with the main challenges identified in current practices for the recoverable resources assessment. A comparison against traditional geostatistical methods is carried out to determine whether the studied approaches are applicable to the mining field. It is clear that CK outperforms most of the popular methods, namely OK and UC, based on the resulted predictions as well as the robustness of CK. In addition, the univariate ML approach overcomes several methods, including CK, UC, OK, and IL. Even though DGM surpasses ML, it may not be a fair comparison due to the fact that DGM uses the true variogram model to obtain the predictions. A sensitivity analysis shows that a moderate variation on the block variance (e.g., 20%) results in a deterioration of the prediction obtained with DGM, implying that it is not a robust option for assessing recoverable resources. Consequently, it is worth noting that the proposed methods may become suitable alternatives in the mineral resource evaluation, especially at preliminary stages where a global characterization of the recoverable resources is required.

Comparing the three proposed approaches reveals that CK is faster than ML in terms of computational calculations. Learning methods require data generation from geostatistical simulations, while CK is more straightforward and does not depend on additional inputs. However, the MLR training itself is a rapid process, especially when compared with other ML techniques such as ANN. After the MLR training is completed, the determination of recovery curves and their corresponding CIs is almost instantaneous. Based on this, it can be inferred that CK is an appropriate alternative because of its simplicity compared to ML techniques, but it cannot provide an uncertainty quantification on the predicted recoverable

resources. Thus, ML methods are suitable options to assess their uncertainty.

A summary of features found in the proposed techniques is presented in Table 8.1. The checkmark indicates whether the approach is able to deal with or can be used for the properties stated on the left.

Table 8.1 Summary of features in the proposed geostatistical and machine learning techniques

Property	**CK**	**ML**	**Multivariate ML**
Change of support	✓	✓	✓
Avoid the smoothing effect	✓	✓	✓
Univariate predictions	✓	✓	
Multivariate predictions			✓
Uncertainty quantification		✓	✓
Non-parametric		✓	✓
Avoid variogram fitting		✓	✓
Global assessment	✓	✓	✓
Local assessment	✓		
Robustness against parameter misspecification	✓	✓	✓
Robustness against model assumptions	✓	✓	✓

ML techniques are capable of meeting more properties than CK as they can be employed for uncertainty assessment on the predicted recoverable resources, avoiding complex parameter definitions and strong assumptions (stationarity and multi-normality) found in traditional approaches. Hence, ML techniques should be the preferred method of choice when performing mineral resource evaluation, and depending on the ore deposit under study, the univariate or multivariate ML technique may be selected. Either the characterization of each SMU grade is required or a quick evaluation is needed, then, it is highly recommended to utilize CK to provide a local assessment of the resources.

CHAPTER 9 CONCLUSION AND RECOMMENDATIONS

The techniques available for resources assessment have been extended by proposing three complementary methods to conduct univariate and multivariate predictions, and also, to deal with the main challenges identified in the context of recoverable resource evaluation. The general objective of this research is successfully reached since the proposed approaches enrich current practices in the mining industry. The approaches aim to characterize recoverable resources at initial stages of mining projects, improving the decision-making process throughout the life-of-mine. This is due to the fact that precise predictions are provided along with a measure of their uncertainty, helping to generate mitigation plans during the development of mining projects.

The research is significantly relevant as it extends CK for the recoverable resources assessment and introduces novel techniques (i.e., machine learning). Although ML methods have gained extensive attention over the years, there is no research that addresses the prediction of recoverable mineral resources and their corresponding uncertainty. Hence, this gap in the state-of-the-art is filled by testing and validating the proposed methods, utilizing synthetic datasets and real ore bodies (gold and nickel deposits) as case studies.

9.1 Summary of Works

CK enables the prediction of non-smoothed block grades for the element of interest to accurately assess the recoverable resources. This method performs better than similar geostatistical predictors since it avoids the smoothing effect of OK and allows local predictions of the resources (for each individual SMU) to be obtained, overcoming the limitation of UC. Moreover, CK does not rely on strong assumptions about the data distribution and can be directly applied as OK is employed today. The validation of CK is carried out using one synthetic and two real case studies. The prediction performance for assessing the recovery functions exhibits appropriate results. Furthermore, CK shows robustness under different kriging neighborhood configurations. Based on these findings, CK becomes a promising alternative method to predict recoverable resources, instead of UC or LUC.

Machine learning can be utilized for the assessment of recoverable mineral resources and their associated uncertainty. The proposed ML approach considers the use of geostatistical simulations to compute a series of input-output variables. A key aspect is that there is no need to specify a unique variogram model as is usually done when CS is applied. Firstly,

MLR and ANN perform similarly and thus, the simplest and computationally much faster approach (i.e., MLR) is established as the studied ML technique. Secondly, MLR outperforms traditional geostatistical methods, non-linear approaches, and change-of-support models in predicting the recoverable resources. A sensitivity analysis verifies that MLR is able to surpass its competitor (i.e., DGM) when a misspecification on the variogram model affects DGM. In addition, when the true variogram is used, DGM is slightly more precise than MLR, but it does not provide CIs on the predicted resources. The efficiency of the ML approach is tested using two synthetic cases and a real gold deposit, providing an accurate quantification of the uncertainty on the predicted resources and a proper characterization of the recoverable resources in each case study. Therefore, ML is deemed to be part of current practices to properly assess global recoverable resources.

A multivariate extension of the MLR approach is provided to account for predicting multiple elements of interest and their corresponding uncertainty quantification in ore deposits. To this end, the recovery curve is extended to the concept of recovery surfaces, which describe the joint predicted resources in a bivariate context. The proposed MLR approach considers geostatistical simulation to generate the training set used in the learning phase. The resulting predicted surface models can determine the resources of both a primary variable and a primary variable constrained by thresholds of a secondary variable. A suitable prediction performance and uncertainty assessment are proved by employing a synthetic and lateritic nickel deposit. Comparing univariate and multivariate predictions obtained through the MLR approach confirms that the incorporation of the dependence relationships between correlated variables allows for enhancement of the evaluation of resources. Hence, a significant value can be derived from including the proposed approach into current methodologies to assess recoverable resources. Additional results verify the robustness of the ML approach in deposits where the multiGaussian distribution cannot be assumed. The ML approach is validated by three analyses: the effect of the sampling density properly exhibited in the predicted CIs, the adequate quantification of measured and indicated resources and their uncertainty, and an appropriate prediction of the conventional benefit.

In summary, the three complementary methods presented herein expand the range of approaches considered within the mining industry, providing novel solutions for specific challenges identified in current practices. These methods can be jointly applied, for instance, to determine the global recoverable resources and their uncertainty employing the ML approach, and subsequently, localize the ore grades by using CK.

9.2 Limitations

Even though the proposed methods can be considered as proper alternatives for the evaluation of recoverable resources, some limitations remain.

Up to now, CK has been applied only for univariate predictions (probably because their main applications have been carried out in the environment field) and is not able to provide a complete measure of the uncertainty on the predictions. Since the non-smoothness is guaranteed, deterioration may occur for the precision of the estimates, as seen in Table 4.4 for the gold deposit. However, its overall performance and robustness for the parameter definition of the kriging neighborhood can overcome this effect. The proposed ML approaches cannot localize the predicted resources because they are not designed for this purpose. As seen in current literature, numerous applications can predict ore grades at unsampled locations using ML techniques; however, these approaches are not considered in this research as they are out of the scope.

An additional restriction of ML methods is the computation time required to generate the predictive models. This is non-restrictive since proper simulation algorithms and parallel computing can surpass this limitation.

9.3 Future Research

Further studies may include seven lines of research to enhance the approaches carried out in the thesis.

Research should be focused on a multivariate extension of CK, which may be capable of including information on other variables of interest. Since orebodies are typically multi-element deposits, this study would have the particularity of generating non-smoothed predicted values under more realistic prediction scenarios.

The so-called information effect (Matheron, 1976a) has a direct impact on the selectivity of the recovery curves. This is generated by misclassifying ore and waste material based on the ultimate information available when the classification is performed. Consequently, further work should be focused on incorporating the information effect into the recoverable mineral resources prediction through the use of the proposed techniques. It should be noted that neither most resource studies nor NI-43-101 resources assessment reports have incorporated this effect.

Future research is also required to apply the proposed methods to other types of ore deposits, such as porphyry copper or iron deposits. This is key to verify their appropriateness and

robustness thoroughly.

Fitting an LCM is the default decision to characterize the spatial structure of variables hosted in multi-element ore deposits. The process can be especially challenging when several variables are simultaneously analyzed. Alternative methods for the LCM fitting process (i.e., Bayesian inference and PPMT) lead to unfavorable results in tests that are not reported in the thesis. In addition, further research should explore the non-linear coregionalization models (Marcotte, 2016) or utilize novel parametric covariance models that offer flexibility to represent the joint spatial correlation structure of coregionalized variables. For instance, Gneiting et al. (2010) and Apanasovich et al. (2012) provide validity conditions for the multivariate Matérn covariance model, in which each direct or cross-covariance can possess proper scale and shape parameters. Other parametric families such as the hypergeometric models in Euclidean spaces (Emery & Alegría, 2021) or models in other spaces such as spheres (Emery et al., 2021) that could possibly be adapted to define new models in Euclidean spaces.

The research could be extended using the proposed approach to predict the profit of the mineral resources and its uncertainty when the operational cut-off is known. This can be understood to be an extension of the conventional benefit assessment incorporating the real expected prices and costs.

In this thesis, three variables have been simulated for the nickel deposit, but the predicted resources are associated with nickel and the silica-magnesia ratio; therefore, the MLR training is performed as bivariate. Adaptations are needed to extend the proposed multivariate approach to more than two variables for the MLR training (e.g., nickel, cobalt, and chromium). The dimensionality of the problem likely implies that the training time would increase; however, this would not be a major obstacle to determining the recoverable resources.

Finally, the thesis applies ML techniques since no previous research has been conducted to assess recoverable mineral resources and quantify their uncertainty. However, the question still remains as to whether more sophisticated approaches (e.g., deep learning) will be suitable for improving or optimizing the obtained results. Ideally, deep learning should directly use raw data to predict the recovery functions without defining input and outputs variables. Even when more research is needed in this regard, it is expected that the computing power will be a considerable limitation for next years due to the deposit sizes, large amount of data, and complexity of the required networks.

REFERENCES

Abzalov, M. (2006). Localised uniform conditioning (LUC): A new approach for direct modelling of small blocks. *Mathematical Geology*, *38*, 393–411. URL: https://doi.org/10.1007/s11004-005-9024-6. doi:10.1007/s11004-005-9024-6.

Adeli, A., Dowd, P., Emery, X., & Xu, C. (2021). Using cokriging to predict metal recovery accounting for non-additivity and preferential sampling designs. *Minerals Engineering*, *170*, 106923. URL: https://www.sciencedirect.com/science/article/pii/S0892687521001527. doi:https://doi.org/10.1016/j.mineng.2021.106923.

Afeni, T., Lawal, A., & Adeyemi, R. (2020). Re-examination of Itakpe iron ore deposit for reserve estimation using geostatistics and artificial neural network techniques. *Arabian Journal of Geosciences*, *13*, 657. URL: https://doi.org/10.1007/s12517-020-05644-9. doi:10.1007/s12517-020-05644-9.

Alabert, F. (1987). The practice of fast conditional simulations through the LU decomposition of the covariance matrix. *Mathematical Geology*, *19*, 369–386. doi:10.1007/BF00897191.

Aldworth, J. (1998). *Spatial prediction, spatial sampling and measurement error*. Ph.D. thesis Iowa State University.

Aldworth, J., & Cressie, N. (1999). Sampling designs and prediction methods for Gaussian spatial processes. In S. Ghosh (Ed.), *Multivariate Analysis, Design of Experiments, and Survey Sampling* (pp. 1–54). New York volume 159.

Aldworth, J., & Cressie, N. (2003). Prediction of nonlinear spatial functionals. *Journal of Statistical Planning and Inference*, *112*, 3–41. doi:https://doi.org/10.1016/S0378-3758(02)00321-X.

Apanasovich, T., Genton, M., & Sun, Y. (2012). A valid Matérn class of cross-covariance functions for multivariate random fields with any number of components. *Journal of the American Statistical Association*, *107*, 180–193. doi:10.1080/01621459.2011.643197. arXiv:https://doi.org/10.1080/01621459.2011.643197.

Armstrong, M. (1984). Improving the estimation and modelling of the variogram. In G. Verly, M. David, A. G. Journel, & A. Marechal (Eds.), *Geostatistics for Natural Resources*

Characterization: Part 1 (pp. 1–19). Dordrecht: Springer Netherlands. URL: https://doi.org/10.1007/978-94-009-3699-7_1. doi:10.1007/978-94-009-3699-7_1.

Assibey-Bonsu, W., Deraisme, J., García, E., Gómez, P., & Ríos, H. (2014). Production reconciliation of a multivariate uniform conditioning technique for mineral resource modelling of a porphyry copper gold deposit. *Journal of The Southern African Institute of Mining and Metallurgy*, *114*, 285–292.

Assibey-Bonsu, W., & Muller, C. (2014). Limitations in accepting localized conditioning recoverable resource estimates for medium-term, long-term, and feasibility-stage mining projects, particularly for sections of an ore deposit. *Journal of the Southern African Institute of Mining and Metallurgy*, *114*, 619 – 625. URL: http://www.scielo.org.za/scielo.php?script=sci_arttext&pid=S2225-62532014000800012&nrm=iso.

Balamurali, M., L., K., & Melkumyan, A. (2019). A comparison of t-sne, som and spade for identifying material type domains in geological data. *Computers & Geosciences*, *125*, 78 – 89. URL: http://www.sciencedirect.com/science/article/pii/S0098300418306010. doi:https://doi.org/10.1016/j.cageo.2019.01.011.

Barnett, R., Manchuk, J., & Deutsch, C. (2014). Projection pursuit multivariate transform. *Mathematical Geosciences*, *46*, 337–359. URL: https://doi.org/10.1007/s11004-013-9497-7. doi:10.1007/s11004-013-9497-7.

Battalgazy, N., & Madani, N. (2019). Categorization of mineral resources based on different geostatistical simulation algorithms: A case study from an iron ore deposit. *Natural Resources Research*, *28*, 1329–1351. URL: https://doi.org/10.1007/s11053-019-09474-9. doi:10.1007/s11053-019-09474-9.

Benndorf, J. (2013). Application of efficient methods of conditional simulation for optimising coal blending strategies in large continuous open pit mining operations. *International Journal of Coal Geology*, *112*, 141–153.

van den Boogaart, K. G., Mueller, U., & Tolosana-Delgado, R. (2017). An affine equivariant multivariate normal score transform for compositional data. *Mathematical Geosciences*, *49*, 231–251.

Boucher, A., & Dimitrakopoulos, R. (2009). Block simulation of multiple correlated variables. *Mathematical Geosciences*, *41*, 215–237. URL: https://doi.org/10.1007/s11004-008-9178-0. doi:10.1007/s11004-008-9178-0.

Boucher, A., & Dimitrakopoulos, R. (2012). Multivariate block-support simulation of the Yandi iron ore deposit, Western Australia. *Mathematical Geosciences*, *44*, 449–468. URL: https://doi.org/10.1007/s11004-012-9402-9. doi:10.1007/s11004-012-9402-9.

Boyle, C. (2010). Kriging neighbourhood analysis by slope of regression and weight of mean - evaluation with the Jura data set. *Mining Technology*, *119*, 49–58. doi:10.1179/037178410X12741755140804.

Brooker, P. (1985). Two-dimensional simulation by turning bands. *Mathematical Geology*, *17*, 81–90. URL: https://doi.org/10.1007/BF01030369. doi:10.1007/BF01030369.

Bérubé, C., Olivo, G., Chouteau, M., Perrouty, S., Shamsipour, P., Enkin, R., Morris, W., Feltrin, L., & Thiémonge, R. (2018). Predicting rock type and detecting hydrothermal alteration using machine learning and petrophysical properties of the Canadian Malartic ore and host rocks, Pontiac Subprovince, Québec, Canada. *Ore Geology Reviews*, *96*, 130–145. URL: https://www.sciencedirect.com/science/article/pii/S0169136817308338. doi:https://doi.org/10.1016/j.oregeorev.2018.04.011.

Camus, Y., & Desharnais, G. (2015). *Practical Application of Kriging Neighbourhood Analysis for the selection of Interpolation Parameters. White Paper, 9 p.* Technical Report SGS.

Carrasco, P., Chilès, J.-P., & Séguret, S. (2008). Additivity, metallurgical recovery, and grade. In *Proceedings of the 8th International Geostatistics Congress*. Santiago, Chile volume 1188.

Carvalho, A., Ramos, F., & Chaves, A. (2011). Metaheuristics for the feedforward artificial neural network (ANN) architecture optimization problem. *Neural Computing and Applications*, *20*, 1273–1284.

Caté, A., Perozzi, L., Gloaguen, E., & Blouin, M. (2017). Machine learning as a tool for geologists. *The Leading Edge*, *36*, 215–219. doi:10.1190/tle36030215.1.

Caté, A., Schetselaar, E., Mercier-Langevin, P., & Ross, P.-S. (2018). Classification of lithostratigraphic and alteration units from drillhole lithogeochemical data using machine learning: A case study from the Lalor volcanogenic massive sulphide deposit, Snow Lake, Manitoba, Canada. *Journal of Geochemical Exploration*, *188*, 216–228. doi:10.1016/j.gexplo.2018.01.019.

Chatterjee, S., Bhattacherjee, A., Samanta, B., & Pal, S. (2006). Ore grade estimation of a limestone deposit in India using an artificial neural network. *Applied GIS*, *2*, 1–20. doi:10.2104/ag060003.

Chilès, J.-P., & Delfiner, P. (2012). *Geostatistics: Modeling Spatial Uncertainty*. (2nd ed.). New York: Wiley.

Chiquini, A., & Deutsch, C. (2020). Mineral resources evaluation with mining selectivity and information effect. *Mining, Metallurgy & Exploration*, *37*, 965–979. URL: https://doi.org/10.1007/s42461-020-00229-2. doi:10.1007/s42461-020-00229-2.

Cracknell, M., & Reading, A. (2014). Geological mapping using remote sensing data: A comparison of five machine learning algorithms, their response to variations in the spatial distribution of training data and the use of explicit spatial information. *Computers & Geosciences*, *63*, 22–33. doi:10.1016/j.cageo.2013.10.008.

Cressie, N. (1993). Aggregation in geostatistical problems. In A. Soares (Ed.), *Geostatistics Tróia '92* (pp. 25–36). Dordrecht: Springer Netherlands volume 1.

Cressie, N., & Aldworth, J. (1997). Spatial statistical analysis and its consequences for spatial sampling. In E. Baafi, & N. Schofield (Eds.), *Geostatistics Wollongong '96* (pp. 126–137). volume 1.

Cressie, N., & Johannesson, G. (2001). Kriging for cut-offs and other difficult problems. In P. Monestiez, D. Allard, & R. Froidevaux (Eds.), *geoENV III — Geostatistics for Environmental Applications* (pp. 299–310). Dordrecht: Springer Netherlands.

CSA (2016). *Standards of disclosure for mineral projects: National Instrument 43-101*. Canadian Securities Administration.

David, M. (1977). *Geostatistical ore Reserve estimation*. New York: Elsevier.

Davis, B., & Jalkanen, G. (1988). Nonparametric estimation of multivariate joint and conditional spatial distributions. *Mathematical Geology*, *20*, 367–381.

Davis, M. (1987). Production of conditional simulations via the LU triangular decomposition of the covariance matrix. *Matematical Geology*, *19*, 91–98.

De-Vitry, C., Vann, J., & Arvidson, H. (2007). A guide to selecting the optimal method of resource estimation for multivariate iron ore deposits. In *Iron ore conference* (pp. 67–77). Melbourne: Australasian Institute of Mining and Metallurgy Publication Series.

Demange, C., Lajaunie, C., Lantuejoul, C., & Rivoirard, J. (1987). Global recoverable reserves: Testing various changes of support models on uranium data. In G. Matheron, & M. Armstrong (Eds.), *Geostatistical Case Studies* (pp. 135–147). Dordrecht: Springer Netherlands. doi:10.1007/978-94-009-3383-5_11.

Deraisme, J., & Assibey-Bonsu, W. (2012). Comparative study of localized block simulations and localized uniform conditioning in the multivariate case. In P. Abrahamsen, R. Hauge, & O. Kolbjørnsen (Eds.), *Geostatistics Oslo 2012* (pp. 309–320). Dordrecht: Springer Netherlands. URL: https://doi.org/10.1007/978-94-007-4153-9_25. doi:10.1007/978-94-007-4153-9_25.

Deraismes, J., Rivoirard, J., & Carrasco, P. (2008). Multivariate uniform conditioning and block simulations with discrete gaussian model: application to Chuquicamata deposit. In *Proceedings of the 8th International Geostatistics Congress* (pp. 69–78). Santiago, Chile.

Desbarats, A., & Dimitrakopoulos, R. (2000). Geostatistical simulation of regionalized pore-size distributions using min/max autocorrelation factors. *Mathematical Geology*, *32*, 919–942. doi:10.1023/A:1007570402430.

Deutsch, C., & Journel, A. (1998). *GSLIB: Geostatistical Software Library and User's guide* volume 37. (2nd ed.). New York: Oxford University Press.

Deutsch, J., Szymanski, J., & Deutsch, C. (2014). Checks and measures of performance for kriging estimates. *Journal of the Southern African Institute of Mining and Metallurgy*, *114*, 223–230.

Dhaher, G., & Lee, M. (2013). A comparison between the performance of kriging and cokriging in spatial estimation with application. *Matematika: Malaysian Journal of Industrial and Applied Mathematics*, *29*, 33–41. doi:https://doi.org/10.11113/matematika.v29.n.357.

Dimitrakopoulos, R. (1998). Conditional simulation algorithms for modelling orebody uncertainty in open pit optimisation. *International Journal of Surface Mining, Reclamation and Environment*, *12*, 173–179. doi:10.1080/09208118908944041. arXiv:https://doi.org/10.1080/09208118908944041.

Dominy, S. (2007). Sampling - a critical component to gold mining project evaluation. In *Proj. Eval. Conf.* (pp. 89 – 96). Melbourne: Australasian Institute of Mining and Metallurgy Publication Series volume 23.

Dominy, S., Noppé, M., & Annels, A. (2002). Errors and uncertainty in mineral resource and ore reserve estimation: The importance of getting it right. *Exploration and Mining Geology*, *11*, 77–98. URL: https://doi.org/10.2113/11.1-4.77. doi:10.2113/11.1-4.77.

Dumakor-Dupey, N. K., & Arya, S. (2021). Machine learning—a review of applications in mineral resource estimation. *Energies*, *14*. URL: https://www.mdpi.com/1996-1073/14/14/4079. doi:10.3390/en14144079.

Dutaut, R., & Marcotte, D. (2019). A comparison of indirect lognormal and discrete gaussian change of support methods for various variogram estimators. *Journal of the Southern African Institute of Mining and Metallurgy*, *119*, 1–9.

Emery, X. (2005). Simple and ordinary multigaussian kriging for estimating recoverable reserves. *Mathematical Geology*, *37*, 295–319. URL: https://doi.org/10.1007/s11004-005-1560-6. doi:10.1007/s11004-005-1560-6.

Emery, X. (2007). On some consistency conditions for geostatistical change-of-support models. *Mathematical Geology*, *39*, 205–223.

Emery, X., & Alegría, A. (2021). The Gauss hypergeometric covariance kernel for modeling second-order stationary random fields in euclidean spaces: its compact support, properties and spectral representation. *arXiv e-prints*, (p. arXiv:2101.09558). arXiv:2101.09558.

Emery, X., Arroyo, D., & Mery, N. (2021). Twenty-two families of multivariate covariance kernels on spheres, with their spectral representations and sufficient validity conditions. *Stochastic Environmental Research and Risk Assessment*, . URL: https://doi.org/10.1007/s00477-021-02063-4. doi:10.1007/s00477-021-02063-4.

Emery, X., & Lantuéjoul, C. (2006). TBSIM: A computer program for conditional simulation of three-dimensional gaussian random fields via the turning bands method. *Computers & Geosciences*, *32*, 1615 – 1628. doi:10.1016/j.cageo.2006.03.001.

Emery, X., & Ortiz, J. (2004). Shortcomings of multiple indicator kriging for assessing local distributions. *Applied Earth Science : IMM Transactions section B*, *113*, 249–259. doi:10.1179/174327504X27242.

Emery, X., & Ortiz, J. (2011). Two approaches to direct block-support conditional cosimulation. *Computers & Geosciences*, *37*, 1015–1025. doi:10.1016/j.cageo.2010.07.012.

Emery, X., Ortiz, J., & Rodríguez, J. (2006). Quantifying uncertainty in mineral resources by use of classification schemes and conditional simulations. *Mathematical Geology*, *38*, 445–464. URL: https://doi.org/10.1007/s11004-005-9021-9. doi:10.1007/s11004-005-9021-9.

Emery, X., & Peláez, M. (2011). Assessing the accuracy of sequential Gaussian simulation and cosimulation. *Computational Geosciences*, *15*, 673. doi:10.1007/s10596-011-9235-5.

Emery, X., Porcu, E., & White, P. (2021). Flexible validity conditions for the multivariate Matérn covariance in any spatial dimension and for any number of components. *arXiv e-prints*, (p. arXiv:2101.04235). arXiv:2101.04235.

Emery, X., & Torres, J. F. S. (2005). Models for support and information effects: A comparative study. *Mathematical Geology*, *37*, 49–68. URL: https://doi.org/10.1007/s11004-005-8747-8. doi:10.1007/s11004-005-8747-8.

Englund, E., & Heravi, N. (1993). Conditional simulation: Practical application for sampling design optimization. In A. Soares (Ed.), *Geostatistics Tróia '92: Volume 1* (pp. 613–624). Dordrecht: Springer Netherlands. URL: https://doi.org/10.1007/978-94-011-1739-5_48. doi:10.1007/978-94-011-1739-5_48.

Ertunç, G., Tercan, A., Hindistan, M., Ünver, B., Ünal, S., Atalay, F., & Kıllıoğlu, S. (2013). Geostatistical estimation of coal quality variables by using covariance matching constrained kriging. *International Journal of Coal Geology*, *112*, 14 – 25. doi:10.1016/j.coal.2012.11.014.

Eze, P., Madani, N., & Adoko, A. (2019). Multivariate mapping of heavy metals spatial contamination in a Cu-Ni exploration field (Botswana) using turning bands co-simulation algorithm. *Natural Resources Research*, *28*, 109–124. URL: https://doi.org/10.1007/s11053-018-9378-3. doi:10.1007/s11053-018-9378-3.

Faria, P. H., Costa, J. F. C. L., & Bassani, M. A. A. (2021). Multivariate geostatistical simulation with PPMT: an application for uncertainty measurement. *Applied Earth Science*, *130*, 174–184. URL: https://doi.org/10.1080/25726838.2021.1892364. doi:10.1080/25726838.2021.1892364. arXiv:https://doi.org/10.1080/25726838.2021.1892364.

Fouedjio, F., & Klump, J. (2019). Exploring prediction uncertainty of spatial data in geostatistical and machine learning approaches. *Environmental Earth Sciences*, *78*, 38. URL: https://doi.org/10.1007/s12665-018-8032-z. doi:10.1007/s12665-018-8032-z.

Ghezelbash, R., Maghsoudi, A., Bigdeli, A., & Carranza, E. J. M. (2021). Regional-scale mineral prospectivity mapping: Support vector machines and an improved data-driven multi-criteria decision-making technique. *Natural Resources Research*, *30*, 1977–2005. URL: https://doi.org/10.1007/s11053-021-09842-4. doi:10.1007/s11053-021-09842-4.

Glacken, I., & Snowden, D. (2001). Mineral resource estimation. In A. Edwards (Ed.), *Mineral resource and ore reserve estimation—the AusIMM guide to good practice.* (pp. 189–198). Melbourne: The Australasian Institute of Mining and Metallurgy volume 23.

Gneiting, T., Kleiber, W., & Schlather, M. (2010). Matérn cross-covariance functions for multivariate random fields. *Journal of the American Statistical Association*, *105*, 1167–1177. doi:10.1198/jasa.2010.tm09420. arXiv:https://doi.org/10.1198/jasa.2010.tm09420.

Goldsmith, T. (2002). Resource and reserves - their impact on financial reporting, valuations and the expectations gap. In *CMMI Congress* (pp. 1–5). Australasian Institute of Mining and Metallurgy.

Goovaerts, P. (1993a). Spatial orthogonality of the principal components computed from coregionalized variables. *Mathematical Geology*, *25*, 281–302. doi:10.1007/BF00901420.

Goovaerts, P. (1993b). Spatial orthogonality of the principal components computed from coregionalized variables. *Mathematical Geology*, *25*, 281–302. URL: https://doi.org/10.1007/BF00901420. doi:10.1007/BF00901420.

Goovaerts, P. (1997). *Geostatistics for Natural Resource Evaluation* volume 42. New York: Oxford University Press.

Govindsammy, V. (2016). The practical implementation of uniform conditioning at AngloGold Ashanti African Operations, and a case study as applied for potential underground mining at Nyankanga pit, Geita gold mine, Tanzania. *Journal of the Southern African Institute of Mining and Metallurgy*, *116*, 621 – 628. URL: http://www.scielo.org.za/scielo.php?script=sci_arttext&pid=S2225-62532016000700005&nrm=iso.

Granian, H., Hassan, S., Asadi, H., & Carranza, E. (2015). Multivariate regression analysis of lithogeochemical data to model subsurface mineralization: a case study from the Sari Gunay epithermal gold deposit, NW Iran. *Journal of Geochemical Exploration*, *148*, 249–258. URL: https://www.sciencedirect.com/science/article/pii/S0375674214003446. doi:https://doi.org/10.1016/j.gexplo.2014.10.009.

Gringarten, E., & Deutsch, C. (2001). Teacher's aide variogram interpretation and modeling. *Mathematical Geology*, *33*, 507–534. doi:10.1023/A:1011093014141.

Guertin, K. (1984). Correcting conditional bias. In G. Verly, M. David, A. Journel, & A. Marechal (Eds.), *Geostatistics for Natural Resources Characterization: Part 1* (pp. 245–260). Dordrecht: Springer Netherlands. doi:10.1007/978-94-009-3699-7_15.

Guibal, D. (2001). Variography, a tool for the resource geologist. In A. Edwards (Ed.), *Mineral Resource and Ore Reserve Estimation – The AusIMM Guide to Good Practice. The Australasian Institute of Mining and Metallurgy* (pp. 85–90). Melbourne volume 23.

Guibal, D., & Remacre, A. (1984). Local estimation of the recoverable reserves: Comparing various methods with the reality on a porphyry copper deposit. In G. Verly, M. David, A. Journel, & A. Marechal (Eds.), *Geostatistics for Natural Resources Characterization: Part 1* (pp. 435–448). Dordrecht: Springer Netherlands. doi:10.1007/978-94-009-3699-7_25.

Hagan, M., & Menhaj, M. (1994). Training feedforward networks with the Marquardt algorithm. *IEEE transactions on Neural Networks*, *5*, 989–993.

Halotel, J., Demyanov, V., & Gardiner, A. (2020). Value of geologically derived features in machine learning facies classification. *Mathematical Geosciences*, *52*, 5–29. doi:10.1007/s11004-019-09838-0.

Halton, J. (1960). On the efficiency of certain quasi-random sequences of points in evaluating multi-dimensional integrals. *Numerische Mathematik*, *2*, 84–90. doi:10.1007/BF01386213.

Hansmann, K. (2016). When should uniform conditioning be applied? *Journal of the Southern African Institute of Mining and Metallurgy*, *116*, 645–654. doi:10.17159/2411-9717/2016/v116n7a6.

Harris, J., & Grunsky, E. (2015). Predictive lithological mapping of Canada's North using random forest classification applied to geophysical and geochemical data. *Computers & Geosciences*, *80*, 9–25. doi:10.1016/j.cageo.2015.03.013.

Harvey, A., & Fotopoulos, G. (2016). Geological mapping using machine learning algortihms. *International Archives of the Photogrammetry, Remote Sensing and Spatial Information Sciences*, *41*, 423–430. doi:10.5194/isprs-archives-XLI-B8-423-2016.

Hasterok, D., Gard, M., Bishop, C., & Kelsey, D. (2019). Chemical identification of metamorphic protoliths using machine learning methods. *Computers & Geosciences*, *132*, 56–68. doi:10.1016/j.cageo.2019.07.004.

Hofer, C., Borer, F., Bono, R., Kayser, A., & Papritz, A. (2013). Predicting topsoil heavy metal content of parcels of land: An empirical validation of customary and constrained lognormal block kriging and conditional simulations. *Geoderma*, *193*, 200 – 212. doi:https://doi.org/10.1016/j.geoderma.2012.08.034.

Hofer, C., & Papritz, A. (2010). Predicting threshold exceedance by local block means in soil pollution surveys. *Mathematical Geosciences*, *42*, 631–656.

Hofer, C., & Papritz, A. (2011). ConstrainedKriging: An R-package for customary, constrained and covariance-matching constrained point or block kriging. *Computers & Geosciences*, *37*, 1562 – 1569. doi:10.1016/j.cageo.2011.02.009.

Hornik, K., Stinchcombe, M., & White, H. (1989). Multilayer feedforward networks are universal approximators. *Neural Networks*, *2*, 359 – 366. URL: http://www.sciencedirect.com/science/article/pii/0893608089900208. doi:https://doi.org/10.1016/0893-6080(89)90020-8.

Hosseini, E., Gallichand, J., & Marcotte, D. (1994). Theoretical and experimental performance of spatial interpolation methods for soil salinity analysis. *Transactions of the ASAE. American Society of Agricultural Engineers*, *37 (6)*, 1799–1807.

Hosseini, S., & Asghari, O. (2019). Multivariate geostatistical simulation on block-support in the presence of complex multivariate relationships: Iron ore deposit case study. *Natural Resources Research*, *28*, 125–144. URL: https://doi.org/10.1007/s11053-018-9379-2. doi:10.1007/s11053-018-9379-2.

Hosseini, S., Asghari, O., & Emery, X. (2017). Direct block-support simulation of grades in multi-element deposits: application to recoverable mineral resource estimation at Sungun porphyry copper-molybdenum deposit. *Journal of the Southern African Institute of Mining and Metallurgy*, *117*, 577–585. URL: http://www.scielo.org.za/scielo.php?script=sci_arttext&pid=S2225-62532017000600011&nrm=iso.

Hundelshaussen, R., Costa, J., Marques, D., & Arcari, M. (2018). Localised kriging parameter optimisation based on absolute error minimisation. *Applied Earth Science*, *127*, 153–162. doi:10.1080/25726838.2018.1539536.

Isaaks, E., & Srivastava, R. (1989). *An Introduction To Applied Geostatistics* volume 33. New York: Oxford University Press.

Isaaks, I. (2004). The kriging oxymoron: A conditionally unbiased and accurate predictor (2nd edition). In O. Leuangthong, & C. Deutsch (Eds.), *Geostatistics Banff* (pp. 363–374). Springer Netherlands volume 14.

Ishitsuka, K., Ojima, H., Mogi, T., Kajiwara, T., Sugimoto, T., & Asanuma, H. (2021). Characterization of hydrothermal alteration along geothermal wells using unsupervised machine-learning analysis of X-ray powder diffraction data. *Earth Science Informatics*, . doi:10.1007/s12145-021-00694-3.

Jafrasteh, B., Fathianpour, N., & Suárez, A. (2018). Comparison of machine learning methods for copper ore grade estimation. *Computational Geosciences*, *22*, 1371–1388. URL: https://doi.org/10.1007/s10596-018-9758-0. doi:10.1007/s10596-018-9758-0.

Jalloh, A., Kyuro, S., Jalloh, Y., & Barrie, A. (2016). Integrating artificial neural networks and geostatistics for optimum 3D geological block modeling in mineral reserve estimation: A case study. *International Journal of Mining Science and Technology*, *26*, 581 – 585. doi:https://doi.org/10.1016/j.ijmst.2016.05.008.

Jones, O., Aspandiar, M., Dugdale, A., Leggo, N., Glacken, I., & Smith, B. (2019). *The Business of Mining: Mineral Deposits, Exploration and Ore-Reserve Estimation*. CRC Press. doi:10.1201/9780429057540.

Journel, A. (1974). Geostatistics for conditional simulation of ore bodies. *Economic Geology*, *69*, 673–687. doi:10.2113/gsecongeo.69.5.673.

Journel, A., & Huijbregts, C. (1978). *Mining Geostatistics*. Academic Press, Inc.

Journel, A., & Kyriakidis, P. (2004). *Evaluation of mineral reserves: a simulation approach*. Oxford University Press.

Journel, A., Kyriakidis, P., & Mao, S. (2000). Correcting the smoothing effect of estimators: A spectral postprocessor. *Mathematical Geology*, *32*, 787–813. doi:10.1023/A:1007544406740.

Kalam, S., Khan, R. A., Khan, S., Faizan, M., Amin, M., Ajaib, R., & Abu-Khamsin, S. (2021). Data-driven modeling approach to predict the recovery performance of low-salinity waterfloods. *Natural Resources Research*, *30*, 1697–1717. URL: https://doi.org/10.1007/s11053-020-09803-3. doi:10.1007/s11053-020-09803-3.

Kapageridis, I. (2005). Input space configuration effects in neural network-based grade estimation. *Computers & Geosciences*, *31*, 704–717. URL: https://www.

sciencedirect.com/science/article/pii/S009830040500004X. doi:https://doi.org/10.1016/j.cageo.2005.01.001.

Karbalaei Ramezanali, A., Feizi, F., Jafarirad, A., & Lotfi, M. (2020). Geochemical anomaly and mineral prospectivity mapping for vein-type copper mineralization, Kuhsiah-e-Urmak area, Iran: Application of sequential gaussian simulation and multivariate regression analysis. *Natural Resources Research*, *29*, 41–70. URL: https://doi.org/10.1007/s11053-019-09565-7. doi:10.1007/s11053-019-09565-7.

Keskinkilic, E. (2019). Nickel laterite smelting processes and some examples of recent possible modifications to the conventional route. *Metals*, *9*, 974–989. URL: https://www.mdpi.com/2075-4701/9/9/974. doi:10.3390/met9090974.

Khakestar, M., Madani, H., Hassani, H., & Moarefvand, P. (2013). Determining the best search neighbourhood in reserve estimation, using geostatistical method: A case study anomaly No 12A iron deposit in central Iran. *Journal of the Geological Society of India*, *81*, 581–585. URL: https://doi.org/10.1007/s12594-013-0074-y. doi:10.1007/s12594-013-0074-y.

Kirkwood, C., Cave, M., Beamish, D., Grebby, S., & Ferreira, A. (2016). A machine learning approach to geochemical mapping. *Journal of Geochemical Exploration*, *167*, 49–61. doi:10.1016/j.gexplo.2016.05.003.

Kitanidis, P. (1986). Parameter uncertainty in estimation of spatial functions: Bayesian analysis. *Water Resources Research*, *22*, 499–507. doi:https://doi.org/10.1029/WR022i004p00499.

Kotsiantis, S., Kanellopoulos, D., & Pintelas, P. (2006). Data preprocessing for supervised learning. *International Journal of Computer Science*, *1*, 111–117.

Krige, D. (1997). A practical analysis of the effects of spatial structure and of data available and accessed, on conditional biases in ordinary kriging. In E. Baafi, & N. Schofield (Eds.), *Geostatistics Wollongong '96* (pp. 799–810). Dordrecht: Kluwer Academic Publishers volume 1.

Kuhn, M., Johnson, K. et al. (2013). *Applied predictive modeling*. New York: Springer.

Lajaunie, C. (2000). Introduction to the modelling of the support effect. In H. Pandalai, & P. Saraswati (Eds.), *Geological data analysis: statistical methods* (pp. 155–171). New Delhi: Hindustan Publishing.

Lantuejoul, C. (1988). On the importance of choosing a change of support model for global reserves estimation. *Mathematical Geology*, *20*, 1001–1019. URL: https://doi.org/10.1007/BF00892976. doi:10.1007/BF00892976.

Lantuéjoul, C. (2002). *Geostatistical Simulation*. Berlin, Heidelberg: Springer.

Lantuéjoul, C. (1990). Cours de sélectivité: Course notes C-140, Centre de géostatistique. Ecole des Mines de Paris, Fontainebleau, France.

Le Ravalec, M., Noetinger, B., & Hu, L. (2000). The FFT moving average generator: An efficient numerical method for generating and conditioning Gaussian simulations. *Mathematical Geology*, *32*, 701–722.

Leuangthong, O., & Deutsch, C. (2003). Stepwise conditional transformation for simulation of multiple variables. *Mathematical Geology*, *35*, 155–173. URL: https://doi.org/10.1023/A:1023235505120. doi:10.1023/A:1023235505120.

MacCormack, K., Arnaud, E., & Parker, B. (2017). Using a multiple variogram approach to improve the accuracy of subsurface geological models. *Canadian Journal of Earth Sciences*, *55*, 786–801. doi:10.1139/cjes-2016-0112.

Machuca-Mory, D., Babak, O., & Deutsch, C. (2008). Flexible change of support model suitable for a wide range of mineralization styles. *Mining Engineering*, *60*, 63–72.

Madani, N., & Ortiz, J. (2017). Geostatistical simulation of cross-correlated variables: a case study through Cerro Matoso nickel-laterite deposit. In *The 26th international symposium on mine planning and equipment selection*. Nazarbayev University School of Mining and Geosciences.

Maitre, J., Bouchard, K., & Bédard, L. (2019). Mineral grains recognition using computer vision and machine learning. *Computers & Geosciences*, *130*, 84 – 93. URL: http://www.sciencedirect.com/science/article/pii/S0098300419301037. doi:https://doi.org/10.1016/j.cageo.2019.05.009.

Marcotte, D. (1994). Direct conditional simulation of block grades. In R. Dimitrakopoulos (Ed.), *Geostatistics for the Next Century: An International Forum in Honour of Michel David's Contribution to Geostatistics, Montreal, 1993* (pp. 245–252). Dordrecht: Springer Netherlands. doi:10.1007/978-94-011-0824-9_29.

Marcotte, D. (2016). Spatial turning bands simulation of anisotropic non-linear models of coregionalization with symmetric cross-covariances. *Computers & Geosciences*, *89*, 232–238. doi:https://doi.org/10.1016/j.cageo.2016.01.004.

Marcotte, D., & David, M. (1985). The Bi-Gaussian approach: A simple method for recovery estimation. *Mathematical Geology*, *17*, 625–644. URL: https://doi.org/10.1007/BF01030857. doi:10.1007/BF01030857.

Matheron, G. (1963). Principles of geostatistics. *Economic Geology*, *58*, 1246–1266. doi:10.2113/gsecongeo.58.8.1246.

Matheron, G. (1974). Les fonctions de transfert des petits panneaux. Internal report N-127: Centre de géostatistique. Ecole des Mines de Paris, fontainebleau, france.

Matheron, G. (1976a). Forecasting block grade distributions: The transfer functions. In M. Guarascio, M. David, & C. Huijbregts (Eds.), *Advanced Geostatistics in the Mining Industry* (pp. 237–251). Dordrecht: Springer Netherlands.

Matheron, G. (1976b). A simple substitute for conditional expectation: The disjunctive kriging. In M. Guarascio, M. David, & C. Huijbregts (Eds.), *Advanced Geostatistics in the Mining Industry* (pp. 221–236). Dordrecht: Springer Netherlands.

Matheron, G. (1980). Modèles isofactoriels pour l'effet zéro. Internal report N-659: Centre de géostatistique. Ecole des Mines de Paris, fontainebleau, france.

Matheron, G. (1984). The selectivity of the distributions and "the second principle of geostatistics". In G. Verly, M. David, A. Journel, & A. Marechal (Eds.), *Geostatistics for Natural Resources Characterization: Part 1* (pp. 421–433). Dordrecht: Springer Netherlands. URL: https://doi.org/10.1007/978-94-009-3699-7_24. doi:10.1007/978-94-009-3699-7_24.

Matías, J., Vaamonde, A., Taboada, J., & González-Manteiga, W. (2004). Comparison of kriging and neural networks with application to the exploitation of a slate mine. *Mathematical Geology*, *36*, 463–486. URL: https://doi.org/10.1023/B:MATG.0000029300.66381.dd. doi:10.1023/B:MATG.0000029300.66381.dd.

McKay, G., & Harris, J. (2015). Comparison of the data-driven random forests model and a knowledge-driven method for mineral prospectivity mapping: A case study for gold deposits around the Huritz Group and Nueltin Suite, Nunavut, Canada. *Natural Resources Research*, *25*, 125–143. doi:10.1007/s11053-015-9274-z.

McManus, S., Rahman, A., Coombes, J., & Horta, A. (2021). Uncertainty assessment of spatial domain models in early stage mining projects – a review. *Ore Geology Reviews*, *133*. URL: https://www.sciencedirect.com/science/article/pii/S0169136821001232. doi:https://doi.org/10.1016/j.oregeorev.2021.104098.

Mery, N., & Marcotte, D. (2022). Quantifying mineral resources and their uncertainty using two existing machine learning methods. *Mathematical Geosciences*, . doi:10.1007/s11004-021-09971-9.

Mery, N., Marcotte, D., & Dutaut, R. (2020). Constrained kriging: An alternative to predict global recoverable resources. *Natural Resources Research*, *29*, 2275–2289. URL: https://doi.org/10.1007/s11053-019-09601-6. doi:10.1007/s11053-019-09601-6.

Micheletti, N., Foresti, L., Robert, S., Leuenberger, M., Pedrazzini, A., Jaboyedoff, M., & Kanevski, M. (2014). Machine learning feature selection methods for landslide susceptibility mapping. *Mathematical Geosciences*, *46*, 33–57.

Millad, M., & Zammit, K. (2014). Implementation of localised uniform conditioning for recoverable resource estimation at the Kipoi Copper Project, DRC. In *Proceedings of the Ninth International Mining Geology Conference* (pp. 207–214). Melbourne: Australasian Institute of Mining and Metallurgy.

Minnitt, R., & Deutsch, C. (2014). Cokriging for optimal mineral resource estimates in mining operations. *Journal of the Southern African Institute of Mining and Metallurgy*, *114*, 189–189.

Mitchell, T. (1997). *Machine Learning*. New York: McGraw-Hill.

Montoya, C., Emery, X., Rubio, E., & Wiertz, J. (2012). Multivariate resource modelling for assessing uncertainty in mine design and mine planning. *Journal of the Southern African Institute of Mining and Metallurgy*, *112*, 353–363.

Morley, C., Snowden, V., & Day, D. (1999). Financial impact of resource/reserve uncertainty. *Journal of the Southern African Institute of Mining and Metallurgy*, *99*, 293–301.

Murphy, K. (2012). *Machine learning: a probabilistic perspective*. MIT press.

Myers, D. (1982). Matrix formulation of co-kriging. *Journal of the International Association for Mathematical Geology*, *14*, 249–257. doi:10.1007/BF01032887.

Myers, D. (1983). Estimation of linear combinations and co-kriging. *Journal of the International Association for Mathematical Geology*, *15*, 633–637. doi:10.1007/BF01093416.

Nezamolhosseini, S., Mojtahedzadeh, S., & Gholamnejad, J. (2017). The application of artificial neural networks to ore reserve estimation at Choghart iron ore deposit. *Analytical and Numerical Methods in Mining Engineering*, *6*, 73 – 83.

Nwaila, G., Zhang, S., Frimmel, H., Manzi, M., Dohm, C., Durrheim, R., Burnett, M., & Tolmay, L. (2020). Local and target exploration of conglomerate-hosted gold deposits using machine learning algorithms: A case study of the Witwatersrand gold ores, South Africa. *Natural Resources Research*, *29*, 135–159. doi:10.1007/s11053-019-09498-1.

O'Brien, J., Spry, P., Nettleton, D., Xu, R., & Teale, G. (2015). Using random forests to distinguish gahnite compositions as an exploration guide to Broken Hill-type Pb–Zn–Ag deposits in the Broken Hill domain, Australia. *Journal of Geochemical Exploration*, *149*, 74–86. URL: https://www.sciencedirect.com/science/article/pii/S0375674214003793. doi:https://doi.org/10.1016/j.gexplo.2014.11.010.

Olea, R. (1994). Fundamentals of semivariogram estimation, modeling, and usage. In *Stochastic Modeling and Geostatistics: Principles, Methods, and Case Studies* (pp. 27 – 36). American Association of Petroleum Geologists. doi:10.1306/CA3590C4.

Olea, R., & Pawlowsky, V. (1996). Compensating for estimation smoothing in kriging. *Mathematical Geology*, *28*, 407–417. doi:10.1007/BF02083653.

Owusu, S., & Dagdelen, K. (2019). Critical review of mineral resource classification techniques in the gold mining industry. In *Mining goes Digital: Proceedings of the 39th International Symposium 'Application of Computers and Operations Research in the Mineral Industry' (APCOM 2019)* (pp. 201–209). Wroclaw, Poland. doi:10.1201/9780429320774-23.

Pan, G., Gaard, D., Moss, K., & Heiner, T. (1993). A comparison between cokriging and ordinary kriging: Case study with a polymetallic deposit. *Mathematical Geology*, *25*, 377–398. doi:10.1007/BF00901424.

Paravarzar, S., Emery, X., & Madani, N. (2015). Comparing sequential gaussian and turning bands algorithms for cosimulating grades in multi-element deposits. *Comptes Rendus Geoscience*, *347*, 84 – 93. doi:10.1016/j.crte.2015.05.008.

Pasquier, P., Zarrella, A., & Labib, R. (2018). Application of artificial neural networks to near-instant construction of short-term g-functions. *Applied Thermal Engineering*, *143*, 910 – 921. URL: http://www.sciencedirect.com/science/article/pii/S1359431118305921. doi:https://doi.org/10.1016/j.applthermaleng.2018.07.137.

Ravalec, M., Noetinger, B., & Hu, L. (2000). The FFT moving average (FFT-MA) generator: An efficient numerical method for generating and conditioning Gaussian simulations. *Mathematical Geology*, *32*, 701–723. doi:10.1023/A:1007542406333.

Remacre, A. (1989). Uniform conditioning versus indicator kriging. In M. Armstrong (Ed.), *Geostatistics* (pp. 947–960). Dordrecht: Springer Netherlands.

Rendu, J.-M. (1980). Disjunctive kriging: Comparison of theory with actual results. *Journal of the International Association for Mathematical Geology*, *12*, 305–320. URL: https://doi.org/10.1007/BF01029418. doi:10.1007/BF01029418.

Ripley, B. D. (1987). *Stochastic Simulation*. New York: John Wiley & Sons.

Rivoirard, J. (1987). Two key parameters when choosing the kriging neighborhood. *Mathematical Geology*, *19*, 851–856.

Rivoirard, J. (1994). *Introduction to Disjunctive Kriging and Non-Linear Geostatistics*. Oxford University Press.

Roden, S., & Smith, T. (2001). Sampling and analysis protocols and their role in mineral exploration and new resource development. In A. Edwards (Ed.), *Mineral resource and ore reserve estimation - The AusIMM guide to good practice* (pp. 73 – 78). Melbourne volume 23.

Rossi, M., & Deutsch, C. (2014). *Mineral Resource Estimation*. (1st ed.). Springer Netherlands. doi:10.1007/978-1-4020-5717-5.

Rossi, M., & Parker, H. (1994). Estimating recoverable reserves: Is it hopeless ? In R. Dimitrakopoulos (Ed.), *Geostatistics for the Next Century. Quantitative Geology and Geostatistics* (pp. 259–276). Dordrecht: Springer Netherlands. URL: https://doi.org/10.1007/978-94-011-0824-9_31. doi:10.1007/978-94-011-0824-9_31.

Rouet-Leduc, B., Hulbert, C., Lubbers, N., Barros, K., Humphreys, C., & Johnson, P. (2017). Machine learning predicts laboratory earthquakes. *Geophysical Research Letters*, *44*, 9276–9282. doi:10.1002/2017gl074677.

Sagadin, C., Luidold, S., Wagner, C., & Wenzl, C. (2016). Melting behaviour of ferronickel slags. *JOM*, *68*, 3022–3028. URL: https://doi.org/10.1007/s11837-016-2140-6. doi:10.1007/s11837-016-2140-6.

Samanta, B., Bandopadhyay, S., & Ganguli, R. (2006). Comparative evaluation of neural network learning algorithms for ore grade estimation. *Mathematical Geology*, *38*, 175–197. URL: https://doi.org/10.1007/s11004-005-9010-z. doi:10.1007/s11004-005-9010-z.

Shinozuka, M., & Jan, C. M. (1972). Digital simulation of random processes and its applications. *Journal of Sound and Vibration*, *25*, 111–128.

Silva, D., & Almeida, J. (2017). Geostatistical methodology to characterize volcanogenic massive and stockwork ore deposits. *Minerals*, *7*. URL: https://www.mdpi.com/2075-163X/7/12/238. doi:10.3390/min7120238.

Svoboda, J. (2004). *Magnetic techniques for the treatment of materials*. Springer Science & Business Media.

Tercan, A. (2004). Global recoverable reserve estimation by covariance matching constrained kriging. *Energy Sources*, *26*, 1177–1185.

Tercan, A., & Sohrabian, B. (2013). Multivariate geostatistical simulation of coal quality data by independent components. *International Journal of Coal Geology*, *112*, 53–66. URL: https://www.sciencedirect.com/science/article/pii/S0166516212002480. doi:https://doi.org/10.1016/j.coal.2012.10.007. Special issue on geostatistical and spatiotemporal modeling of coal resources.

Vann, J., Bertoli, O., & Jackson, S. (2002). An overview of geostatistical simulation for quantifying risk. In *Mining Industry–Symposium on Quantifying Risk and Error*. Perth, Western Australia: The Geostatistical Association of Australasia.

Vann, J., & Guibal, D. (2001). Beyond ordinary kriging - an overview of non-linear estimation. In A. Edwards (Ed.), *Mineral Resource and Ore Reserve Estimation - The AusIMM Guide to Good Practice* (pp. 6–25). volume 23.

Vann, J., Guibal, D., & Harley, M. (2000). Multiple indicator kriging–is it suited to my deposit? In *Proceedings of the 4th International Mining Geology Conference* (pp. 187–194). Coolum, Queensland, Australia.

Vann, J., Jackson, S., & Bertoli, O. (2003). Quantitative kriging neighbourhood analysis for the mining geologist - a description of the method with worked case examples. In S. Dominy (Ed.), *5th International Mining Geology Conference* (pp. 215–223). Melbourne, Australia.

Vergara, D., & Emery, X. (2013). Conditional bias for multivariate resources estimation. In J. Ambrus, J. Beniscelli, F. Brunner, J. Cabello, & F. Ibarra (Eds.), *3rd International Seminar on Geology for the Mining Industry* (pp. 27–33).

Verly, G. (1983). The multiGaussian approach and its applications to the estimation of local reserves. *Journal of the International Association for Mathematical Geology*, *15*, 259–286. doi:10.1007/BF01036070.

Verly, G. (1984). The block distribution given a point multivariate normal distribution. In G. Verly, M. David, A. Journel, & A. Marechal (Eds.), *Geostatistics for Natural Resources Characterization: Part 1* (pp. 495–515). Dordrecht: Springer Netherlands. URL: https://doi.org/10.1007/978-94-009-3699-7_29. doi:10.1007/978-94-009-3699-7_29.

Verly, G., & Parker, H. M. (2021). Conditional simulation for mineral resource classification and mining dilution assessment from the early 1990s to now. *Mathematical Geosciences*, *53*, 279–300. URL: https://doi.org/10.1007/s11004-021-09924-2. doi:10.1007/s11004-021-09924-2.

Wackernagel, H. (2003). *Multivariate Geostatistics – An Introduction With Applications*. (3rd ed.). Berlin: Springer.

Wellmer, F.-W., Dalheimer, M., & Wagner, M. (2007). *Economic evaluations in exploration*. Springer Science & Business Media.

Yalçin, E. (2005). Cokriging and its effect on the estimation precision. *Journal of The Southern African Institute of Mining and Metallurgy*, *105*, 223–228.

Yamamoto, J. (2005). Correcting the smoothing effect of ordinary kriging estimates. *Mathematical Geology*, *37*, 69–94. doi:10.1007/s11004-005-8748-7.

Yamamoto, J. (2008). Estimation or simulation? that is the question. *Computational Geosciences*, *12*, 573–591. doi:10.1007/s10596-008-9096-8.

Yamamoto, J. K. (2007). On unbiased backtransform of lognormal kriging estimates. *Computational Geosciences*, *11*, 219–234. doi:10.1007/s10596-007-9046-x.

Yao, L., Huo, Z., Feng, S., Mao, X., Kang, S., Chen, J., Xu, J., & Steenhuis, T. (2014). Evaluation of spatial interpolation methods for groundwater level in an arid inland oasis, northwest China. *Environmental Earth Sciences*, *71*, 1911–1924. doi:10.1007/s12665-013-2595-5.

Yao, T. (1998). Conditional spectral simulation with phase identification. *Mathematical Geology*, *30*, 285–308. doi:10.1023/A:1021728931335.

Yates, S., & Yates, M. (1988). Disjunctive kriging as an approach to management decision making. *Soil Science Society of America Journal*, *52*, 1554–1558.

Zhang, P., Patuwo, E., & Hu, M. (1998). Forecasting with artificial neural networks: The state of the art. *International Journal of Forecasting*, *14*, 35–62. doi:10.1016/S0169-2070(97)00044-7.

Zhang, S., Carranza, E., Xiao, K., Wei, H., Yang, F., Chen, Z., Li, N., & Xiang, J. (2021a). Mineral prospectivity mapping based on isolation forest and random forest: Implication for the existence of spatial signature of mineralization in outliers. *Natural Resources Research*, . URL: https://doi.org/10.1007/s11053-021-09872-y. doi:10.1007/s11053-021-09872-y.

Zhang, S., Nwaila, G., Tolmay, L., Frimmel, H., & Bourdeau, J. (2021b). Integration of machine learning algorithms with gompertz curves and kriging to estimate resources in gold deposits. *Natural Resources Research*, *30*, 39–56. URL: https://doi.org/10.1007/s11053-020-09750-z. doi:10.1007/s11053-020-09750-z.

Zhang, X., Song, S., Li, J., & Wu, C. (2013). Robust LS-SVM regression for ore grade estimation in a seafloor hydrothermal sulphide deposit. *Acta Oceanologica Sinica*, *32*, 16–25. doi:10.1007/s13131-013-0337-x.

Zuo, R., & Xiong, Y. (2020). Geodata science and geochemical mapping. *Journal of Geochemical Exploration*, *209*, 106431. URL: http://www.sciencedirect.com/science/article/pii/S0375674219304960. doi:https://doi.org/10.1016/j.gexplo.2019.106431.

APPENDIX A DISCRETE GAUSSIAN MODEL

The discrete Gaussian model was initially developed by Matheron (1974) to assess the recoverable resources by accounting for the support and information effects. A comprehensive review of the model can be found in Matheron (1976a); Rivoirard (1994); Emery & Torres (2005) and Chilès & Delfiner (2012).

Relating the point- and block-support grade distributions

The point-support grade $Z(x)$ is transformed into a variable $Y(x)$ with a standard Gaussian distribution by an anamorphosis function $\phi(\cdot)$

$$Z(x) = \phi(Y(x)) \tag{A.1}$$

Similarly, the block-support grade Z_v can be also transformed as

$$Z_v = \phi_v(Y_v) \tag{A.2}$$

where ϕ_v is the block-support anamorphosis function.

It is assumed that $Y(\underline{x})$ and Y_v, with $\underline{x}$ uniformly distributed within v, follow a bigaussian distribution with correlation r_v. The anamorphosis transformation at point-support $\phi(\cdot)$ can be derived from the sample data, while the anamorphosis at block-support ϕ_v and r_v can be obtained using the Cartier's relationship (Matheron, 1984; Rivoirard, 1994). This relationship states that the expected grade of a sample randomly located within a block v is equal to the block grade

$$\mathbb{E}[Z(\underline{x})|Z_v] = Z_v \tag{A.3}$$

where $\underline{x}$ stands for a point uniformly distributed within v.

From the bigaussian distribution, the following expressions are derived

$$\mathbb{E}[Y(\underline{x})|Y_v] = r_v Y_v \tag{A.4}$$

$$var(Y(\underline{x})|Y_v) = 1 - r_v^2 \tag{A.5}$$

Then, $Y(\underline{x})$ conditionally on Y_v can be written as

$$Y(\underline{x}) = r_v Y_v + (1 - r_v^2)^{1/2} U \tag{A.6}$$

where $U \sim$N(0,1).

Using the definition of the expectation, it can be obtained

$$Z_v = \phi_v(Y_v) = \mathbb{E}[Z(\underline{x})|Z_v] = \int \phi(r_v Y_v + (1 - r_v^2)^{1/2} u) g(u) du \tag{A.7}$$

where $g(u)$ is a standard Gaussian probability density function. The coefficient $r_v \in [0,1]$ is called the change-of-support coefficient, where 0 is associated with very large blocks and 1 with very small blocks. This coefficient is determined so as to reproduce the correct block-support variance: $var(Z_v) = var(Z(x)) - \overline{\gamma}(v, v)$.

Figure A.1 shows the normalized histogram of variable that follows a lognormal distribution under four different supports. A lower change-of-support coefficient corresponds to a larger support, which implies a less skewed distribution.

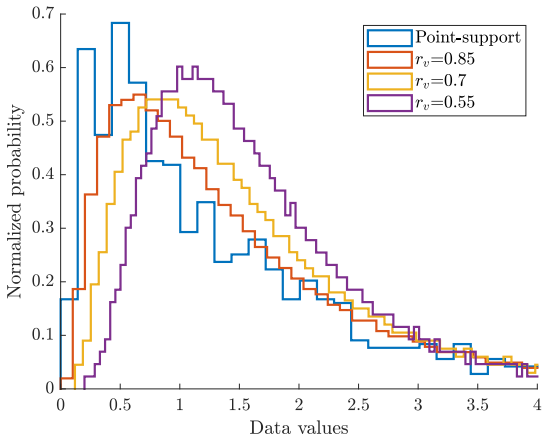

Figure A.1 Normalized probability distribution varying the change-of-support coefficient

Once the distribution of Z_v is determined, any quantity associated with Z_v can be obtained, for instance, the recovery functions. The tonnage $T_v(c)$ and metal quantity $Q_v(c)$ above a cutoff grade c with $c = \phi_v(y_c)$ are defined as

$$T_v(c) = 1 - G(y_c) \tag{A.8}$$

$$Q_v(c) = \int_{y_c}^{\infty} \phi_v(u) g(u) du \tag{A.9}$$

where G is the cumulative probability density function of a standard Gaussian variable.

Determining the distributions and recoverable resources via expansions into Hermite polynomials

The point-support anamorphosis function $\phi(\cdot)$ can be computed via either a graphical transformation of the data (quantile-quantile method), or an expansion into Hermite polynomials $\{H_n : n = 0, 1, ...\}$ as follows

$$\phi(Y(x)) = \sum_{n=0}^{\infty} \phi_n H_n(Y(x)) \tag{A.10}$$

where $\{\phi_n : n = 0, 1, ...\}$ are coefficients determined from the experimental distribution of the point-support data.

In turn, the block-support anamorphosis function (Eq. A.7) can be rewritten as

$$\phi_v(Y_v) = \sum_{n=0}^{\infty} \phi_n r_v^n H_n(Y_v) \tag{A.11}$$

The change-of-support coefficient r_v can be determined from the known variance of the block-support grades considering the following expression

$$var(Z_v) = \sum_{i=1}^{\infty} \phi_n^2 r_v^{2n} \tag{A.12}$$

Alternatively, the metal quantity function of Eq. A.9 can be expressed using the Hermite polynomials as

$$Q_v(c) = \phi_0[1 - G(y_c)] - \sum_{n=1}^{\infty} \phi_n r_v^n n^{-1/2} H_{n-1}(y_c) g(y_c) \tag{A.13}$$

The practice of the discrete Gaussian model

The application of the discrete Gaussian model relies on the following steps:

1. Select the area of study and the SMU size (depending on the mining method)

2. Normal-score transform the point-support data within the area of study, and also, determine the point-support anamorphosis function. A declustering of the data may be needed to obtain representative point-support distribution and point-support anamorphoses. The procedure can be performed by expanding the experimental anamorphosis into Hermite polynomials as:

   2.1 Sort the grade data $z_1, ...z_{n_d}$ in ascending order and determine the Gaussian equivalents $y_1, ..., y_{n_d}$ (quantile-quantile transformation)

   2.2 Choose the order of the polynomial expansion N

   2.3 Evaluate the polynomials $H_n(y_i), n = 0, ..., N$ at each value y_i

   2.4 Evaluate $\phi_n = \frac{1}{n_d} \sum_{i=1}^{n_d} z_i H_n(y_i)$, where n_d is the number of data

   2.5 Compare the experimental values z_i with the values calculated by the polynomial anamorphosis model. The process is stopped when the fit is satisfactory; otherwise, one can increase the degree of the polynomial expansion

3. Calculate the variogram of the original point-support data and compute the variance of Z_v by the block-regularization formulae. The sill of the point-support variogram may be previously corrected in order to match the variance of the point-support data, as determined by the point-support anamorphosis calculated at step 2

4. Determine the change-of-support coefficient r_v based on the point-support anamorphosis, and the block-support variance computed at step 3 using Eq. A.12. An alternative approach is to generate a large amount of values $Y_v \sim N(0, 1)$ and numerically evaluate the integral of Eq. A.7 for each value Y_v and a given r_v. Then, several Z_v values are obtained and used to calculate the experimental variance. Finally, r_v is optimized until the experimental block-support variance coincides with the theoretical variance obtained in step 3

5. The block-support distribution, in particular, the tonnage, quantity of metal, among others, can be estimated once the change-of-support coefficient is known

APPENDIX B UNIFORM CONDITIONING

Extension of the discrete Gaussian model to a panel support

Uniform conditioning (Rivoirard, 1994) is an extension of the discrete Gaussian model, focused on determining the distribution of block-support grades conditional to the grade of a panel V (composed by several small blocks). The Cartier's relationship can also be extended for the block $Z_{\underline{v}}$ and panel Z_V grades as

$$\mathbb{E}[Z_{\underline{v}}|Z_V] = Z_V \tag{B.1}$$

where $\underline{v}$ stands for a block randomly distributed within panel V.

This relationship implies that the expected grade of a block randomly located within a panel is equal to the panel grade.

Assuming that $Y_{\underline{v}}$ and Y_V follow a bigaussian distribution with correlation R, $\mathbb{E}[Y_{\underline{v}}|Y_V] = RY_V$ and $var(Y_{\underline{v}}|Y_V) = 1 - R^2$ can be derived. Therefore, it is possible to obtain an expression similar to Eq. A.7 in order to calculate the panel grade distribution

$$Z_V = \phi_V(Y_V) = \mathbb{E}[Z_{\underline{v}}|Z_V] = \int \phi_v(RY_V + (1-R^2)^{1/2}u)g(u)du \tag{B.2}$$

here $\phi_V(\cdot)$ is the anamorphosis at panel-support.

It can be also supposed that $Y(\underline{x})$ and Y_V follow a bigaussian distribution with correlation r_V; then, the following expression can be obtained

$$Z_V = \phi_V(Y_V) = \mathbb{E}[Z(\underline{x})|Z_V] = \int \phi(r_V Y_V + (1-r_V^2)^{1/2}u)g(u)du \tag{B.3}$$

Eqs. B.3 and B.2 allow the grade distribution to be calculated at panel-support considering the point and block-support distributions, respectively. It ensues $R = r_V/r_v$, linking the change-of-support coefficients between point, block and panel supports. When $v \to V$, then $R \to 1$ and $\phi_V = \phi_v$. Likewise, when $V \to \infty$, then $R \to 0$ and the influence of the panel disappears in Eq. B.2, returning to the global prediction of the discrete Gaussian model (refer to Appendix A).

Hypothetical case when the panel grade is known

Assuming a known value for the panel grade z_V, it is possible to determine any function at block-support within the panel since y_V can be calculated as $y_V = \phi_V^{-1}(z_V)$. Conditional to $Z_V = z_V$, $Y_{\underline{v}}$ follows a Gaussian distribution with mean Ry_V and variance $1 - R^2$. The tonnage and metal quantity above a cutoff grade $c = \phi_v(y_c)$ at block-support within the panel are defined as

$$T_{v|V}(c) = 1 - G\left(\frac{y_c - Ry_V}{\sqrt{1-R^2}}\right) \tag{B.4}$$

$$Q_{v|V}(c) = \int_{y_c}^{\infty} \phi_v(Ry_V + \sqrt{1-R^2}u)g(u)du \tag{B.5}$$

where $u \sim N(0,1)$.

In terms of the Hermite polynomial expansions, the following expression is obtained

$$Q_{v|V}(c) = \sum_{n=0}^{\infty} q_n(c)R^n H_n(y_V) \tag{B.6}$$

where $q_n(c)$ are the coefficients of the Hermite polynomial expansion of $Z_v \mathbb{1}_{Z_v > z_c}$.

Real case when the panel grade is unknown

In practice, one does not perfectly knows the panel grade, so that z_V is replaced with a prediction of the panel grade z_V^* and y_V with the Gaussian equivalent of z_V^*. Typically, z_V^* is obtained by ordinary kriging, which is advantageous in situations where the stationarity assumption is questionable, (e.g., the mean grade is locally constant, but varies at the scale of the deposit) and strictly stationary techniques such as the traditional multigaussian simulation fails at accounting for such a spatially varying mean.

Practical implementation

The implementation of UC is similar to the one described in Appendix A. The main differences are the additional definition of a panel size, the computation of the variance of Z_V, the determination of r_V to compute R, and the estimation of the panel grades by ordinary kriging to determine y_V by Eqs. B.3 or A.12 (defined in terms of the panel grades).